Retardation of organic compound movement in landfills by shredded tires. 1994

Edil, Tuncer B.; Park, Jae K.; Kim, Jae Y.
[s.l.]: [s.n.], 1994

RETARDATION OF ORGANIC COMPOUND MOVEMENT IN LANDFILLS BY SHREDDED TIRES

Principal Investigators
Tuncer B. Edil and Jae K. Park

Graduate Assistant
Jae Y. Kim

The Report for 1993 - 1994

Submitted to
The Bureau of Solid and Hazardous Waste Management
Wisconsin Department of Natural Resources

TABLE OF CONTENTS

LIST OF FIGURES

LIST OF TABLES

NOMENCLATURE

The dimension used are length = L, mass = M, time = T, and mole = MOL.

C	concentration in pore water of a porous medium [ML^{-3}]
$C_{CS_2, i}$	VOC concentration in CS_2 before extraction (mg/L)
$C_{CS_2, f}$	VOC concentration in CS_2 after extraction (mg/L)
C_e	equilibrium concentration of a compound [ML^{-3}]
C_{LR}	concentration in lower boundary (mg/L)
C_{UR}	concentration in upper boundary (mg/L)
$C_{liquid,0}$	initial concentration of a compound in liquid phase (mg/L)
$C_{liquid,e}$	equilibrium concentration of a compound in liquid phase (mg/L)
C_{pw}	concentration of a compound in pore water (mg/L)
C_{solid}	concentration of a compound in solid phase (mg/kg)
$C_{sol'n}$	concentration of a compound in solution (mg/L)
$C_{solid, i}$	VOC concentration in solid before extraction (mg/kg)
$C_{solid, f}$	VOC concentration in solid after extraction (mg/kg)
$C_{pw, i}$	VOC concentration in pore water before extraction (mg/L)
$C_{pw, f}$	VOC concentration in pore water after extraction (mg/L)
D	diffusion coefficient through polymer [L^2T^{-1}]
D_e	effective diffusion coefficient [L^2T^{-1}]
D_h	hydrodynamic dispersion coefficient [L^2T^{-1}]
D_m	mechanical dispersion coefficient [L^2T^{-1}]
D_o	free solution diffusion coefficient [L^2T^{-1}]
d_p	diameter of pore in a porous medium [L]
d_s	molecular diameter of solute [L]

f_{oc}	weight fraction of organic carbon
$F(\lambda)$	restrictive factor
h	head difference [L]
H_{LR}	height of lower reservoir (cm)
H_{UR}	height of upper reservoir (cm)
i	hydraulic gradient [LL^{-1}]
J	mass flux [$ML^{-2}T$]
J_{adv}	advective mass flux [$ML^{-2}T$]
$J_{adv,x}$	one-dimensional advective mass flux [$ML^{-2}T$]
J_{dis}	dispersive mass flux [$ML^{-2}T$]
$J_{dis,x}$	one-dimensional dispersive mass flux [$ML^{-2}T$]
$J_{in,adv}$	advective mass flux from $(n+1)^{th}$ to bottom reservoir ($mg/cm^2 \cdot sec$)
$J_{in,dis}$	dispersive mass flux into bottom reservoir ($mg/cm^2 \cdot sec$)
$J_{out,adv}$	advective mass flux from bottom reservoir to out of system ($mg/cm^2 \cdot sec$)
$J_{out,dis}$	dispersive mass flux from bottom reservoir to out of system ($mg/cm^2 \cdot sec$)
K	partition coefficient [dimensionless]
K_f	Freundlich constant
k_h	hydraulic conductivity [LT^{-1}]
K_l	Langmuir constant [$M^{-1}L^3$]
K_{oc}	partition coefficient between organic carbon and water [$M^{-1}L^3$]
K_{ow}	octanol-water partition coefficient
K_p	partition coefficient [$M^{-1}L^3$]
$K_{p,soil}$	partition coefficient of test soil (L/kg);
L	length of a porous medium [L]
$L_{1/2}$	half thickness of the polymer sheet [L]
L_e	length of a flow channel for a fluid particle [L]

L_s	imaginary length of solution on the each of the plain sheet [L]
M	mass of solid applied in batch tests [M]
M_t	total amount of solute in polymer at time t [M]
MW	molecular weight [M MOL^{-1}]
M_∞	total amount of solute in polymer after infinite time [M]
N_{Avo}	Avogadro's number (= 6.02×10^{23}/mol)
n_e	effective porosity
N_f	Freundlich constant
n_t	total porosity
PV	pore volume
Q	volume of flow [L^3]
Q_o	saturation constant in the Langmuir model [MM^{-1}]
q_{out}	effluent flowrate (cm^3/sec)
r	spherical coordinate [L]
r_p	radius of a sphere [L]
R_f	retardation factor
S	cross-sectional area of soil liner of medium into which solute transport [L^2]
S_{in}	cross-sectional area of inlet (cm^2)
S_{out}	cross-sectional area of outlet (cm^2)
t	elapsed time [T]
V	volume [L^3]
V_{CS_2}	volume of CS_2 (L)
V_{LR}	volume of lower reservoir (cm^3)
V_{UR}	volume of upper reservoir (cm^3)
V_{liquid}	volume of liquid (L)
V_{pw}	volume of pore water (L)

$V_{sol'n}$	volume of a solution (mL)
V_{water}	volume of water (mL)
V_m	molar volume (nm/mol)
v_x	seepage velocity along x [LT^{-1}]
v_z	seepage velocity along z [LT^{-1}]
w	water content (%)
W_{can}	weight of can (g)
W_{water}	weight of pore water in soil (g)
W_{solid}	weight of solid in sample (g)
$W_{soil+can, i}$	weight of (soil + can) before drying (g)
$W_{soil+can, f}$	weight of (soil + can) after drying (g)
x	mass of sorbate sorbed on the solid [M]
γ_1, γ_2	constants in solute diffusion model through polymer
λ	ratio of solute molecular diameter to pore diameter, (d_s/d_p)
ρ_p	dry density of porous medium [ML^{-3}]
ρ_{pw}	density of pore ware [ML^{-3}]
ρ_s	density of a compound [ML^{-3}]
τ	tortuosity, $(L/L_e)^2$
τ_a	apparent tortuosity, (D_e/D_o)

CHAPTER 1
INTRODUCTION

1.1 PROBLEMS

Leachates from municipal and hazardous waste landfills have recently been found to contain a wide variety and range of organic compounds (Plumb et al., 1985; Nelson et al., 1986; Gibbons et al., 1992). These organic compounds can contaminate the surrounding environment and impair the use of groundwater. The organic contaminants in landfill leachates originate from the incoming wastes into landfill or are produced by reactions within landfills (Tchobanoglous et al., 1993).

In the United States, the composite liner consisting of 0.6 m of compacted soil barrier with a hydraulic conductivity of 1×10^{-7} cm/sec or less and a minimum of 0.76 mm (30 mil) flexible membrane liner (FML which is also commonly called a geomembrane) is required as a minimum for municipal solid waste disposal sites by the U.S. Environmental Protection Agency (RCRA Subtitle D). However, states can require more conservative guidelines for the construction of municipal solid waste landfill liners. For example, Illinois and Wisconsin require 1.52 mm HDPE (high density polyethylene) and 1.2 m and 0.9 m of soil with a hydraulic conductivity of 1×10^{-7} cm/sec or less, respectively. The municipal solid waste landfills in Michigan and New York are required to have a double composite liner with a leakage detection system. The double composite liner consists of 0.6 m of soil liner with 1×10^{-7} cm/sec hydraulic conductivity and 1.52 mm HDPE, a leakage detection system, 0.6 m of soil liner (0.45 m in NY.) and 1.52 mm HDPE, from bottom to top.

However, these standards may not satisfactorily prevent the migration of organic contaminants from waste disposal sites during the operational and post-closure monitoring

periods. There is some evidence that organic compounds are not significantly retarded in clay barriers (Johnson et al., 1989; Edil et al., 1991; Myrand et al., 1992). Contaminants are transported through an earthen barrier by advective and diffusive mass transport. The advective mass transport accompanied the water flow. The diffusive mass transport results from the concentration difference of the transporting contaminant in the earthen barrier. Even if the hydraulic conductivity of a barrier is very low, i.e. $< 1 \times 10^{-7}$ cm/sec, some of the organic contaminants could penetrate through the barrier easily by diffusion independently of the advection.

The organic matter in soil material can sorb organic contaminants. The retardation of organic contaminants can be explained in terms of the sorption reaction. The sorption reaction of organic compounds by soil material depends on the amount of the organic matter in the soil material (Karickhoff et al., 1979). However, the organic matter content of typcal soil liner materials is not sufficiently high to sorb a considerable amount of organic contaminants. Thus, the penetration of organic compounds cannot be prevented effectively by earthen barriers alone.

To compensate for the weakness of earthen barriers, plastic materials such as geomembranes have been applied in the contaminant containment systems. However, organic compounds have been found to penetrate through geomembranes even without any holes or cracks on geomembranes (Park et al., 1993). The geomembrane liner in landfills experiences great tension due to the heavy weight of the solid wastes. Under stretched conditions, geomembranes allowed more mass transport of organic compounds through geomembranes than under unstretched conditions (Sakti et al., 1992). During the installation, some holes may be created on the geomembrane, too. For the purpose of design, 5 holes per acre is typically accepted. Thus, earthen liners and geomembranes together may not be sufficient to prevent the transport of organic compounds from waste disposal sites.

In the Unite States, approximately 240 million tires were discarded in 1990 based on the tire industry's estimation. The recovery rate, including heat recovery and rubber reclaiming, is only approximately 17 %. Most of the used tires are landfilled, stockpiled, or illegally dumped (EPA., 1991). The still growing generation rate of new tire production will make the used tire disposal problem more serious. Whole tires are difficult to be landfilled because they tend to float to the surface and also take up a large volume of the valuable landfill space. Most states ban the landfill of whole tires (Eldin and Piekarski, 1993).

Stockpiles of used tires result in public health, environmental, fire, and aesthetic problems (EPA, 1991). Desirable disposal methods should at least include three facets: (1) minimum environmental impact, (2) maximum reutilization of potential resources, and (3) economic feasibility.

1.2 BACKGROUND

Tires are principally composed of vulcanized rubber, rubberized fabric containing reinforcing textile cords, steel or fabric belts, and steel-wire-reinforced rubber beads. Styrene-butadiene rubber (SBR) is the most important synthetic rubber used by the tire industry, while natural rubber is still used in tires. Carbon black, extended oil, sulfur, zinc oxide, and stearic acid are also added (Dodds et al., 1983).

Several different technologies have been studied to reuse used tires. Shredded waste tires were investigated for their suitability for use as drainage material for leachate collection at municipal solid waste landfills (Hall, 1991; Edil et al., 1992). These studies indicated that shredded waste tires are suitable for the drainage material in municipal solid waste landfills.

The potential use of the tire rubber as a sorbent has been considered. Snoeyink and

Weber (1967) have pointed out that the chemical property of carbon black is very similar to that of activated carbon. The internal surface area of carbon black is much less than that of activated carbon. Metal removal by tire rubber has been tested (Hendersen et al., 1977; Knocke et al., 1981; Rowley et al., 1984). Heavy metals such as cadmium, mercury and lead were removed from aqueous phases by tire rubber. Park et al. (1991a) investigated the permeation of organic compounds through SBR gaskets used for potable water distribution systems and found that SBR was capable of sorbing significant amounts of organic compounds.

There have been concerns over detrimental and environmental impacts which may be caused by scrap tires. Leaching tests have been conducted (Rubber Manufacturers Association, 1989; Minnesota Control Protection Agency, 1990; Waste Management Pennsylvania, 1990; Edil and Bosscher, 1992; Glade et al., 1993). EPA's Toxicity Characteristics Leaching Procedure (TCLP) was used for various types of tires under different scrap tire processing scenarios (House of Representatives, 1990). Results reported did not show any significant levels of contaminants. Several bioassay tests have also been conducted to evaluate the potential toxicity of tire leachate to aquatic organisms (Stone et al., 1975; Minnesota Control Protection Agency, 1990; Kellough, 1991; Goude and Barton, 1992; Park, 1992). All tested organisms except one, the rainbow trout, survived.

It is postulated that hazardous organic compounds in landfills can be removed significantly by installing a layer of shredded tire chips in a proper location in landfills. Although the organic compound sorption by tire materials may be reversible, the reduced concentration in the leachate will effectively decrease the mass transport through the landfill liner. Also, it can be said that under typical conditions encountered in landfills, leaching components from scrap tires will not reach the level which may cause any serious environmental impact.

1.3 OBJECTIVES

The objectives of this research are:

1. To estimate the partition and diffusion coefficients of organic compounds onto tire materials;
2. To evaluate factors affecting the organic compound sorption capacity of tire materials under field conditions;
3. To develop a mathematical method to estimate mass transport key parameters from the long-term tank/column test results;

CHAPTER 2
LITERATURE REVIEW

2.1 VOLATILE ORGANIC COMPOUNDS IN LANDFILL LEACHATE

Many hazardous organic compounds have been detected in leachate from hazardous waste and municipal solid waste landfills. Plumb and Pitchford (1985) reported that 725 substances were detected in 183 hazardous waste disposal sites across the United States. Based on the frequency of detection, 9 of the 10 most frequently detected contaminants and 13 of the top 15 were volatile organic compounds (VOCs). The detection frequency of the organic compounds were highly variable and ranged from 51% to less than 1%.

In 1980, the Minnesota Pollution Control Agency (MPCA) initiated sampling and analysis for selected volatile organic compounds at sanitary landfills (Nelson and Book, 1986). Samples were collected from approximately 90 of Minnesota's municipal solid waste landfills for the study. Although some of the landfills had accepted hazardous waste, most of the landfills received only municipal solid waste. Volatile organic compounds were found at most of the Minnesota municipal landfills in the study.

A total of 65 sites, including 12 hazardous waste landfill sites and 36 municipal solid waste landfills, were investigated to evaluate the difference between the hazardous waste landfill leachate and the municipal solid waste landfill leachate (Gibbons et al., 1992). Organic compounds were detected in both municipal and hazardous waste landfills. The concentrations of the detected organic compounds in the hazardous waste disposal sites were higher than those in the municipal solid waste landfills.

There are two basic sources of the organic compounds detected in landfill leachate. They may be contained within the incoming waste. Except the incoming waste related pathway, they may be produced by biotic and abiotic reactions occurring within the

landfills. For example, vinyl chloride is a byproduct of the degradation of di- and trichloroethylene (Tchobanoglous et al., 1993).

According to the cited investigations, volatile organic compounds are expected to exist in landfill leachate, irrespective of whether it is a hazardous or municipal waste landfill, and finally contaminate the surrounding groundwater and soil system. Table 2.1 summarizes the most frequently detected volatile organic compounds at waste disposal sites tested by the previously mentioned studies. Table 2.2 shows the concentration ranges of the most frequently detected volatile organic compounds which are listed in Table 2.1.

2.2 MASS TRANSPORT THROUGH EARTHEN BARRIERS

The primary mechanisms of solute transport through a saturated soil with low hydraulic conductivity are advection and dispersion. The advective mass transport means the mass transport response to hydraulic flow through the soil pore spaces. The dispersive mass transport can be explained by the molecular diffusion and the mechanical dispersion. The molecular diffusion is the movement of solute through the soil pore spaces in response to a concentration gradient. The mechanical dispersion is caused by the local velocity variation.

The density driven migration (e.g., the movement of dense organic contaminants under the influence of gravity) is another potential mass transport mechanism. However, in the case of VOCs of landfill sites, the density driven migration can be ignored because VOCs are diluted in leachate and this may not cause significant density driven migration.

Table 2.1 The most frequently detected volatile organic compounds at waste disposal sites.

Hazardous waste				
Source	Plumb and Pitchford (1985)		Gibbons et al. (1992)	
Rank	Volatile organic compound	Detection (%)	Volatile organic compound	Detection (%)
1	Trichloroethylene	51.3	Acetone	92.0
2	Tetrachloroethylene	36.0	Methylene chloride	85.7
3	1,2-Dichloroethylene	29.1	2-Butanone	82.0
4	Chloroform	28.4	4-Nethyl-2-Pentanone	80.0
5	1,1-Dichloroethylene	25.2	Toluene	75.2
6	Methylene chloride	19.2	Isobutyl alcohol	65.0
7	1,1,1-Trichloroethane	18.9	Trichloroethylene	61.5
8	1,1-Dichloroethane	17.9	1,1-Dichloethane	48.3
9	1,2-Dichloroethane	14.2	1,2-Dichloroethane	48.1
10	Acetone	12.4	p-Dioxane	42.0
11	Toluene	11.6	Vinyl chloride	41.1
12	Benzene	11.2	Ethyl benzene	38.9
13	Vinyl chloride	8.7	Tetrachloroethylene	37.6
14			Chroform	35.3
15			Benzene	35.1
Municipal waste				
Source	Nelson and Book (1986)		Gibbons et al. (1992)	
Rank	Volatile organic compound	Detection (%)	Volatile organic compound	Detection (%)
1	1,2-Dichloroethylene	87.2	Acetone	82.5
2	1,1-Dichloethane	80.0	Toluene	73.7
3	Xylenes (total)	73.7	2-Butanone	67.5
4	Trichloroethylene	69.0	Methylene chloride	63.4
5	Tetrahydrofuran	61.2	4-Methyl-2-Pentanone	53.6
6	Benzene	58.3	Ethyl benzene	52.9
7	1,1,1-Trichloroethane	57.6	Acetonitrile	50.3
8	Toluene	55.0	Benzene	40.6
9	Methylene chloride	54.1	1,2-Dichloroethylene	32.8
10	Ethyl benzene	52.6	Chlorobenzene	28.0
11	Acetone	50.0	1,1-Dichloroethane	22.5
12	Tetrachloroethylene	48.2	Xylenes (total)	20.0
13	Methyl ethyl ketone	47.9	Trichlorofluromethane	15.1
14	1,2-Dichloroethane	47.5	Vinyl chloride	11.2
15	Methylene chloride	46.4	Chloroform	8.0

Table 2.2 The average concentration of the most frequently detected volatile organic compounds at waste disposal sites (Gibbons et al., 1992).

	Concentration in leachate (mg/L)					
	Hazardous waste			Municipal waste		
Volatile organic compound	Min.	Max.	Ave.	Min.	Max.	Ave.
Acetone	0.34	77.50	23.20	0.01	11.00	2.16
Acetonitrile	N.A.	N.A.	N.A.	N.A.	N.A.	N.A.
Benzene	0.09	0.72	0.30	0 <	1.08	0.22
2-Butanone	0.06	42.90	13.60	0.11	27.00	4.15
Chlorobenzene	0.11	2.48	0.48	0.0	0.69	0.13
Chloroform	0.03	7.25	1.94	0.07	1.30	0.20
1,1-Dichloroethane	0.05	1.62	0.18	0.04	44.00	1.72
1,2-Dichloroethane	N.A.	9.04	0.70	0 <	11.00	1.84
1,1-Dichloroethylene	N.A.	N.A.	N.A.	N.A.	N.A.	N.A.
1,2-Dichloroethylene	0.11	1.61	0.17	0 <	4.80	0.57
p-Dioxane	N.A.	N.A.	N.A.	N.A.	N.A.	N.A.
Ethyl benzene	0.16	1.10	0.33	0.01	4.90	0.27
Isobutyl alcohol	N.A.	N.A.	N.A.	N.A.	N.A.	N.A.
Methylene chloride	0.02	56.80	14.10	0 <	220.00	5.35
Methyl ethyl ketone	N.A.	N.A.	N.A.	N.A.	N.A.	N.A.
4-Methyl-2-Pentanone	0.01	3.97	0.78	0.01	0.71	0.31
Tetrachloroethylene	0.01	1.80	0.43	0 <	0.62	0.13
Tetrahydrofuran	N.A.	N.A.	N.A.	0.02	1.30	0.48
Toluene	0.03	33.60	8.34	0.01	18.00	1.02
1,1,1-Trichloroethane	0.04	22.00	1.83	0 <	13.00	0.89
Trichloroethylene	0.01	11.30	2.04	0 <	1.30	0.19
Trichlorofluoromethane	N.A.	N.A.	N.A.	0 <	0.15	0.06
Vinyl chloride	N.A.	N.A.	N.A.	0.01	0.06	0.04
Xylenes (total)	0.06	5.16	1.54	0.03	0.31	0.14

2.2.1 Advective Mass Transport

Mathematically, the advective mass transport can be expressed as Eq. 2.1. The mass tansport through a liner can be considered as one-dimensional flow. The advective mass flow (e.g., x-direction) through a porous medium can be represented by Eq. 2.2:

$$\mathbf{J_{adv}} = n_t \cdot \mathbf{v} \cdot C \tag{2.1}$$

$$J_{adv,x} = n_t \cdot v_x \cdot C \tag{2.2}$$

where $\mathbf{J_{adv}}$ = total advective mass flux (vector) [$ML^{-2}T$];

$J_{adv,x}$ = one-dimensional advective mass flux [$ML^{-2}T$];

n_t = total porosity of the porous medium;

$\mathbf{v}$ = seepage velocity (vector) [LT^{-1}];

v_x = seepage velocity along the direction i [LT^{-1}];

C = concentration of a solute in pore water [ML^{-3}].

The velocity of fluid through a porous medium can be estimated by Darcy's law. Under the constant hydraulic gradient condition, the seepage velocity is expressed as Eq. 2.3.

$$v_x = \frac{k_h \cdot i}{n_e} \tag{2.3}$$

where k_h = hydraulic conductivity of the porous media [LT^{-1}];

i = hydraulic gradient of the flowing system [LL^{-1}]; and

n_e = effective porosity of the porous media.

The effective porosity is defined as the portion of the pore which is effective to the fluid flow. Eq. 2.1 is based on the assumption that the transport of a mass does not influence the pattern of flow. For example, the solute, which has significantly different density from the ambient fluid, will not flow with the ambient fluid through a medium. However, in most of the practical groundwater contamination problems, transported

contaminants can be assumed to move along with groundwater.

2.2.2 Hydrodynamic Dispersive Mass Transport

When a fluid flows through a porous medium, the solute can move faster than the advective front which is estimated by the advection alone. This mass transport phenomenon is explained by hydrodynamic dispersion. If there is a concentration difference between two points, the solute flows from the high concentration point to the low concentration point by diffusion. This mass transport can occur even in reverse of the hydraulic flow direction. If there is a high hydraulic gradient in addition to the concentration gradient, the mechanical dispersion can be significant and the overall mass transport will be more complicated. The hydrodynamic dispersion has been expressed frequently by using the combination of the effective diffusion and mechanical dispersion (Domenico and Schwartz, 1990).

$$D_h = D_e + D_m \tag{2.4}$$

where D_h = hydrodynamic dispersion coefficient [L^2T^{-1}];

D_e = effective diffusion coefficient [L^2T^{-1}]; and

D_m = mechanical dispersion coefficient [L^2T^{-1}].

2.2.2.1 Effective diffusion coefficient, D_e

Mass transport by molecular diffusion is caused by random molecular motions due to the thermal kinetic energy of the solute. Because of molecular spacing, the scattering is larger in gases than in liquids, and larger in liquids than in solids. In general, the effective diffusion coefficient in a porous medium is smaller than the free solution diffusion coefficient in pure liquids primarily because collision with the solids of the medium hinders diffusion (Domenico and Schwartz, 1990). The mass transport by diffusion can be formulated as follows:

$$J_{dif} = - n_t \cdot D_e \cdot \nabla C \tag{2.5}$$

$$J_{dif,x} = - n_t \cdot D_e \cdot \frac{\partial C}{\partial x} \tag{2.6}$$

where J_{dif} = total mass flux by diffusion [$ML^{-2}T^{-1}$];

$J_{dif,x}$ = one dimensional mass flux by diffusion [$ML^{-2}T^{-1}$].

Since the effective diffusion within a porous medium is difficult to estimate, there have been several trials to estimate the effective diffusion coefficient from the free solution diffusion coefficient data. The free solution diffusion coefficient, which is the diffusion coefficient of a solute in a free solution, has been experimentally measured. There have been some attempts to estimate the effective diffusion coefficient using readily measured parameters such as the total porosity, tortuosity of the porous medium, and/or pore size of the porous medium. The following equations have been reported in the literature:

$$\frac{n_t}{(2-n_t)^2} D_o < D_e < \frac{1}{2} D_o \quad \text{(Helfferich, 1966)} \tag{2.7}$$

$$D_e = \sqrt{\tau} \cdot D_o \quad \text{(Greenkorn and Kessler, 1972)} \tag{2.8}$$

$$D_d = \tau \cdot D_o \quad \text{(Gillham et al., 1984)} \tag{2.9}$$

$$D_e = n_t \cdot D_o \quad \text{(Myrand et al., 1992)} \tag{2.10}$$

where D_o = free solution diffusion coefficient [L^2T^{-1}]; and

τ = tortuosity

The tortuosity of a medium is the characteristic of the solute traveling through the medium. Bear (1972) defined the tortuosity as $(L/L_e)^2$. (L, the length of a porous medium sample, and L_e, the length of a flow channel for fluid particles). Thus, the value of tortuosity is always smaller than unity except for perfect capillary-type passages. Even though there are other definitions of tortuosity, tortuosity in this study follows Bear's definition. The values of tortuosity in the granular media was 0.56 to 0.80 (Bear, 1972).

The tortuosity values of the aluminas were between 0.80 to 0.88 (Satterfield, 1973). In the case of soils, the ranges of 0.01 to 0.84, and 0.025 to 0.57 were observed for saturated and unsaturated soils, respectively (Shackelford and Daniel, 1991b).

Tortuosity has been considered to be independent of transport solutes because it is a geometric characteristic of a porous medium (Lin et al., 1994). Also, all of the previous equations were based on the constant tortuosity. Since the pathways of a solute through a porous medium can be affected by the sizes of transporting solutes, the effect of the ratio of solute size to pore size on the effective diffusion coefficient has been tested. The empirical equations derived from the results are as follows:

$$D_e = F(\lambda)\cdot \sqrt{\tau}\cdot D_o \quad \text{(aluminas)} \quad \text{(Satterfield et al., 1973)} \tag{2.11}$$

$$F(\lambda) = (1 - \lambda)^2\cdot(1 - 2.104\lambda + 2.09\lambda^3 - 0.95\lambda^5)$$

$$\text{(porous membranes)} \quad \text{(Renkin, 1954)} \tag{2.12}$$

$$F(\lambda) = (1-\lambda)^4 \quad \text{(porous membranes)} \quad \text{(Beck and Schultz, 1970)} \tag{2.13}$$

$$F(\lambda) = e^{-4.6\cdot\lambda} \quad \text{(aluminas)} \quad \text{(Satterfield et al., 1973)} \tag{2.14}$$

$$F(\lambda) = (1.03)\cdot e^{-4.5\cdot\lambda} \quad \text{(aluminas)} \quad \text{(Chantong and Mossoth, 1983)} \tag{2.15}$$

where $F(\lambda)$ = restrictive factor which is valid up to $\lambda = 0.5$; and

λ = ratio of the solute molecular diameter to pore diameter.

The tortuosity of a system is not a geometric constant but a function of the ratio between the molecular size of diffusing solute and the size of the channel. Under the assumption that the tortuosity is proportional to the porosity of the porous medium and is inverse to the restrictive factor, Farrell and Reinhard (1994) suggested the following equation for the estimation of tortuosity:

$$\tau = \frac{n_t^2}{F(\lambda)} \tag{2.16}$$

Although the previous equations were very consistent over wide ranges of λ, it is

not easy to apply the equation to the soil and groundwater problems. The equations were derived from membranes and aluminas, the pores of which were relatively uniform and easily measured. All the previous studies found that the effective diffusion coefficient in porous media increases with increasing porosity and tortuosity. Also, the effective diffusion coefficient can be said to be equal to or slightly less than the free solution diffusion coefficient of a concerned solute.

Shackelford (1991) suggested the following relationship containing an overall parameter, the apparent tortuosity, which explains the relationship between the effective diffusion coefficient and the free solution diffusion coefficient:

$$D_e = \tau_a \cdot D_o \quad \text{(Shackelford, 1991a)} \tag{2.17}$$

where τ_a = apparent tortuosity.

The apparent tortuosity includes not only the geometric tortuosity, but also all of the solute-solute and solute-solvent interactions.

Diffusion cell tests were conducted by using clayey soil and six inorganic chemicals (Shackelford and Daniel , 1991b). The ions which have the same hydrated radii and have different valences showed completely different apparent tortuosities. This cannot be explained by the relative size of the channel. The values of the apparent tortuosity of several inorganic and organic chemicals obtained from laboratories were relatively high and some of them were even higher than one (Sackelford and Daniel, 1991b; Barone et al., 1992; Wayne, 1993). The apparent tortuosity is a different concept from the traditional tortuosity. If the traditional tortuosity is the relative travelling length, the apparent tortuosity is the relative mass transport.

2.2.2.2 Mechanical dispersion coefficient, D_m

Mechanical dispersion is mixing that occurs as a consequence of local variations in

velocity around some mean velocity of flow. The main cause of the variation in the direction and rate of transport is the non-uniformity of the porous medium . Mechanical dispersion is an advective process and is affected by the fluid velocity and grain size. Evidence exists that groundwater velocity in compacted clay is low enough to ignore the effect of mechanical dispersion (Bear, 1972; Rowe, 1987; Shackelford, 1990).

In a one-dimensional flow, the total mass flux of an inactive solute through a porous medium under the combined effects of advection and hydrodynamic dispersion can be expressed as Eq. 2.18.

$$J = - n_t \cdot D_h \cdot \frac{\partial C}{\partial x} + n_t \cdot v_x \cdot C \tag{2.18}$$

and

$$\frac{\partial C}{\partial t} = D_h \cdot \frac{\partial^2 C}{\partial x^2} - v_x \cdot \frac{\partial C}{\partial x} \tag{2.19}$$

2.2.3 Retardation Factor, R_f

As a solute migrates through a soil layer, the solute may be uptaken by soil particles from the pore water in soil pore spaces. This reaction decreases the concentration of the solute in the pore water and consequently reduces the rate of the solute migration. The retardation factor, R_f, has been most frequently used to estimate contaminant mobility. The retardation factor can be defined as the ratio of the solute velocity to the ground water velocity (Domenico and Schwartz, 1990). The exact determination of the sorption capacity is very important, because it is one of the main parameters included in transport equations in the form of the retardation factor, R_f. Retardation factor is related to the partition coefficient. The partition coefficient which is also called the distribution coefficient, can be estimated (1) directly from batch isotherm sorption tests, (2) indirectly from equations based on a compound's octanol-water partition coefficient, K_{ow}, and the weight fraction of

organic carbon, f_{oc}, in the soil material concerned, (3) indirectly from the breakthrough curve of a column test, and (4) directly from the equilibrium concentrations in the pore water and solid phases.

2.2.3.1 Measurements of partition coefficient

Batch isotherm tests : When a solution containing solutes (sorbate) is mixed with a solid medium (sorbent) and allowed to equilibrate, a mass partitioning between the solution and the solid phase occurs. The partitioning of a solute between the solid phase and the aqueous phase is affected by the solubility of the solute. A high solubility means that the solute prefers to remain in the aqueous phase rather than in the solid phase. The solubility of a chemical depends on temperature. During the batch test, the temperature is kept constant; thus, the batch test is called isotherm.

The isotherms can be linear, concave, convex or a complex combination of several of these shapes. Four of the most common relationships are the linear model, Freundlich model, Langmuir model, and thermodynamic model. The Langmuir model is based on three assumptions: (1) population of bonding sites are all uniform with equal heat of adsorption and no interaction between adsorbate and adsorbent molecules, (2) adsorbate molecules are fixed and cannot migrate across the surface, and (3) no surface accumulation is permitted (monolayer adsorption). The Freundlich model permits multilayer accumulation and is based on the nonuniform heat of adsorption. The thermodynamic model was proposed by Park and Bontoux (1992). This model is a variation of the Langmuir model. This model is expressed in terms of the solubility of a solute in a solution.

In a one-dimensional mass transfer, the retardation factor can be derived differently based on the following mass balance equation, Eq. 2.20, and each sorption model applied. The mathematical expressions of the models are listed in Table 2.3.

$$\frac{\partial C}{\partial t} + \frac{\rho_p \cdot (1-n_t)}{n_t} \cdot \frac{\partial (x/M)}{\partial t} = D_h \cdot \frac{\partial^2 C}{\partial x^2} - v_x \cdot \frac{\partial C}{\partial x} \qquad (2.20)$$

where x = mass sorbed on the solid [M];

M = mass of solid applied [M]; and

ρ_p = dry density of porous medium.

Table 2.3 The mathematical expressions of isotherm and retardation models.

	Isotherm model	Retardation model
Linear model	$\frac{x}{M} = K_p \cdot C_e$ (2.21) K_p = partition coefficient [$M^{-1}L^3$] C_e = equilibrium concentration [ML^{-3}]	$1 + \frac{\rho_p \cdot K_p \cdot (1-n_t)}{n_t}$ (2.22)
Freundlich model	$\frac{x}{M} = K_f \cdot C_e^{N_f}$ (2.23) K_f = Freundlich constant N_f = Freundlich constant.	$1 + \frac{\rho_p \cdot (1-n_t)}{n_t} N_f \cdot K_f \cdot C_e^{(N_f-1)}$ (2.24)
Langmuir model	$\frac{x}{M} = \frac{Q_o \cdot K_l \cdot C_e}{1 + (K_l \cdot C_e)}$ (2.25) K_l = Langmuir constant [$M^{-1}L^3$] Q_o = saturation constant [MM^{-1}]	$1 + \frac{\rho_p \cdot (1-n_t) \cdot Q_o \cdot K_l}{n_t \cdot (1 + C_e \cdot K_l)^2}$ (2.26)
Thermodynamic model	$\frac{1}{(x/M)} = a + \frac{b}{(C_e/S)}$ (2.27) S = solubility of solute [ML^{-3}] a, b = constants	$1 + \frac{\rho_p \cdot (1 - n_t)}{n_t \cdot b \cdot S \cdot (1 + \frac{a \cdot C_e}{(b \cdot S)})^2}$ (2.28)

Except in the linear model, the retardation factors are not constants but functions of the equilibrium concentrations of the solute. Therefore, the retardation factor estimated by the models, except the linear model, can be changed by the experimental conditions, e.g., the solid/solution ratio.

In the soil and groundwater system, the linear sorption isotherm appears to be a reasonable assumption at low solute concentrations, although nonlinear isotherms are common at high concentrations (Rao and Davidson, 1979; Karickhoff, 1984; Yiacoumi and

Tien, 1994). The greatest advantage of the linear model is its simplicity. It contains only one parameter, K_p, partition coefficient.

Indirect estimation by K_{ow} and f_{oc} : In a soil-water system, numerous soil properties including organic carbon content, partitcle size distribution, clay mineral composition, moisture content, pH, and cation exchange capacity, have been identified as the factors affecting the mechanism and degree of organic compound sorption onto soil. However, the organic carbon content in soils has been considered to be the predominant factor. This suggests that the organic compound sorption onto soil can be simplified to the sorption onto organic carbon in soils. Several studies have shown that the partition coefficients of organic compounds are proportional to the weight fraction of organic carbon in soils (Karickhoff, 1984).

$$K_p = K_{oc} \cdot f_{oc} \tag{2.29}$$

where K_{oc} = partition coefficient between aqueous solution and organic carbon $[M^{-1}L^3]$;

and

f_{oc} = weight fraction of organic carbon.

There is a good correlation between log K_{ow} and log K_{oc} because the partitioning of an organic compound between water and organic carbon is not much different from water and octanol. Regression equations in practice describe the relationship between K_{oc} and K_{ow}.

$$\log K_{oc} = \log K_{ow} - 0.21 \text{ (Karickhoff et al., 1979)} \tag{2.30}$$

$$\log K_{oc} = 0.72 \cdot \log K_{ow} + 0.49 \text{ (Schwarzenbach and Westall, 1981)} \tag{2.31}$$

$$\log K_{oc} = 1.029 \cdot \log K_{ow} - 0.18 \text{ (Rao et al., 1982)} \tag{2.32}$$

$$\log K_{oc} = 0.909 \cdot \log K_{ow} + 0.088 \text{ (Hassett et al., 1983)} \tag{2.33}$$

$$\log K_{oc} = 0.69 \cdot \log K_{ow} + 0.22 \text{ (Piwoni and Banerjee, 1989)} \tag{2.34}$$

$$\log K_{oc} = 0.98 \cdot \log K_{ow} - 0.26 \text{ (Shimizu, 1992)} \tag{2.35}$$

Breakthrough curves of column test : Based on the linear model, the partition coefficient can be estimated from the breakthrough curve of a column test. As mentioned above, the retardation factor can be calculated from the breakthrough curves of the tracer and solute. The retardation factor is the ratio of the required pore volume of tracer to reach C/Co = 0.5 to that of solute. Figure 2.1 shows the estimation of the retardation factor using a column test data. Finally, the partition coefficient can be estimated using the retardation factor estimated from breakthrough curves and Eq. 2.22.

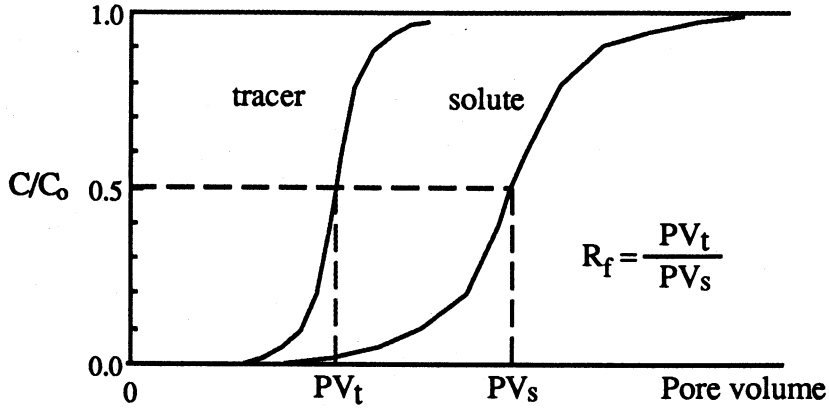

Figure 2.1 Breakthrough curves of tracer and solute.

Concentratation measurements in column test : The partition coefficient can be estimated directly by measuring the equilibrium concentrations of a solute in the both pore water and solid phases.

2.2.3.2 Comparison between different estimation techniques

If different laboratory techniques are used to estimate the partition coefficient, the resulting retardation factors may have different values. The sorption capacity of clay rocks for different metals (Cd, Co, Cr, Cs, Cu, Pb, Sr, and Zn) was analyzed in a series of batch and column experiments (Kurt and Wagner, 1991). The values of R_f measured from the batch tests are much bigger, 10 to 100 times bigger than estimated from the column tests.

The partition coefficients of several organic compounds obtained from batch tests and column tests were compared (Myrand et al., 1992). The partition coefficients of organic compounds derived from batch tests were one order greater than the values from column tests. However, according to another study (Wambold, 1993), the partition coefficients of organic compounds based on batch tests, column sectioning, and empirical equations had the same order.

The first reason of the higher partition coefficient estimation by batch tests than column tests was the parameters influencing the determination of the sorption capacity, e.g., contact time, pH, and chemistry of solution, clay/solution ratio, etc. In the case of organic compounds, the effect of pH on the sorption onto soil has mostly been ignored. As the pH increases, the humic materials in a soil system are elongated and the surface charge of the soil increases. Therefore, the sorption of organic compounds onto humic materials may decrease as pH increases. However, the effect of pH on the overall sorption of organic compounds onto soil materials is relatively small and negligible (Kan and Tompson, 1990).

The second reason was that sorbent particles are present in the batch solution as isolated particles and all the surfaces of the clay particles are accessible for the solutes. However, this is not the case for the column test, where the solute is following only specific migration paths and a very small part of the clay surface is in contact with the solute. The preparation of soil samples for the batch test can affect the results. Grinding or sieving may clean the surface of the soil particle which is covered with a wide variety of coatings in a natural system.

The dependence of the partition coefficient determined in batch tests on the soil/solution ratio was found (Voice et al., 1983; Barone et al., 1992). According to these studies, the observed K_p of organic compounds decreased with increasing the soil/solution ratio. Soluble organic compounds of soil particles may dissolve in the aqueous phase

during batch tests and increase the solubility of the solute in the aqueous phase. It was recommended to conduct batch tests under a low soil/solution ratio condition (Barone et al., 1992). However, in the case of the soil with a low solute uptake capacity, as the ratio decreases, it becomes more difficult to decrease the organic compound concentration significantly at the end of the sorption test.

Laboratory column tests were conducted by using a geological material obtained from an outwash aquifer and seven volatile organic compounds (VOCs) - 1,4-dioxane, tetrahydrofuran, diethyl ether, 1,2-dichloroethane, chloroform, 1,1-dichloroethylene, and benzene (Priddle and Jackson, 1991). The retardation factors of seven organic compounds estimated from column experiments were higher than the value calculated by the empirical correlation of Schwarzenbach and Westall (Eq. 2.31). These results were consistent with a latter study; the partition coefficients of organic compounds obtained from compacted clay column tests were one order larger than those derived from the organic content of soil (Myrand et al., 1992).

Field-measured values were compared with the value calculated from an empirical equation. Retardation factors calculated from the equation of Schwarzenbach and Westall were 35% - 85% lower than field-measured values (Curtis et al., 1986). It agreeds with the results from the Priddle and Jackson's study (1991). The empirical correlation of Schwarzenbach and Westall's results was based on organic compounds with much higher log K_{ow} (2.6 - 4.7) and sorbents with organic content greater than 0.1%. This underestimation was explained by the fact that empirical correlations did not account for sorption onto mineral surfaces (Myrand et al., 1992). Several studies showed that soil mineral fraction contributes to organic solute uptake, especially for soils with low organic matter (Karickhoff, 1984; Rebhun et al., 1992; Shimizu et al., 1992).

Priddle and Jackson (1991) compared the R_f values measured from the column tests and those estimated from the field tests. The measured R_f values compared with those

derived from contaminant plume lengths and are in reasonable agreement.

Although Priddle and Jackson (1991) showed the agreement of column test results to field condition, the estimated retardation factor by column tests may have very different values from the field or larger scale tests. This is related to differences in the scale of solute migration. In the field, much more heterogeneity exists in the porous media than in columns, and the less retained compounds would be more likely to migrate into low permeability zones, thereby increasing field retardation values. Once the retardation of more hydrophobic compounds, which have relatively high partition coefficients, is controlled by partitioning into sedimentary organic material, then the difference in retardation is relatively minor between laboratory column and field tests.

The pore water velocity may affect retardation measurement (Bahr, 1989). At higher velocities, sorption and desorption of hydrophobic compounds cannot proceed at a rate sufficient to reach local equilibrium. In the column test, the solute breakthrough curves of Cl^-, Ca^{+2}, and CH_3OH became more asymmetric with increasing pore water velocity or, shorter column residence time (Nkedi-Kizza et al., 1983).

Retardation factors have been found to vary with time and distance in the field. In a natural gradient experiment, a steady increase in retardation factors was found for a number of solutes over a two-year observation period (Roberts et al., 1986). The retardation factors increase by an amount ranging from 40% to 130% over the test period. The rate of increase is initially rapid, and then slow toward the end of the observation period. This can be attributed to a sorption rate limitation - slow uptake of the organic solutes.

2.3 MASS TRANSPORT THROUGH POLYMERS

Diffusion is the process by which a matter is transported from one part of a system to another as a result of random molecular motions. Fick recognized an obvious analogy

between heat transfer and mass transfer and put diffusion on a quantitative basis by adopting the mathematical equation of heat conduction derived by Fourier. The mathematical theory of diffusion in isotropic substances is based on the hypothesis, Fick's first law of diffusion, that the rate of transfer of the diffusing substance through a unit area of a section is proportional to the concentration gradient measured normal to the section.

The diffusion coefficient can be reasonably taken as constant while it depends very markedly on the concentration in some cases. The statement expressed mathematically by Eq. 2.28 is generally consistent only for an isotropic medium. It means that the structure and diffusion properties in the neighborhood of any point are relatively the same to all directions. Because of this symmetry, the flow of the diffusing substance at any point is along the normal to the surface of constant concentration through the point.

The fundamental differential equation of diffusion in an isotropic medium can be derived from Fick's first law of diffusion. Under isotropic conditions, all diffusion equations can be expressed in terms of the nomenclature of vector analysis as follows:

$$\frac{\partial C}{\partial t} = D \cdot \nabla^2 C \tag{2.36}$$

If diffusion is one-dimensional, Eq. 2.36 can be simplified to the following equation (Fick's second law of diffusion):

$$\frac{\partial C}{\partial t} = D \cdot \frac{\partial^2 C}{\partial x^2} \tag{2.37}$$

If the diffusion is radial, the diffusion equation will be as follows:

$$\frac{\partial C}{\partial t} = D \cdot \left(\frac{\partial^2 C}{\partial r^2} + \frac{2}{r} \frac{\partial C}{\partial r} \right) \tag{2.38}$$

where r = spherical coordinate [L].

When a piece of polymer is suspended in a limited volume of the solution which contains a solute and is stirred well, the diffusion coefficient of the solute through the polymer can be estimated by monitoring the concentration change of the solute in the solution over time. The ratio between the amount of the solute in the polymer at a certain time and the amount of the solute at equilibrium can be determined from the following equations (Carman and Haul, 1954; Crank, 1964):

Plain sheet polymer:

$$\frac{M_t}{M_\infty} = (1+\alpha)\cdot\left(1 - e\,\mathrm{erfc}\sqrt{\frac{T}{\alpha^2}}\right) \tag{2.39}$$

$$\alpha = \frac{L_s}{K\cdot L_{1/2}} \tag{2.40}$$

$$T = \frac{D\cdot t}{L_{1/2}^2} \tag{2.41}$$

$$e\,\mathrm{erfc}(x) = \exp(x^2)\cdot\mathrm{erfc}(x) \tag{2.42}$$

$$\mathrm{erfc}(x) = 1 - \mathrm{erf}(x) \tag{2.43}$$

where K = partition coefficient of the solute [dimensionless];

L_s = imaginary length of solution on each of the plain sheets [L];

$L_{1/2}$ = half thickness of the polymer sheet [L];

M_t = total amount of solute in polymer at time t [M];

M_∞ = total amount of solute in polymer after infinite time [M]; and

t = elapsed time [T].

Sphere polymer:

$$\frac{M_t}{M_\infty} = (1+\alpha)\cdot\left[1 - \frac{\gamma_1}{\gamma_1+\gamma_2}\,e\,\mathrm{erfc}\left(\frac{3\cdot\gamma_1}{\alpha}\sqrt{\frac{D\cdot t}{r_p^2}}\right) - \frac{\gamma_2}{\gamma_1+\gamma_2}\,e\,\mathrm{erfc}\left(\frac{3\cdot\gamma_2}{\alpha}\sqrt{\frac{D\cdot t}{r_p^2}}\right)\right]$$

$$+ \text{higher terms} \tag{2.44}$$

$$\alpha = \frac{3\cdot V}{4\cdot\pi\cdot r_p^3\cdot K} \tag{2.45}$$

$$\gamma_1 = \frac{1}{2}\{\sqrt{(1+\frac{4}{3}\alpha)} + 1\} \quad (2.46)$$

$$\gamma_1 - \gamma_2 = 1 \quad (2.47)$$

where r_p = radius of the sphere [L]; and

V = solution volume in which the sphere polymer is suspended [L^3].

Both cases:

$$C_t = (1 - \frac{M_t}{M_\infty})\cdot C_0 + \frac{M_t}{M_\infty} C_\infty \quad (2.48)$$

The higher terms in Eq 2.44 are extremely complex, but have no practical role (Carman and Haul, 1954). To develop the analytical solutions mentioned above, several assumptions were applied. The concentration of a solute in the solution is always uniform. The partition and diffusion coefficients are assumed to be constant. The polymer is assumed to be homogeneous and the diffusion coefficient is identical over the entire polymer. In the case of the plain shape polymer model, the diffusion of a solute from the surrounding solution into the polymer is assumed to happen only in two of the wider sides, not in four of the side faces. The imaginary distance in the case of the plain sheet polymer, L_s, can be calculated as follows:

$$L_s = \frac{V}{2\cdot S} \quad (2.49)$$

where S = area of the surface into which solute diffuses [L^2].

2.4 USED TIRES

2.4.1 Chemical Composition of Tires

Tires are principally composed of vulcanized rubber, rubberized fabric containing reinforcing textile cords, steel or fabric belts, and steel-wire-reinforced rubber beads. The

manufacturing of tires varies among the different manufacturers. However, the basic process is approximately the same. Dozens of different chemicals are used in preparing the rubber for use in tires.

Tires are produced by mixing natural or synthetic rubber and chemicals. Styrene-butadiene rubber (SBR) is the most important synthetic rubber used by the tire industry. This is the result of its good mechanical and physical properties coupled with its favorable cost. Other elastomers such as natural rubber (*cis* -polyisoprene), synthetic *cis*-polyisoprene, and *cis*-polybutadiene are also used in tires in varying amounts. SBR is made by copolymerizing 75% butadiene and 25% styrene.

Sulfur is the basic chemical agent in vulcanization. The vulcanizing agent reacts with the double bonds in adjacent polymer chains to cause cross-linking, which hardens the rubber and prevents excessive deformation at elevated temperatures. The accelerator is typically an organo-sulfur compound such as 2-mercaptobenzothiazole which acts as a catalyst for the vulcanization process. Zinc oxide and stearic acid also act to control the vulcanization process and in addition enhance the physical properties of the rubber. Carbon black is used to strengthen the rubber and aid abrasion resistance. The extender oil is a mixture of aromatic hydrocarbons which serves to soften the rubber and improve workability (Dodds et al., 1983). A typical composition of tire rubber is shown in Table 2.4.

2.4.2 Current Conditions of Used Tires

The disposal of used tires has become a growing problem. Stockpiles of scrap tires are located in many communities, resulting in public health, environmental, fire, and aesthetic problems. It has been known that tires serve as ideal breeding grounds for mosquitoes especially when tires are stockpiled in large numbers. Because of the shape and impermeability of tires, they may hold water for long periods of time and provide sites

for mosquito larvae development. It has also been known that tires are a fire hazard. Tire fires are particularly bad because of the difficulty in extinguishing them. The fact that 75% of a whole waste tire is void space makes it difficult to either extinguish the fire with water or cut off the oxygen supply. Soil contamination can happen by pyrolytic oil which is often produced by the water on tire fires. Toxic gases like polyaromatic hydrocarbons (PAHs), CO, SO_2, NO_2, HCl, etc. are emitted from tire fires (EPA, 1991).

Table 2.4 Typical composition of tire rubber.

Component	% Weight
SBR	62.1
Carbon black	31.0
Extender oil	1.9
Zinc oxide	1.9
Stearic acid	1.2
Sulfur	1.1
Accelerator	0.7

It is commonly accepted in the tire industry that about one tire per person per year is discarded. Based on the Rubber Manufacturers Association (RMA) records, about 16.3 million were recycled, 26 million were recovered for energy, about 12 million were exported, and the remaining 188 million were landfilled, stockpiled, or illegally dumped (EPA, 1991). The recycled or recovered rate of scrap tire in 1990 was only 17.4%. Two options to reduce the number of tires disposed are the extension of the tire life time and the improvement of the recycled or recovered rate. Even though the life time of tire is being extended, the production rate of tire is not decreasing because 2.2% of average annual growth in tire production is still expected during the 1993-1997 period (Reisch, 1993). Reclaiming rubber is not cost effective because basic raw rubber material is not expensive. Reclaimed raw material is two to three times more expensive than virgin material. Regrinding and reusing old tires in the production of highway asphalt is not economic,

either. The cost of transporting used tires to an incinerator may be more than the value of energy recovered when the tires are burned.

Concerns regarding disposal of waste tires were voiced at the federal level in the early 1960's. This led to the enactment of the Federal Solid Waste Disposal Act in 1965, which includes legislation on scrap tires, and encouraged studies such as that conducted by the Federal Bureau of Solid Waste Management in 1968. At the state level, many state governments have adopted laws to regulate the hauling, storing, and disposing of scrap tires. Table 2.5 summarizes the current storage/processing/hauling regulations and landfill restrictions (Eldin and Piekarski, 1993).

2.4.3 Applications of Used Tires in Construction

Interest in the roadway applications of scrap tires has grown. Roadway crash barriers, roadway sub-grade supporters, road pavements, slope erosion control, waste disposal facility construction material, etc. have been suggested.

The construction of a roadway across soft wetland soil deposits usually presents stability problems. One method of dealing with this problem is to substitute a lightweight fill material for the heavy fill soil materials (Edil and Bosscher, 1992). Conventional lightweight fill consists of woodchips or sawdust. Shredded waste tires were suggested as an alternative to the biodegradable woodchips.

The energy absorbing properties and durability of tires can be utilized in the construction of roadway crash barriers. The use of scrap tires as crash barriers was studied in the late 1970s by the Texas Transportation Institute. Stacked whole waste tires bound by a steel cable and enclosed with fiberglass would reduce or absorb the impact of automobiles traveling up to 114 km per hour. However, this application has not been used widely because it is more difficult to erect and dismantle and has less impact absorbing capacity than the sandfilled crash barrier (EPA, 1991).

Table 2.5 Summary of tire disposal regulations and landfill restrictions (Eldin and Piekarski, 1993).

State	Regulations Controlling			Landfill Restrictions
	Store	Processes	Haul	
Arizona	X	-	-	bans whole tire
California	X	X	-	-
Colorado	X	X	-	-
Connecticut	X	-	-	-
Florida	X	X	X	must be cut
Illinois	X	X	X	-
Indiana	X	-	-	-
Iowa	-	-	-	bans whole tire
Kansas	X	X	X	must be cut
Kentucky	X	-	-	must be cut
Louisiana	X	-	-	must be cut
Maine	X	X	X	-
Maryland	X	X	X	-
Michigan	X	X	X	-
Missouri	X	-	X	bans whole tire
Minnesota	X	X	X	bans whole tire
Nebraska	-	-	-	-
New Hampshire	X	-	-	-
North Carolina	X	X	X	must be cut
Ohio	-	-	-	must be cut
Oklahoma	X	X	X	must be cut
Oregon	X	X	X	must be cut
Pennsylvania	X	-	-	-
Rhode Island	X	X	-	-
South Dakota	X	X	-	must be cut
Tennessee	-	-	-	bans whole tire
Texas	X	-	-	bans whole tire
Utah	-	-	-	-
Virginia	-	-	-	-
Vermont	-	-	-	must be cut
Washington	X	X	X	-
Wisconsin	X	X	X	must be cut

Crumb rubber originated from waste tires can be combined with asphalt for use as a paving material. Crumb rubber is made by either mechanical or cryogenic size reduction of tires. Typically tires are shredded to reduce them to 1.9 cm chips. Then all steel and polyester fragments are removed by magnetic separators and fiber separators. A series of screening and grinding operations achieves the desired crumb size. Durability and flexibility can be increased by crumb rubber addition compared to conventional asphalt pavements. The recyclability of this material is one of the concerns. Heating for reclamation may catch fire or produce toxic smoke (EPA, 1991).

The California Office of Transportation Research has designed and tested several erosion control applications of waste tires. Tires were banded together and partially or completely buried on unstable slopes. Construction costs were reduced from 50 to 75 % of the lowest cost alternatives such as rock, gabion, or concrete protection. This application was reported not to be appropriate for all sites (EPA, 1991).

A recent study by the Cold Regions Research and Engineering Laboratory (CRREL) in Hanover, ME., showed another application of used tires to road construction (ASCE, 1994). The potential as an insulating layer beneath a gravel-surfaced road in cold regions was evaluated. The tire layer can minimize penetration of freezing temperatures into the underlying frost-susceptible soils because tire rubber has a significantly lower thermal conductivity than soil. Frost penetrates deep into the layers of soil beneath unpaved roadbeds, causing uneven surface frost heaving. During the spring, the water, having no place to go except upward to the road surface, causes the road to become muddy. The demonstration project was conducted on 180 m of a gravel road in ME. The tire chip layer was proven effective. The project will continue to be monitored for three to five years to validate engineering specifications and thickness design.

Research for the use of scrap tires as a drainage media in the leachate collection system of solid waste landfill has been conducted. When the simulated waste thickness

and the hydraulic gradient were 10.7 m and 0.41, respectively, the measured hydraulic conductivity of 3.8 cm tire chips was 1.88 cm/sec (Hall, 1991). The simulated waste thickness was obtained from 740 kg/m^3 (1,250 lb/yd^3) of inplace density of waste. The compression of shredded tire material did not appear to significantly reduce its hydraulic conductivity. The average hydraulic conductivity under no confining pressure was 2.23 cm/sec. Two different sizes of tire chips, 1.9 and 3.8 cm were tested to evaluate the size effect on the hydraulic conductivity. The difference was only 7% and the size of the tire chips did not appear to significantly affect the hydraulic conductivity.

The hydraulic conductivity of waste tire chips and their mixtures with sand under different hydraulic gradients and vertical overburden pressures were tested. Tire chips 3.8 $\times$ 7.6 cm in size have high hydraulic conductivity when unconfined (> 1.0 cm/sec). Under 138 kN/m^3 (20 psi) of overburden pressure, which is equivalent to about 18 m of waste based on the same inplace density of waste with Hall's study, the hydraulic conductivity of tire chips was on the order of 10^{-1} cm/sec (Edil et al., 1992).

One geotextile-wrapped layer of shredded tire was installed in Lowry Landfill Superfund site. The collection system was constructed for seepage collection and surface runoff conveyance. The tire chips 3.8 $\times$ 7.6 cm in size were applied. The hydraulic conductivity values ranged between 45.7 and 79.2 cm/sec. Construction benefits of the shredded tires included light unit weight ranging between 3.9 and 5.7 kN/m^3, and excellent placement and spreading characteristics. No tears or punctures from exposed steel radials were observed in the enveloping geotextile. Overall, a cost savings of 42% for the drainage material was realized by utilizing shredded tires rather than the Class 3 aggregate (Glade et al., 1993).

According to previous studies, as the overburden pressure increases, tire chips were significantly compressed and the hydraulic conductivity decreases. For example, 30% of compression under 10.7 m simulated waste height (Hall, 1991) and 40% under

690 kN/m^2 were observed (Edil et al., 1992). However, the hydraulic conductivity of tire chips meets the minimum requirement of 10^{-3} cm/sec for most leachate collection system design situations under high overburden pressure. In the case of the shredded tire application of the Lowry Landfill, the on-site availability of waste tires could reduce the construction cost significantly. Other various applications of scrap tires to landfills are being considered, for example, the liner protective cover (Waste Management of Pennsylvania, 1990).

2.4.4 Environmental Applications of Used Tires

At the Camden City Sewage Sludge Co-composting Facility, a pilot scale and full scale study were conducted using shredded tires as a bulking agent (Higgins et al., 1980). The tire chips containing fiber and steel, produced by hammer mill crushing and maceration, were used for both the pilot and full scale study. The estimated size of the tire chips was 3-5 cm in width, 5-8 cm in length, and 1-1.2 cm in thickness. The major advantages of using shredded tires over the most conventional bulking agent, wood chips were 1) high, more than 99%, of bulking agent recoverability, 2) lower cost of composting due to lower cost of shredded tires than wood chips, and 3) waste tire reuse. Shredded tires were used as an alternative bulking agent to wood chips in a full scale composting program without adverse effects or significant degrading of the quality of the finished compost material.

There have been many investigations of the use of tire rubber in metal removal processes. Mercury removal was the most frequently studied. Tharin (1974) showed that vulcanized rubber removed mercury in almost any physical or chemical form over a wide range of concentration, temperature and pH values. Griffith (1975) developed cation and anion exchange resins for mercury removal using tire rubber as an exchange base. Comparison of ion exchange capacities showed that the waste rubber material was

competitive with certain ion resins, especially at lower mercury concentration. Netzer and Winkinson (1974) observed the sorption of a range of 12 metals by vulcanized rubber. Knocke and Hempell (1981) have investigated the mechanism of the mercury(II) adsorption by scrap rubber. Rowley et al. (1984) conducted the test of cadmium(II), mercury(II), and lead(II) uptake by shredded rubber.

There has been much evidence which showed the metal sorption ability of tire material. However, the mechanism of metal uptake is not clear yet. There were several different suggestions about the mechanism of the metal uptake phenomenon. The reaction between mercury and cross-linked sulfur which is present in the tire rubber was speculated to be the mechanism of the mercury removal from a solution (Tharin, 1974). Griffith (1975) had the similar opinion that the mechanism of mercury removal was related to the disulfide bonds in vulcanized rubber. In contrast, the adsorption by carbon black was considered the principal mechanism of metal uptake and the interaction with sulfur residues or other constituents of vulcanizates was of secondary importance (Netzer and Winkinson, 1974). Also, it was suggested that sulfur is not essential to the mercury sorption process and a reaction between mercury. Sulfur was not the only viable factor in the rubber sorption process and the carbon black may well provide the main site of interaction (Knocke and Hempell, 1981). The mechanism of metal uptake by tire rubber was explained depending on the metal being sorbed because mercury and cadmium uptake were accompanied by displacement of zinc and therefore involved an ion exchange reaction. Lead adsorption involved no zinc displacement and is not competitive with cadmium or mercury uptake (Rowley et al., 1984).

There was another application of tire rubber to inorganic compounds sorption (Scheels, 1993). A pilot test was performed to evaluate the potential use of ground tires for the removal of odorous, particularly hydrogen sulfide, gas emitted from a gravity belt thickener dewatering of anaerobic digester sludge. According to the comparison between

glass bead and tire rubber, it was revealed that the hydrogen sulfide removal was promoted by tire rubber. The carbon existing in tire rubber was suspected to play an important role in the study.

Shredded rubber tires may be good for absorbing oil and clean-up of oil spills (Beckman et al., 1974). The tire materials revealed to possess good capacity for absorbing the oil and can be collected easily for final disposal. After absorbing the oil, it can be used for road construction as an asphalt material by heating.

Recent investigations have found that organic chemicals may contaminate drinking water by permeating buried plastic pipes and gasket materials. Park et al. (1991a) conducted the organic compound permeation test by using several different types of plastic pipe and gasket materials used for potable water distribution systems. They tested seven organic compounds. They found that organic compounds permeated through SBR gaskets and SBR had a high organic compound sorption capacity. As mentioned above, SBR is one of the most widely used rubber in tire industry. The estimated partition and diffusion coefficients are listed in Table 2.6.

Table 2.6 Summary of permeation parameters for SBR and seven organic compounds.

Organic compounds	K_v [1]	K_w [2]	D [3] ($\times 10^{-8}$ cm^2/sec)
Methyl ethyl ketone	310	2	2.1
1,2-Dichlorobezene	28,000	473	1.2
n -Hexane	220	8,074	1.0
Tetrachloroethylene	3,300	3,927	1.2
Toluene	2,100	517	1.7
1,1,1-Trichloroethane	330	56	1.7
o -Xylene	12,000	2,628	0.9

1: Vapor-polymer partition coefficient.

2: Aqueous-polymer partition coefficient (estimated by using Henry's law constants).

3. Vapor diffusion coefficient through polymer.

Relationships between the octanol-water partition coefficient and partition coefficient and between the molecular diameter and diffusion coefficient were found. As the octanol-water partition coefficient of the organic compound increased, the partition coefficient of the compound increased. Also, the diffusion coefficient decreased with the increased molecular diameter.

Waste tires seem to have a good potential to sorb organic compounds in the surrounding solution. The mechanism of organic removal by tire material is not clear yet, nor understood. Compared to metal removals, the interaction with sulfur or ion exchange do not seem to be important. The partitioning and diffusion of organic compounds through tire rubber is considered the principal mechanism.

2.5 THE IMPACTS OF TIRE APPLICATION ON ENVIRONMENT

Several studies were conducted to evaluate the impact of tire applications on the surrounding environment. The studies included the physical compatibility of tires, the chemical characterization of leachate from tires, and biological impact.

2.5.1 Physical Compatibility

A visual compatibility test was performed to evaluate the application of shredded tires on the drainage material (Glade et al., 1993). The shredded tires were immersed in site seepage water for a period of five months. No visual evidence of a color change and surface disintegration was observed in the shredded tires. The shredded tires were chemically compatible with the seepage constituent of the site. Like most geosynthetics, the tires are composed of high molecular weight polymers which are inert to the dilute organic compounds detected in waste disposal sites.

Natural rubber and SBR, a synthetic rubber, are the major components of tires.

The physical properties are listed in Table 2.7 (Hall et al., 1972). Tire materials have high tensile strength and a wide range of service temperature. Thus, tires would not deteriorate easily under the pressure and temperature which are typical in waste disposal sites.

Table 2.7 Physical properties of natural rubber and SBR.

	Natural rubber	SBR
Durometer hardness range	20 - 100	40 - 100
Tensile strength at room temperature, kN/m^2	6,900 - 27,600	6,900 - 24,100
Elongation at room temperature, %	100 - 700	100 - 700
Temperature range of service, ^oC	-55 - 80	-55 - 110
Weather resistance	Fair	Fair

2.5.2 Chemical Characterization of Leachate from Tire Materials

The Jaca Corporation (1988) conducted leaching tests with rain water using the standard Extraction Procedure (EP) method. The study revealed that no appreciable concentrations of toxic metals, cyanide, phenol, or organics were leached. Of the 72 parameters tested, only three of them were detectable and within Safe Drinking Water Act limits. Other studies also revealed agreeable results (Rubber Manufacturers Association, 1989; Waste Management of Pennsylvania, 1990).

The potential for the tire chips to release contaminants when they are exposed to leachate was assessed by J & L Testing Company Inc., Canonsburg, PA (Waste Management of Pennsylvania, 1990). Leachate column tests were performed using leachate from a landfill over a 90-day period. Cyanides, sulfides, arsenic, barium, cadmium, chromium, lead, mercury, selenium, silver, and pH were monitored. According to this test, no appreciable changes in concentrations occurred during the test period.

When shredded tires were exposed to extreme pH's, significant leaching was observed by Twin City Testing Corporation, St. Paul, MN (Minnesota Pollution Control

Agency, 1990). Laboratory leaching tests and water and soil analysis from scrap tire sub-grade road bed sites and tire stockpile sites were conducted. Acidic conditions favored metal leaching, while basic conditions favored the leaching of PAHs (Polynuclear Aromatic Hydrocarbons) and TPHs (Total Petroleum Hydrocarbons). Barium, cadmium, chromium, lead, selenium, and zinc were released under acidic conditions. The worst-case conditions in which the highest concentrations of metals and organics were found were pH 3.5 and 8.0, respectively. Drinking Water Recommended Allowable Limits (RAL) may be exceeded under "worst-case" conditions for certain parameters.

Extensive testing of tires using EPA's TCLP (Toxicity Characteristics Leaching Procedure) protocol tests were conducted (House of Representatives, 1990). Differently processed scrap tires were also compared and 34 organics and 8 metals were tested. Very small quantities of heavy metals were leached from scrap tires. Arsenic, barium, chromium, and lead were detected. In a few cases, some organic compounds, including carbon disulfide, methyl ethyl ketone, 1,1,1-trichloroethane, toluene, and phenol were detected. The leaching contaminants from scrap tires significantly varied quantitatively and qualitatively between scrap processings. For example, arsenic was detected only in the uncured passenger automobile tires. Barium was detected consistently in all differently processed scrap tires. Ground cured light truck tires did not leach phenol.

EP toxicity and American Foundry Society (AFS) leaching tests were performed on tire chip samples by the Wisconsin State Laboratory of Hygiene (Edil and Bosscher, 1992). The shredded tires appeared to release no base-neutral regulated organics. The tire samples showed detectable but very low leaching patterns for all substances tested and a declining concentration with continued leaching for most substances. Four metallic elements, barium, iron, manganese, and zinc exhibited increasing concentrations with continued leaching. The highest concentrations for iron and manganese were at or above their applicable drinking water standards, while those of barium and zinc were below their

standards.

According to previous studies, the leaching solution from tires contains some components which were added during the tire manufacturing process. Also, the leaching components will not reach the level which can cause serious environmental impact.

2.5.3 Bioassay Tests

Laboratory studies were conducted to determine whether automobile tire leaching contaminants are toxic to aquatic organisms. In the study by Stone et al. (1975), fish were exposed to tires in 2,000 L glass aquaria for periods lasting 21 days or longer. The test fish were pinfish (*Lagodon rhomboides*) and black sea bass (*Centropristis striata*). The tests were conducted under flow through conditions which involved the condition of fresh salt water at the rate of 15 L/min (about 11 tank volumes per day). Under these conditions, they did not observe any adverse effects of tires on the survival of pinfish and black sea bass.

Kellough (1991) exposed whole tires and cut tires in tanks containing a fixed volume of water (300 L) for periods of 30 to 60 days. Testing of the overlying water caused the complete mortality of rainbow trout, but had no effect on *Daphnia magna.* No detectable levels of organochlorine pesticides were found in the overlying water.

Three different types of tires, including used tires removed from an existing floating tire breakwater, scrap tires, and new tires, were tested (Park, 1992). Rainbow trout, fathead minnows, and *Daphnia magna* were tested. The tires from the breakwater were exposed to lake water for approximately 10 years. Tires were individually exposed in glass aquaria containing 300 L of clean water for periods of a maximum of 40 days. Contaminants released from both used and new tires within about five days were found only to be toxic to rainbow trout. However, leachates generated from breakwater tires were not acutely lethal to any species tested.

On the other hand, Goude and Barton (1992) exposed whole tire pieces under static renewal conditions which involved daily replacement of the overlying water. Under these conditions, tires were shown to release materials which were acutely toxic to rainbow trout, *Daphnia magna, Ceriodaphnia* and bioluminescent bacteria. The acutely toxic concentration was reached within 24 hours. The chemical characterization of the overlying water was not conducted.

The specific contaminants contributing to toxicity have not been identified. However, there were some suggestions about the nature of toxicity (Park, 1992). Leachate toxicity is not related to the presence of volatile materials and is water soluble because toxicity remained relatively stable over time even after removal of the test tires from the aquaria. Leachate toxicity is not related to heavy metals because no increase in the levels of heavy metals was observed. The toxic contaminants are quickly released and stop leaching.

A general vegetation survey of two scrap tire sub-grade road bed sites was conducted by Minnesota Control Protection Agency (1990). The vegetation survey indicated no observable difference in vegetation composition at tire applied sites and background sites.

The toxicity can be easily removed before it may affect the surrounding environment since the toxicity leaching will be finished in a relatively short time and the leachate will be pumped out from waste disposal sites periodically through the leachate pumping system. Reasons for the conflicting results of several bioassay tests reported may be related to the conditions under which tires were exposed, e.g., the duration of tire exposure, the ratio of tire to water, or sensitivity differences of the laboratory culture stocks.

CHAPTER 3
EXPERIMENTAL MATERIALS AND METHODS

3.1 MATERIALS

3.1.1 Tires

The Firestone-Bureau of Mines Destructive Distillation process turns scrap rubber into char, oil, and hydrogen gas. The composition of scrap tire (by weight) was obtained from the destructive distillation process. The results are listed in Table 3.1 (Hudson and Lake, 1977).

Table 3.1 Components of scrap tire.

Component	Content (% by wt.)
Carbon	83.2
Hydrogen	7.1
Oxygen	2.5
Sulfur	1.2
Nitrogen	0.3
Ash	5.7

In this study, two types of tire were used: non-processed chips, which contained textile and steel materials, and ground tire granules, which do not contain as much textile and steel material as the non-processed chips. Ground tire granules were obtained from Tire Technology, Inc., Rockton, IL. No attempt was made to separate the tires based on different manufacturers or sizes. The particle size of the ground tire was estimated by sieving.

The density of the tire chip was measured in the laboratory based on the soil

analysis technique. The density of raw used tire which contains textile and steel was estimated to be 1.22 g/cm^3. The ground tire which do not have significant amount of textile and steel has a density of 1.15 g/cm^3 (Edil et al., 1992). This value is consistent with the density of SBR, 1.13 g/cm^3 (Park et al., 1991a). The surface of ground tire was measured by a Surface Area Analyzer (Micromertics Co., ACCQUSORB 2100B) and the value ranged from 0.16 to 0.56 m^2/g. The pore size of ground tire was measured by a porosity meter. The pore diameter ranged from 0.003 to 3.0 μm and the average was 0.0385 μm.

3.1.2 Clay

The soil used in this study is Kirby Lake Till, obtained from the Outagamie County Landfill, Appleton, Wisconsin. The organic carbon content of the liner clay is an important factor for the attenuation of VOCs (Park et al., 1991). The organic matter content of Kirby Lake Till was tested by the Soil & Plant Analysis Lab., Madison, Wisconsin to be 1.8 % (by weight). The specific gravity was 2.7. The physical characteristics of the clay are listed in Table 3.2 (Heim, 1992).

Table 3.2 Characteristics of Kirby Lake Till.

Geologic origin	Fines content (%)	Clay content (%)	Liquid limit (%)	Plastic limit (%)	Exchangeable cations[1] (mg/kg)	Organic carbon content (%)
Glacial	83	47	33	16	494	0.91

1: Exchangeable cations include Ca^{+2}, Mg^{+2}, K^+, and Na^+.

Compaction and grain size distribution for Kirby Lake Till were characterized by Heim (1992). The maximum dry density and optimum moisture content were found to be about 17.76 kN/m^3 (113 lb/ft^3), 15.5%, respectively. The compaction procedures followed ASTM D-698. Sieve and hydrometer analyses were performed to determine the

grain size distribution of Kirby Lake Till. The sieve and hydrometer tests were performed in accordance with ASTM D-422. D_{30} and D_{60} were approximately 0.002 and 0.011 mm, respectively.

3.1.3 Organic Chemicals

Chloroform(CF), ethylbenzene(EB), methylene chloride(MC), toluene(TOL), 1,1,1-trichloroethane(1,1,1-TCA), trichloroethylene(TCE), and *m*-xylene(m-XYL) were selected for testing. These organic chemicals are the most frequently detected compounds at the waste disposal sites (Plumb et al., 1985). The physical/chemical properties of these organic compounds are summarized in Table 3.3. These organic compounds were selected based on the availability of analysis and reasonable ranges of solubility and molecular weight. The properties of the selected organic compounds were listed in Table 3.3 (Verschueren, 1983).

If the molecules of organic compounds were assumed to occupy a cubic, the molecular diameters of the organic compounds were calculated by using the molecular weights of compounds and Avogadro's number (Frendsdorff, 1964). The molecular diameters listed in Table 3.3 are calculated values. The calculation can be expressed as follows:

$$d_s = (V_m / N_{Avo})^{1/3}$$
$$= [MW / (\rho_s \times 6.02 \times 10^{23})]^{1/3} \times 10^7 \qquad (3.1)$$

where d_s = molecular diameter (nm);

V_m = molar volume (nm^3/mol);

N_{Avo} = Avogadro's number (= 6.02×10^{23}/mol);

MW = molecular weight (g/mol); and

ρ_s = density of organic compound (g/cm^3).

The free solution diffusion coefficients of most organic compounds are available (Bonoli and Witherspoon, 1968; Acar and Haider, 1990; Barone et al., 1992). The free solution diffusion coefficients of organic compounds can also be estimated by the following empirical equation (Wilke and Chang, 1955):

$$D_{o,1} = D_{o,2} \cdot \frac{(MW_2/\rho_2)}{(MW_1/\rho_1)} \qquad (3.2)$$

where $D_{o,1}$, $D_{o,2}$ = free diffusion coefficient of organic compounds 1 and 2 (cm^2/sec);

MW_1, MW_2 = molecular weight of organic compounds 1 and 2 (g/mol); and

ρ_1, ρ_2 = density of organic compounds 1 and 2 at their boiling points (g/cm^3).

The density of organic compounds at various temperatures are available in the literature. Also, densities at a standard temperature generally provide relative diffusion coefficients within ± 10 % of experimental values (Myrand et al., 1992).

Table 3.3 Properties of organic compounds tested.

Chemicals	Molecular weight (g/mol)	Specific gravity	Solubility (mg/L)	log K_{ow}[1]	Molecular diameter (nm)	D_o ($\times 10^{-6}$) (cm^2/sec)
MOH	32.04	0.792[2]	∞	-0.82/-0.66	0.407	14.65[4]
CF	119.38	1.489	8,000	1.97	0.511	11.10[6]
EB	106.17	0.867	152	3.15	0.588	7.54[4]
MC	84.93	1.327[2]	20,000	1.25[2]	0.474	11.12[4]
TOL	92.10	0.867	515	2.69	0.561	8.50[5]
TCA	133.41	1.350	4,400	2.47[2]	0.548	8.53[4]
TCE	131.50	1.460	1,100[3]	2.53[2]	0.531	9.89[4]
m-XYL	106.16	0.864	200[2]	3.20	0.589	7.25[6]

MOH: methanol (CH_3OH), CF: chloroform ($CHCl_3$), EB: ethylbenzene ($C_6H_5C_2H_5$), MC: methylene chloride (CH_2Cl_2), TOL: toluene ($C_6H_5CH_3$), TCA: 1,1,1-trichloroethane (CCl_3CH_3), TCE: trichloroethylene (CCl_2=CHCl), and *m*-XYL: *m*-xylene ($C_6H_4(CH)_2$)

1 : Octanol-water partition coefficient.

2 : Dostal (1990).
3 : At 25 °C.
4 : Acar and Haider (1990).
5 : Bonoli and Witherspoon (1968).
6 : Average of the values estimated by using the other compounds data and Wilke and Chang's equation.

3.1.4 Tracer

In a hydrogeological point of view, a tracer is matter or energy carried by groundwater which will give information concerning the direction of movement and/or velocity of the water and potential contaminants which might be transported by the water. An ideal ground-water tracer is non-toxic, is inexpensive, moves with the water, is easy to detect in trace amounts, does not alter the natural direction of the flow of the water, is chemically stable for a desired length of time, is not present in large amounts in the water being studied, and is neither filtered nor sorbed by the soil medium through which the water moves (Davis et al., 1980).

Tracers can be classified to several types, including water temperature, solid particles (yeast, bacteria, spores, etc.), ions, organic acids, dyes, and radioactive tracers. Among them, ions such as chloride (Cl^-), bromide (Br^-), lithium (Li^+), ammonium (NH_4^+), magnesium (Mg^{2+}), potassium (K^+), iodide (I^-), sulfate (SO_4^{2-}), organic anions, etc. have been used extensively. Table 3.4 shows the characteristics of the ionic tracers widely used (Davis et al., 1985).

In this study, the synthetic leachate was made of tap water. Tap water contains several different kinds of ionic materials and their background concentrations are relatively high. Thus, bromide was selected as the tracer because in addition to the advantages mentioned in Table 3.4, it can be easily analyzed by HPLC (High Performance Liquid Chromatograph) and anion tracers are known to be less affected by clay minerals (Davis et al., 1985). Bromide was injected as the LiBr salt.

Table 3.4 Characteristics of ionic tracers.

Tracer	Advantages	Disadvantages
Cl^-	Sharp elusion curve	High background concentration The danger of altering the hydraulic conductivity of clay by ion exchange Density effects (e.g., NaCl)
Br^-	The most commonly used ionic tracer Low background concentration Biologically stable Resistent to precipitation, adsorption, or absorption	
Li^+	Low background concentration	Some loss by ion exchange
NH_4^+		High loss by ion exchange Relatively difficult analysis
Mg^{2+}	Relatively simple analysis	High loss by ion exchange and sorption
K^+	Low background concentration Relatively simple analysis	Some loss by ion exchange and sorption
I^-	Very low background concentration	High loss by sorption Can be affected microbiologically

3.1.5 Disinfectants

In this study, any reaction caused by biological activity was not considered. Thus, the biological activity which can occur during batch isotherm tests and long-term tank and column tests was prevented by the addition of disinfectants. For the purpose of this study, organic pesticides could not be applied.

Sodium azide, NaN_3, and mercuric chloride, $HgCl_2$, were used in some previous studies. Gillham and O'Hannesin (1990) conducted several batch tests to investigate the sorption of aromatic hydrocarbons by monitoring construction materials well. The dosage of sodium azide they used was 0.05% by weight. *Standard Methods* recommended

adding 40 mg-$HgCl_2$/L to the sample when samples are to be stored before analysis. Myrand et al. (1992) used both of the disinfectants in a column study.

Sodium azide was used for the batch tests and both of them, solium azide and mercuric chloride, were added to the long-term tank tests. In the long-term tank tests, the effluent contained high concentrations of nitrate or nitrite. Nitrate and nitrite interfere with the detection of the tracer, bromide ion. The nitrogen in sodium azide is considered as the source of these oxidized nitrogens. Thus, in the column tests, only mercuric chloride is added.

3.2 BATCH ISOTHERM TESTS

3.2.1 Procedure

The batch sorption tests were conducted to estimate the partition and diffusion coefficients of the organic chemicals in sorbents. The batch isotherm test consists of submerging a fixed amount of sorbent into a reactor containing organic compounds and monitoring the concentrations of organic compounds. The concentrations of organic compounds were monitored to estimate the diffusion coefficient and the required time to reach the equilibrium condition. The monitored concentration change was compared with the analytical solution of the mathematical model to estimate the diffusion coefficient. To estimate the partition coefficients, the equilibrium concentrations of organic compounds were measured.

In order to monitor the changes in concentration, the 350 mL-glass reactor was used in the batch isotherm tests (Figure 3.1). Each column is 15.24 cm (6 in.) long and 5.08 cm (2 in.) in diameter with a sampling port and Teflon® plugs.

Two types of screw-capped glass tubes with a Teflon®-coated septum, about 43 or 25 mL were also used for the batch isotherm tests with rotation. The glass tubes were used

to measure the equilibrium concentration. For example, the required time for the ground tire and the tire chip were 2 and 6 days, respectively. Reactors and tubes were tumbled end-over-end by the Millipore® Rotary Agitator (Millipore Co.) during the experiments.

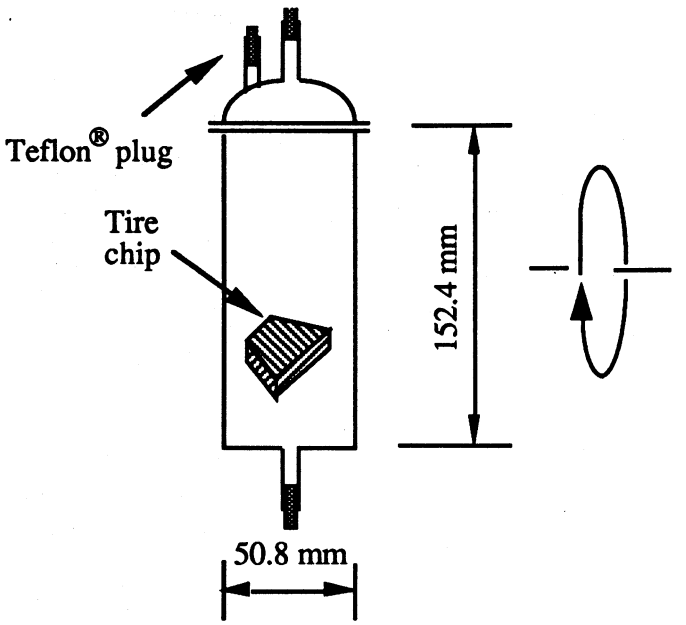

Figure 3.1 Diagram of the reactor used in batch isotherm tests.

To prevent bacterial growth, sodium azide was added during each test at a concentration of 0.05% (by wt.). An aliquot of 1% sodium azide stock solution was made to be diluted further.

Soil and ground tires were sieved to collect similar size samples and to remove gravel or dust, then air dried, and stored in a desiccator at room temperature before conducting the tests. The average size of a sorbent was estimated by taking the geometric mean of the opening of the sieves. Tire chips were used after distilled water-washing and air drying.

The organic compounds tested vaporizes easily. Thus, the head space within the test tube was kept as small as possible. For the concentration correction in the glass reactor tests, the control reactor filled with only the solution was also run with the sample reactors.

The control tubes, which contained no sorbent, were used one for every four sample tubes. For tube tests, the initial concentrations of organic compounds in the liquid phase were re-calculated proportionally based on the concentrations of the control tubes.

For soil batch isotherm tests, the soil was pretreated before the tests. The weighed dry soil was put in test tubes with distilled water to be saturated. After one day, the test tubes containing soil and water were filled with the compound containing solution. This method may reduce the air which may be attached to dried soil. For better accuracy, the volume of the solution added to the test tubes was measured by weighing the tubes. The target compound concentration in the solution cannot be kept constant while filling the test tubes. The blank tubes, which have no solid, were located between filling tubes to adjust the exact concentration in the solution when the solution was added to the test tubes.

3.2.2 Experimental Design

Landfill leachate is composed of the liquid produced from the decomposition of the wastes, the liquid which is originally contained in the wastes, the surface water and the groundwater flowing into the site. The composition of landfill leachate is site specific and is also changing according to the time passed. Tables 3.5 and 3.6 are the summary of the inorganic ions and pH in leachate observed by several researchers (Pohland, 1980; Ehrig, 1983; Lee et al., 1991).

The four variables, the presence of inorganic ions in solution, pH of solution, surrounding temperature, and the size of ground tire, were selected as the major factors affecting the sorption of VOCs into the tire material in the multi-component system. The effect of each factor was tested by conducting multicomponent batch sorption tests. The experimental design of the tests are listed in Table 3.7.

Table 3.5 Concentration ranges for inorganic components of municipal landfill leachate.

inorganic ions	Ehrig[1]	Lee and Jones	Pohland[2]
Arsenic	0.126	NA	NA[3]
Cadmium	0.0052	0.001 - 0.1	< 0.2
Calcium	80 - 1,300	100 - 3,000	260 - 2,850
Chloride	2,119	100 - 2,000	178 - 862
Chromium	0.275	0.05 - 1	< 0.4
Cobalt	0.05	NA	NA
Copper	0.065	0.02 - 1	NA
Iron	15 - 925	10 - 1,000	39 - 900
Lead	0.087	0.1 - 1	NA
Magnesium	250 - 650	30 - 500	76 - 264
Manganese	0.65 - 24	NA	1.6 - 73.7
Nickel	0.166	0.1 - 1	NA
Potassium	1,085	NA	311 - 1,070
Sodium	1,343	200 - 1,500	515 - 1,175
Strontium	0.94 - 7.2	NA	NA
Sulfate	884 - 1,745	10 - 1,000	< 750
Zinc	0.64 - 5.6	0.5 - 30	0.1 - 2.65

1: Some data are the average values of methanogenic phase and acid phase.

2: Original data were classified into "initial", "intermediate", and "final" phases.

3: Not Available

Table 3.6 pH ranges of municipal landfill leachate.

Sources	Phases	pH
Ehrig	Acid phase	6.1
	Methanogenic phase	8.0
Lee and Jones		5.0 - 7.5
Pohland	Initial	5.3
	Intermediate	6.1
	Final	6.7

Table 3.7 Experimental design for batch isotherm tests.

	Inorganic ions	pH	Particle size (sieve opening) (mm)	Temperature (°C)
Control	-[1]	7	2.00 < d < 2.38	20
1	+[2]	7	2.00 < d < 2.38	20
2	-	2	2.00 < d < 2.38	20
3	-	9	2.00 < d < 2.38	20
4	-	11	2.00 < d < 2.38	20
5	-	7	2.38 < d < 2.83	20
6	-	7	1.41 < d < 2.00	20
7	-	7	2.00 < d < 2.38	4
8	-	7	2.00 < d < 2.38	55

1: The medium solution was made with distilled water.

2: The medium solution contained Na^+ (350 mg/L), Mg^{2+} (350 mg/L), Ca^{2+} (500 mg/L), Cl^- (1,424 mg/L), and SO_4^{2-} (1,383 mg/L). The ionic strength of this soluton was 68.7 mM.

3.3 LONG-TERM TANK TESTS

3.3.1 Procedure

Four tank experiments, using clay liner specimens 610 mm in diameter and 914 mm high are under way to determine long-term behavior of the mass transport through a clay layer and retardation by shredded tires. These four experiments were supplemented by three tank tests performed by Heim (1992) and Wambold (1993).

The influent and the effluent were supplied and collected by means of reservoirs. This means of collection permits the water to flow evenly across the entire soil layer. The driving head was around 900 mm because the design hydraulic gradient was 3. A sketch of the tank is shown in Figure 3.2. These tests were performed in a constant temperature

room (20°C).

Tap water was used as the permeant liquid for the long-term tank tests. In the hydraulic conductivity tests, the type of permeant water should be specified and it shall be reported with the hydraulic conductivity results because the observed hydraulic conductivity can be affected by the species of permeant liquids. ASTM D-5084 recommended tap water if no specification is made.

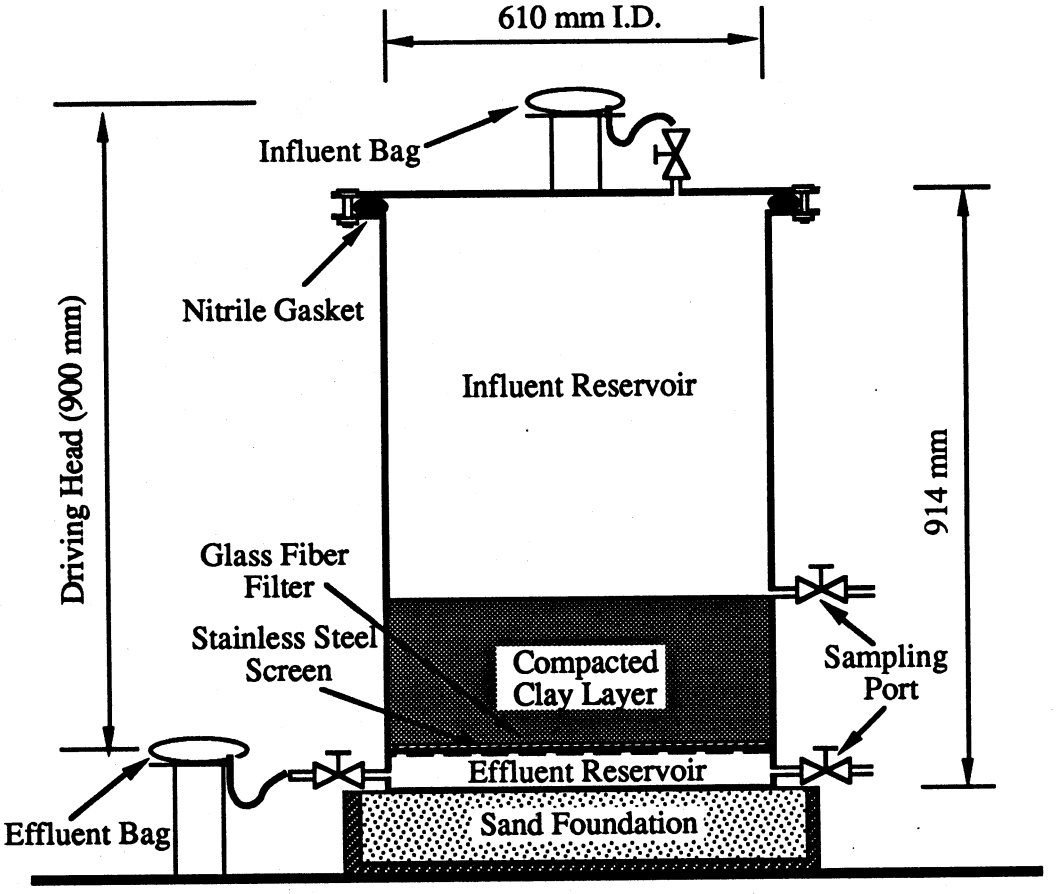

Figure 3.2 Design of the tank used in the long-term experiments.

All parts used were made of Teflon® or stainless steel. Three sampling ports were installed and the sampling ports consisted of Teflon® septa and sampling needles. Since there can be concentration gradients in the top reservoir, three different depths of samples were collected to measure the concentrations of chemicals in the last four tank experiments.

Teflon® bags were used for the influent storage bag and the effluent storage bag. All tubings were made of Teflon®. To support the compacted clay layer, a stamped stainless steel screen which rested on a dozen stainless steel rings 102 mm (4 in.) in diameter and 25 mm (1 in.) high was used.

Soil used in the preparation of samples was ground and passed through a no. 4 sieve (opening = 47.6 mm), as is recommended by Benson and Daniel (1990) for compacted clay hydraulic barriers. By passing the soil through the no. 4 sieve, clods, large particles of bonded and cemented clay, were removed to insure the production of low hydraulic conductivity specimens. Also, by removing clods, the soil was relatively uniform for the preparation of all specimens, which was necessary to create specimens with similar porosity, density, and hydraulic conductivity.

The soil was hydrated manually to obtain the desired moisture content. Hydration was completed by spraying water onto the ground soil and then mixing the soil and water with trowels. The water was sprayed in stages to prevent the soil from lumping together and producing clod size particles. Also, the soil hydrated more uniformly by spraying the water in separate stages. The hydrated soil was then wrapped up in plastic garbage bags and left to sit for 24-hours prior to compaction.

The target value of the hydraulic conductivity was 1×10^{-8} to 1×10^{-7} cm/sec. The compaction procedure as described by Heim (1992) and Wambold (1993) was followed. The liner was designed to have six lifts. Clay in the tanks was compacted with a 12.25 kg hammer, using 60 blows applied to the lower three lifts and 75 blows applied to the top three lifts. The hammer was dropped from a height of 46 cm. Each lift consisted of 31.0 kg of soil and the target water content was 17%. The surface of each lift was scarified and a wet slurry of soil was applied to the walls of the tank before addition of the subsequent lift to make good contact between the compacted lifts and the tank wall. Additional compaction effort was applied to the clay around the edge after the main compaction was

completed. This additional compaction was done by dropping a smaller diameter, 4.54 kg hammer from a height of 46 cm.

3.3.2 Experimental Design

The experimental design of the four tank tests is explained in Table 3.8. Tire chips weighing 2 and 10 kg occupy about 1 and 5 % of the upper reservoir volume, respectively. Styrofoam weighing 220 g has the same volume as 10 kg of tire chips.

Table 3.8 Experimental design for tank tests.

Tank	Contaminant	Sorbent	Initiation Date	VOC Spiking Date	Termination Date
2A	MC, TCE & TOL LiBr	10 kg of Tire chips & 220 g of Styrofoam	05/24/92	09/13/92	Ongoing
4	MC, TCE & TOL LiBr	10 kg of Tire chips	06/16/92	10/19/92	Ongoing
5	MC, TCE & TOL LiBr	Only soil (Control)	06/12/92	09/20/92	Ongoing
6	MC, TCE & TOL LiBr	2 kg of Tire chips	06/12/92	09/02/92	Ongoing

3.4 LONG-TERM COLUMN TESTS

3.4.1 Procedure

Six small-scale column experiments were designed to study the dispersive mass transport of VOCs through soil medium. These experiments were supplemented by the data of nine column experiments performed by Wambold (1993). The schematic dimensions of the test column are shown in Figure 3.3. These tests were performed in the same constant temperature room (20°C) with the long-term tank tests.

To remove interference of any ionic material in tap water, ASTM D-5084 recommended solution (0.005 N $CaSO_4$ solution (6.8 g-$CaSO_4$/10 L)) was applied. This solution is thought to neither increase nor decrease the hydraulic conductivity of clayey soil significantly. Also mercuric chloride was added at 40 mg/L as a disinfectant.

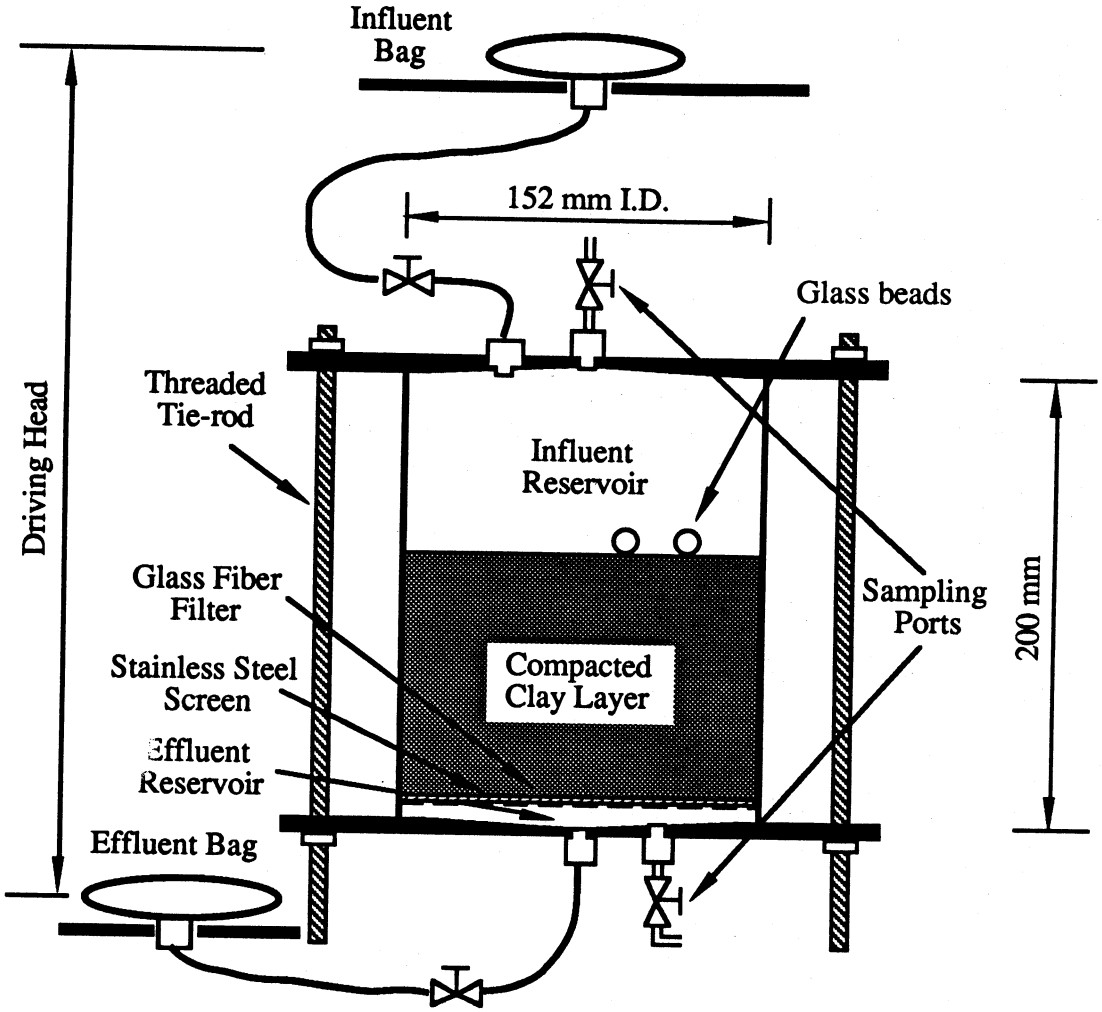

Figure 3.3 Design of the column used in the long-term column tests.

All parts of the test columns were made of brass. Two sampling ports were installed to take influent and effluent samples and consisted of Teflon® septa and sampling needles. All tubings, and the influent and effluent storage bags were made of Teflon®. A stamped stainless steel screen which rested on a stainless steel ring with 0.85 cm height

was used to support the compacted clay layer. Two different sizes of stainless steel rings with 10 mm height were used: 8.25 cm I.D. with 0.29 cm thickness for columns 1, 2, and 3 and 7.82 cm I.D. with 0.56 cm thickness for columns 4, 5, and 6. The different sizes of rings make different effective volumes of lower reservoirs. As explained later, the volume of the lower reservoir is a factor in the column/tank breakthrough analysis. Two glass beads with 1.27 cm in diameter were added into the columns to mix the upper reservoir. Mixing of the upper reservoir will be conducted by rolling the glass beads periodically.

Soil preparation and compaction for these tests were performed as stated by Heim (1992) and Wambold (1993). The no. 4 sieve passed and clods removed soil was hydrated to meet the target water content of 17 %. A 24-hour aged soil after hydration was compacted in brass columns. Each column consisted of three lifts of soil. The compaction was performed by dropping 4.54 kg (10 lb) modified Proctor hammer from 46 cm. 15 blows were applied to each lift. Each surface of lift was scarified and a wet slurry of soil was applied to the walls of the column before the addition of the subsequent lift.

3.4.2 Experimental Design

Six column experiments using clay liner specimens in brass columns were prepared. The purpose of these tests was concentrated on the effect of the hydraulic gradient on the hydrodynamic dispersion coefficient of the VOCs. Two different hydraulic gradients will be applied: zero (pure diffusion case) and three (a typical landfill case, the same as tank tests). The tests will run in triplicate. Table 3.9 lists the experimental design for the column tests.

The tracer, lithium bromide (LiBr) and seven VOCs, chloroform (CF), ethylbenzene (EB), methylene chloride (MC), toluene (TOL), 1,1,1-trichloroethane (TCA), trichloroethylene (TCE), and *m*-xylene (*m*-XYL) will be injected together after the hydraulic conductivity becomes stable.

Table 3.9 Experimental design for column tests.

Column	Contaminant	Sorbent	Hydraulic Gradient
1J	7 VOCs LiBr	Only Soil	3 (the same with Tank tests)
2J	7 VOCs LiBr	Only Soil	0 (Pure Diffusion)
3J	7 VOCs LiBr	Only Soil	0 (Pure Diffusion)
4J	7 VOCs LiBr	Only Soil	0 (Pure Diffusion)
5J	7 VOCs LiBr	Only Soil	3 (the same with Tank tests)
6J	7 VOCs LiBr	Only Soil	3 (the same with Tank tests)

3.5 SOIL CORING AND SECTIONING

The breakthrough curve and concentration-depth profile are the two important data in analyzing the column or tank test. The breakthrough curve can be obtained by monitoring influent and effluent concentrations. To obtain a concentration-depth profile, soil samples should be cored and sectioned. The VOCs in pore water and sorbed into soil should be estimated separately in each section.

The coring and sectioning techniques will follow the methods used by Heim (1992) and Wambold (1993). The steel Shelby tubes with diameters of 68.5 mm will be used for coring in long-term tank tests. Smaller diameter tubes were found to disturb soil samples to a great extent. The soil specimen of long-term column tests will be extruded by a hydraulic jack.

A pore fluid extractor will be used to squeeze the pore water from each sectioned

soil sample. The moisture contents of each section of soil sample will be measured both before and after squeezing the pore water. The pore water squeezing will be conducted by the methods developed in the previous two studies and ASTM D-4542.

The VOCs sorbed into soil material can be extracted with solvents. The extraction procedure is nearly the same as the batch isotherm sorption test. There are no standardized collection and handling procedures only general guidelines. Test Methods for Evaluating Solid Wastes (1986) suggests storing the soil samples in Teflon® lined glass tubes at 4°C, analyzing it within 14 days, and extracting the soil samples with methanol.

Previous studies used several different solvents like deionized water, carbon disulfide, hexane, methanol, methylene chloride, and so on. The efficiencies of solvents have not been determined yet. A drastic change of the organic compound extraction was observed with increased incubation time (Karickhoff, 1984). The extraction with hexane recovered over 90 % of sorbed compounds within approximately 3 minutes. After 3 to 5 hours of incubation, the recovery decreased to 50 %. Furthermore, after the next few days, the recovery was in 20 to 40 %. The estimation procedure of the amounts of VOCs in liquid and solid phase will be explained later.

According to previous studies (Heim, 1992; Wambold, 1993), it is very difficult to prevent the loss of VOCs from the soil sample during the coring and sectioning process. VOCs are easily vaporized during coring, sectioning, and pore water squeezing. Also, the efficiency of the VOC extraction technique by carbon disulfide was not sufficient. It is more desirable to analyze the column test using the breakthrough curve under a constant upper boundary condition or the upper reservoir concentration monitoring than the concentration-depth profile.

3.6 SOLUTION PREPARATION AND SAMPLING

For the long term tank tests, the stock solution containing the mixture of target organic compounds was used as the feeding solution. The calculation which was needed to obtain the required amount of each organic compound for the stock solution was explained in Appendix D. The target compounds were methanol, methylene chloride, TCE, and toluene. An aliquot of 20 mL of stock solution was prepared. The volumes of four organic compounds within 20 mL of stock solution were 6.56, 3.91, 3.54, and 5.99 mL, respectively. Since the target concentration of each organic compound in the tank tests was 16 mg/L, the feeding solution for the tank was made by diluting 123 μL of stock solution into 2 L of tap water. Bromide was injected separately into the feeding solution.

Stock solution was stored at below 0°C in a 25 mL screw-capped glass tube with Teflon®-coated septum. The stock solution was diluted with water and mixed by magnetic stirrers for at least 24 hours to mix the organic compounds with water completely.

VOC samples were collected by using a gas tight glass syringe and 2 mL screw-capped glass vials with Teflon®-coated septum. The sample containing vials and feeding solutions were stored in the low-temperature room (4°C) before VOC analysis or feeding. VOC samples were analyzed within two weeks. Heim (1992) showed that the VOC losses were less than 3% when the samples were stored for periods up to three weeks before analysis.

3.7 ANALYTICAL METHODS

Gas chromatographic analysis was performed on a Varian 3600 gas chromatograph with 60 m × 0.25 mm I.D. Supelcowax-10 megabore column and a flame ionization detector (FID). An aliquot of 1.0 μL liquid sample was directly injected into the column

using a gas-tight micro-syringe or an autosampler. Helium was used as the carrier gas.

The column temperature was programmed to initially hold at 50°C for five minutes, then to climb to 85°C at a rate of 5.0°C/min and to climb again immediately to 230°C at a rate of 40°C/min and finally to hold for two minutes. A Varian 1093 Septum Equipped Programmable Injector (SPI) was programmed to initially hold at 50°C for 0.5 minute and immediately climb to 230°C at a rate of 225°C/min, and then hold for five minutes.

Calibration curves were produced using standards at 0, 10, 20, 30, 40, and 50 mg/L. Below some values of peak area, the calculated concentrations were not convincible because of the recording noise of the gas chromatograph system. Thus, detection limits were approximately 0.5 mg/L for chloroform, methylene chloride, 1,1,1-TCA, and TCE, and 0.1 mg/L for ethylene benzene, toluene, and *m* -xylene, respectively.

The Beckman System Gold High Performance Liquid Chromatography (HPLC) equipped with a conductivity detector was used to analyze the bromide ion. The dimension of the HPLC column was 150 mm × 4.6 mm and it was packed with Universal Anion 10u. 4 mM Phthalic acid adjusted to pH 4 with NaOH was used as the eluant. The column temperature was programmed to hold at 45°C without any change.

An aliquot of 80 μL liquid sample was injected into the column using an autosampler. Calibration curves were produced using standards at 1, 5, 10, and 20 mg/L. Before samples were injected into the HPLC system, samples and the eluant were filtered through 0.45 μm glass fiber filter to prevent the contamination of the column.

All weighings were performed on the analytic scale, Sartorius A200S made by Brinkmann Instruments, Inc. The scale could weigh to 10^{-4} g order.

CHAPTER 4
DATA ANALYSIS

4.1 PARTITION COEFFICIENT

4.1.1 Batch Isotherm Test

In order to estimate the partition coefficient, the concentrations in the liquid and solid phases need to be measured in batch isotherm tests. The concentration in the liquid phase is easily measured. However, the concentration in the solid phase cannot be measured directly. If the initial concentration of the target compound in the solid phase is assumed to be zero and the initial and equilibrium conditions in the liquid phase are known, the concentration in the solid phase can be estimated.

$$K_p = \frac{C_{solid}}{C_{liquid}} \tag{4.1}$$

$$C_{solid} = \frac{(C_{liquid,0} - C_{liquid,e}) \times V_{liquid}}{W_{solid}} \tag{4.2}$$

where K_p = partition coefficient (L/kg);

C_{solid} = concentration of a compound in the solid phase (mg/kg);

$C_{liquid,0}$ = initial concentration of the target compound in the liquid phase (mg/L);

$C_{liquid,e}$ = equilibrium concentration of the target compound in the liquid phase (mg/L);

V_{liquid} = volume of liquid (L); and

W_{solid} = weight of the solid material (kg).

For the batch isotherm tests, the test soil was hydrated by adding water before conducting the test. Thus, the initial organic compound concentration in the liquid concentration was estimated based on the mass balance.

$$C_{liquid,0} = C_{sol'n} \times \frac{V_{sol'n}}{V_{sol'n} + V_{water}} \quad (4.3)$$

where $C_{sol'n}$ = target compound concentration in the solution which is introduced into the vial after soil saturation (mg/L);

$V_{sol'n}$ = volume of the solution added after soil saturation (mL); and

V_{water} = volume of the water added for soil saturation (mL).

Volumes of solution and water added were estimated by weighing them. The partition coefficient can be estimated by finding the slope of the best fitting line by linear regression to the experimentally obtained concentrations in each phase at equilibrium (Mackay, 1991).

4.1.2 Column Test - Soil Extraction

In the case of column tests, the partition coefficient of soil material could be estimated in different ways from batch isotherm tests. The partition coefficient of a VOC is the ratio between the solid and liquid phase concentrations. The partition coefficient can be expressed as follows:

$$K_{p,soil} = \frac{C_{soil}}{C_{pw}} \quad (4.4)$$

where $K_{p,soil}$ = partition coefficient of test soil (L/kg);

C_{solid} = concentration of a VOC in soil (mg/kg); and

C_{pw} = concentration of a VOC in pore water (mg/L).

The concentration of VOC in the pore water can be measured directly. However, the concentration of VOC in solids cannot be measured directly and can be estimated by the mass balance of the extraction. The toal mass of VOC in the extraction vial before extraction should be the same with that after extraction.

$$C_{CS_2,\,i} \cdot V_{CS_2} + C_{solid,\,i} \cdot W_{solid} + C_{pw,\,i} \cdot V_{pw} = C_{CS_2,\,f} \cdot V_{CS_2} + C_{solid,\,f} \cdot W_{solid} + C_{pw,\,f} \cdot V_{pw} \quad (4.5)$$

where $C_{CS_2,\,i}$ = VOC concentration in CS_2 before extraction (mg/L);

$C_{solid,\,i}$ = VOC concentration in solid before extraction (mg/kg);

$C_{pw,\,i}$ = VOC concentration in pore water before extraction (mg/L);

$C_{CS_2,\,f}$ = VOC concentration in CS_2 after extraction (mg/L);

$C_{solid,\,f}$ = VOC concentration in solid after extraction (mg/kg);

$C_{pw,\,f}$ = VOC concentration in pore water after extraction (mg/L);

V_{CS_2} = volume of CS_2 (L);

V_{pw} = volume of pore water (L); and

W_{solid} = weight of extracted solid (kg).

During extraction, the loss of VOCs, the weight change of solids, and the volume change of solution were ignored. Before the extraction, the concentration of VOC in CS_2 is assumed to be zero ($C_{CS_2,i} = 0$). After the extraction, the concentration of VOC in solids is assumed to be zero. Usually, the extraction solution which is used for this type of experiment is relatively insoluble in water. However, in the case of CS_2 extraction, the extraction solution has relatively high water solubility (2,300 mg/L) and cannot be separated from the pore water. Thus, the VOC in the pore water cannot be extracted completely and the VOC concentrations in the pore water will be similar to the VOC concentrations in CS_2 after extraction. Thus, Eq. 4.5 can be simplified as follows:

$$C_{solid,\,i} \cdot W_{solid} + C_{pw,\,i} \cdot V_{pw} = C_{CS_2,\,f} (V_{CS_2} + V_{pw}) \quad (4.6)$$

and

$$C_{solid,\,i} = \frac{C_{CS_2,\,f} (V_{CS_2} + V_{pw}) - C_{pw,\,i} \cdot V_{pw}}{W_{solid}} \quad (4.7)$$

The weight of solids and the volume of pore water are calculated by using the water content test. The water content test was conducted by drying soil samples at about 100°C. The water content, the weight of solids, and the volume of pore water can be calculated as follows:

$$w = \frac{W_{pw}}{W_{solid}} \times 100 = \frac{W_{soil+can,\,i} - W_{soil+can,\,f}}{W_{soil+can,\,f} - W_{can,\,f}} \times 100 \tag{4.8}$$

$$W_{solid} = \frac{W_{soil}}{(1 + w/100)} \tag{4.9}$$

$$V_{pw} = \frac{W_{pw}}{\rho_{pw}} = \frac{W_{soil} - W_{solid}}{\rho_{pw}} = \frac{W_{soil}/\rho_{pw}}{(1 + 100/w)} \tag{4.10}$$

where w = water content (%);

W_{water} = weight of pore water in soil (g);

W_{solid} = weight of solid in soil (g);

$W_{soil+can,\,i}$ = weight of (soil + can) before drying (g);

$W_{soil+can,\,f}$ = weight of (soil + can) after drying (g);

W_{can} = weight of can (g); and

ρ_{pw} = density of pore water (g/cm^3).

Teflon® centrifuge tubes and carbon disulfide CS_2 were used for this test. After squeezing the soil sample with a pore water squeezing equipment, the VOC concentrations in the pore water were analyzed. Approximately 30 mg of squeezed soil was weighed, and moved into the Teflon® centrifuge tube immediately. Then, 25 mL of the extraction solution, CS_2, was added to the Teflon tube and mixed with the squeezed soil. The tubes were rotated to make good contact between the extraction solution and the extracted VOCs. After at least three days passed, the tubes were centrifuged for about ten minutes. The VOCs concentrations in the supernatant were analyzed. The density of the pore water for the estimation of the pore water volume was assumed to be 1.0 g/cm^3.

4.2 DIFFUSION COEFFICIENT

The diffusion coefficient of an organic compound through a medium, e.g., tire or soil particle, can be estimated by monitoring the concentration drop of the organic compound in batch isotherm tests. The concentration drop can be formulated using the equations discussed in Chapter 2.

$$C_t = (1 - \frac{M_t}{M_\infty}) \cdot C_0 + \frac{M_t}{M_\infty} C_\infty \tag{2.48}$$

Plain sheet polymer:

$$\frac{M_t}{M_\infty} = (1+\alpha) \cdot \left(1 - e\,\mathrm{erfc}\sqrt{\frac{T}{\alpha^2}}\right) \tag{2.39}$$

$$\alpha = \frac{L_s}{K \cdot L_{1/2}} \tag{2.40}$$

$$T = \frac{D \cdot t}{L_{1/2}^2} \tag{2.41}$$

$$L_s = \frac{V}{2 \cdot S} \tag{2.49}$$

$$e\,\mathrm{erfc}(x) = \exp(x^2) \cdot \mathrm{erfc}(x) \tag{2.42}$$

$$\mathrm{erfc}(x) = 1 - \mathrm{erf}(x) \tag{2.43}$$

where K = partition coefficient of the solute [dimensionless];

L_s = imaginary length of solution on each of the plain sheets [L];

$L_{1/2}$ = half thickness of the polymer sheet [L];

M_t = total amount of solute in polymer at time t [M];

M_∞ = total amount of solute in polymer after infinite time [M];

S = area of the surface into which solute diffuses [L^2]; and

t = elapsed time [T].

Sphere polymer:

$$\frac{M_t}{M_\infty} = (1+\alpha)\cdot\left[1 - \frac{\gamma_1}{\gamma_1+\gamma_2}\,e\ \mathrm{erfc}\left(\frac{3\cdot\gamma_1}{\alpha}\sqrt{\frac{D\cdot t}{r_p^2}}\right) - \frac{\gamma_2}{\gamma_1+\gamma_2}\,e\ \mathrm{erfc}\left(\frac{3\cdot\gamma_2}{\alpha}\sqrt{\frac{D\cdot t}{r_p^2}}\right)\right] \tag{2.44'}$$

$$\alpha = \frac{3\cdot V}{4\cdot\pi\cdot r_p{}^3\cdot K} \tag{2.45}$$

$$\gamma_1 = \frac{1}{2}\left\{\sqrt{\left(1+\frac{4}{3}\alpha\right)} + 1\right\} \tag{2.46}$$

$$\gamma_1 - \gamma_2 = 1 \tag{2.47}$$

where r_p = radius of the sphere [L]; and

V = solution volume in which a sphere polymer is suspended [L^3].

The diffusion coefficient can be estimated by a curve fitting technique. The partition coefficeint estimated from batch isotherm tests were used for the estimation of the diffusion coefficient. The best fitting line was obtained by changing the value of the diffusion coefficient in the mass transport equation for given experimental conditions.

4.3 HYDRAULIC CONDUCTIVITY

The hydraulic conductivity, k_h, was determined by measuring inflow into the specimen and outflow from the specimen. The following constant-head equation was used to calculate k_h (ASTM D-2434):

$$k_h = \frac{V}{S\times i\times\Delta t} = \frac{V\times L}{S\times h\times\Delta t} \tag{4.11}$$

where h = head difference [L];

i = hydraulic gradient;

L = thickness of clay liner [L];

V = volume of permeant discharged [L^3];

S = cross-sectional area of soil specimen [L^2]; and

Δt = elapsed time [T].

The hydraulic conductivity was measured by weighing the change in both the inflow and outflow bags. Therefore, it was possible to compare the hydraulic conductivity with respect to inflow and outflow. Averages were taken from inflow and outflow hydraulic conductivity measurements as well as a composite average, which includes both inflow and outflow values. The averages will be used in modeling of concentration breakthrough curves in order to determine the hydrodynamic dispersion coefficient.

4.4 COLUMN/TANK TEST ANALYSIS I - ANALYTICAL SOLUTIONS

4.4.1 Constant Upper and Lower Boundary Conditions

The constant upper and lower boundary conditions are the most frequently used boundary conditions for the analysis of column tests. Also with a relatively large volume of the upper reservoir and the slow mass transport through the soil layer, these conditions can be applied during the whole testing period.

Ogata and Banks (1961) developed an analytical solution for the one-dimensional mass transport equation (Eq. 2.19). The analytical solution and initial and boundary conditions are as follows:

$$C(z,t) = \left(\frac{C_o}{2}\right)\left[\operatorname{erfc}\left\{\frac{R_f \cdot z - v_z \cdot t}{2\cdot(R_f \cdot D_h \cdot t)^{1/2}}\right\} + \exp\left(\frac{v_z \cdot z}{D_h}\right)\cdot \operatorname{erfc}\left\{\frac{R_f \cdot z + v_z \cdot t}{2\cdot(R_f \cdot D_h \cdot t)^{1/2}}\right\}\right] \quad (4.12)$$

$$C(z,0) = 0 \qquad 0 < z < \infty \quad (4.13a)$$

$$C(0,t) = C_o \qquad 0 < t \quad (4.13b)$$

$$C(\infty,t) = 0 \qquad 0 < t \quad (4.13c)$$

4.4.2 Changing Upper Boundary Condition

When the mass transport of solutes are relatively fast through the soil layer, the concentration in the upper reservoir may not be considered constant during the testing period. Consequently, the constant upper boundary condition is not appropriate in analyzing the column test. Thus, under this condition, a decreasing upper boundary may be better to analyze the tank or column experiment.

The assumptions of this model are as follows:

(1) The upper reservoir has no concentration gradient along the reservoir depth;

(2) The diffusion at the top of the upper reservoir is ignored; and

(3) The influent concentration into the upper reservoir is constant during the whole testing period.

The technique to estimate key parameters in mass transport through soil columns by monitoring the upper reservoir concentration has some advantages: (1) short testing period; (2) reduction in the potential losses of the compounds due to the short testing period; and (3) elimination of organic compound loss during sectioning and/or extraction. This analytical approach is applicable before the breakthrough of a target compound occurs.

$$\frac{\partial C}{\partial t} = \frac{D_h}{R_f} \cdot \frac{\partial^2 C}{\partial z^2} - \frac{v_z}{R_f} \cdot \frac{\partial C}{\partial z} \qquad (2.19)$$

$$R_f = 1 + \frac{\rho_p \cdot K_p \cdot (1 - n_t)}{n_t} \qquad (2.22)$$

$$C(z,0) = 0 \qquad 0 < z < \infty \qquad (4.13a)$$

$$C(0,t) = C_{UR}(t) \qquad 0 < t \qquad (4.13b')$$

$$C(\infty,t) = 0 \qquad 0 < t \qquad (4.13c)$$

Define the Laplace transformation of C(z,t) as $\overline{C}(z,s)$:

$$\pounds\{C(z,t)\} = \int_0^\infty C(z,t) \cdot \exp(-s \cdot t)\, dt = \overline{C}(z,s) \qquad (4.14)$$

$$\mathcal{L}\{f'(x)\} = s\cdot\mathcal{L}\{f(x)\} - f(0) \tag{4.15}$$

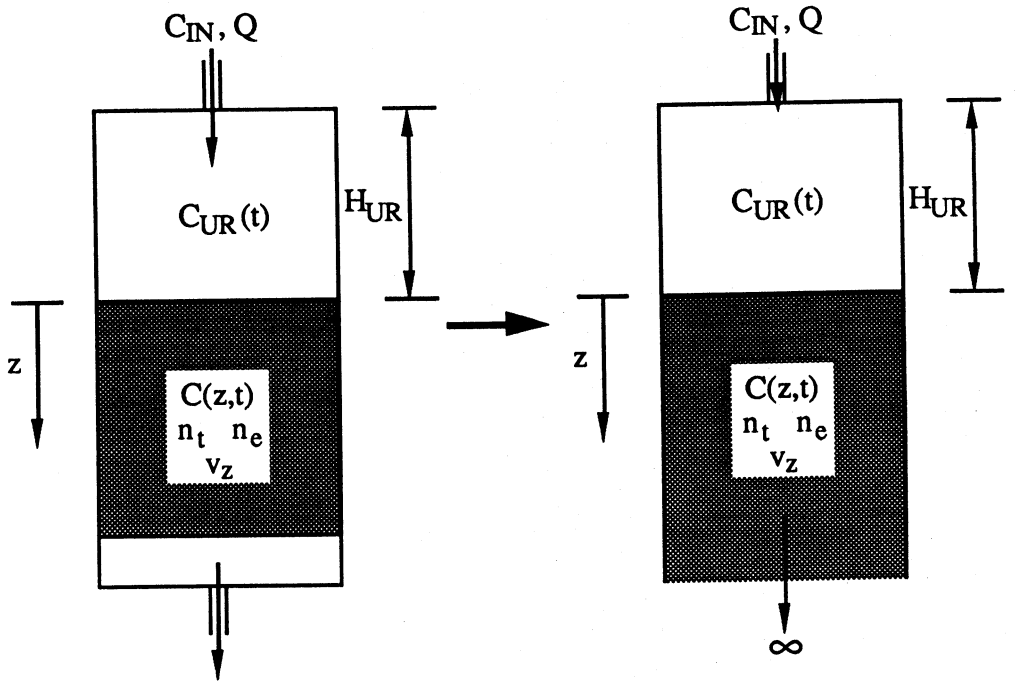

Figure 4.1. Schematic diagram of semi-infinite column model development.

The application of Eqs. 4.14 and 4.15 to 2.19 yields;

$$s\cdot\overline{C} = \frac{D_h}{R_f}\cdot\frac{\partial^2\overline{C}}{\partial z^2} - \frac{v_z}{R_f}\cdot\frac{\partial\overline{C}}{\partial z} \tag{4.16a}$$

$$\frac{\partial^2\overline{C}}{\partial z^2} - \frac{v_z}{D_h}\cdot\frac{\partial\overline{C}}{\partial z} - \frac{R_f\cdot s}{D_h}\cdot\overline{C} = 0 \tag{4.16b}$$

$$\overline{C}(z,0) = \mathcal{L}\{C(z,0)\} = 0 \qquad 0 < z < \infty \tag{4.17a}$$

$$\overline{C}(0,s) = \mathcal{L}\{C(0,t)\} = \mathcal{L}\{C_{UR}(t)\} = \overline{C_{UR}}(s) \qquad 0 < s \tag{4.17b}$$

$$\overline{C}(\infty,s) = \mathcal{L}\{C(\infty,t)\} = 0 \qquad 0 < s \tag{4.17c}$$

The general solution of the Eq.4.16b type differential equation is:

$$\overline{C}(z,s) = A\cdot\exp(\alpha\cdot z) + B\cdot\exp(\beta\cdot z) \tag{4.18a}$$

$$\alpha,\beta = \frac{1}{2}\left\{\frac{v_z}{D_h} \pm \sqrt{\left(\frac{v_z}{D_h}\right)^2 + \frac{4\cdot R_f\cdot s}{D_h}}\right\} \qquad (\alpha > \beta) \tag{4.18b}$$

$$\overline{C}(\infty,s) = A\cdot\exp(\infty) + B\cdot\exp(-\infty) = 0 \tag{4.19a}$$

$$A = 0 \tag{4.19b}$$

$$\overline{C}(0,s) = B \cdot \exp(0) = B = \overline{C_{UR}}(s) \tag{4.19c}$$

Thus, Eqs. 4.18a and 4.18b can be rearranged as follows:

$$\overline{C}(z,s) = \overline{C_{UR}}(s) \cdot \exp\left[\frac{z}{2} \cdot \left\{\frac{v_z}{D_h} - \sqrt{\left(\frac{v_z}{D_h}\right)^2 + \frac{4 \cdot R_f \cdot s}{D_h}}\right\}\right] \tag{4.20}$$

In the upper reservoir the mass balance can be expressed as follows:

$$V_{UR} \cdot \frac{\partial C_{UR}}{\partial t} = Q \cdot C_{IN} - \left\{- n_t \cdot S \cdot D_h \cdot \frac{\partial C}{\partial z}_{z=0} + Q \cdot C(0,t)\right\} \tag{4.21a}$$

Q and V_{UR} can be expressed as follows:

$$Q = k_h \cdot i \cdot S \tag{4.22}$$

$$V_{UR} = H_{UR} \cdot S \tag{4.23}$$

Inserting Eqs. 4.22 and 4.23 into Eq. 4.21a yields:

$$H_{UR} \cdot \frac{\partial C_{UR}}{\partial t} = k_h \cdot i \cdot \{C_{IN} - C(0,t)\} + n_t \cdot D_h \cdot \frac{\partial C}{\partial z}_{z=0} \tag{4.21b}$$

Laplace transformation of Eq. 4.21b with respect to time, t, bcomes:

$$H_{UR} \cdot \{s \cdot \overline{C_{UR}}(s) - C_{UR}(0)\} = k_h \cdot i \cdot C_{IN} \cdot \frac{1}{s} - k_h \cdot i \cdot \overline{C}(0,s) + n_t \cdot D_h \cdot \frac{\partial \overline{C}}{\partial z}_{z=0} \tag{4.24}$$

From Eq. 4.20, the derivative of $\overline{C}(z,s)$ at $z = 0$ can be obtained as follows:

$$\frac{\partial \overline{C}}{\partial z}_{z=0} = \frac{\overline{C_{UR}}(s)}{2} \cdot \left\{\frac{v_z}{D_h} - \sqrt{\left(\frac{v_z}{D_h}\right)^2 + \frac{4 \cdot R_f \cdot s}{D_h}}\right\} \tag{4.25}$$

Inserting Eqs. 4.19c and 4.25 into 4.21b yields:

$$\overline{C_{UR}}(s) = \frac{H_{UR} \cdot C_{UR}(0) + k_h \cdot i \cdot C_{IN} \cdot s^{-1}}{\left(k_h \cdot i - \frac{n_t \cdot v_z}{2}\right) + H_{UR} \cdot s + \sqrt{\left(\frac{n_t \cdot v_z}{2}\right)^2 + \left(n_t^2 \cdot D_h \cdot R_f\right) \cdot s}} \tag{4.26a}$$

or

$$\overline{C_{UR}}(s) = \frac{H_{UR}\cdot C_{UR}(0)}{\left(k_h\cdot i - \frac{n_t\cdot v_z}{2}\right) + H_{UR}\cdot s + \sqrt{\left(\frac{n_t\cdot v_z}{2}\right)^2 + \left(n_t^2\cdot D_h\cdot R_f\right)\cdot s}} + \frac{k_h\cdot i\cdot C_{IN}}{\left[\left(k_h\cdot i - \frac{n_t\cdot v_z}{2}\right) + H_{UR}\cdot s + \sqrt{\left(\frac{n_t\cdot v_z}{2}\right)^2 + \left(n_t^2\cdot D_h\cdot R_f\right)\cdot s}\right]\cdot s} \quad (4.26b)$$

Eq. 4.26b can be simplified as follows:

$$\overline{C_u}(s) = \frac{a}{b + c\cdot s + \sqrt{d + e\cdot s}} + \frac{f}{\left\{b + c\cdot s + \sqrt{d + e\cdot s}\right\}\cdot s} \quad (4.26c)$$

where $a = H_{UR}\cdot C_{UR}(0)$ (4.27a)

$$b = \left(k_h\cdot i - \frac{n_t\cdot v_z}{2}\right) \quad (4.27b)$$

$c = H_{UR}$ (4.27c)

$$d = \left(\frac{n_t\cdot v_z}{2}\right)^2 \quad (4.27d)$$

$e = n_t^2\cdot D_h\cdot R_f$ and (4.27e)

$f = k_h\cdot i\cdot C_{IN}$ (4.27f)

When $F(s) = \pounds\{f(t)\}$,

$$\pounds\{f_1(t) + f_2(t)\} = \pounds\{f_1(t)\} + \pounds\{f_2(t)\} = F_1(s) + F_2(s) \quad (4.28)$$

and

$$F(s + k_1) = \pounds\{\exp(-k_1\cdot t)\cdot f(t)\} \quad (4.29)$$

When $F(s) = (\sqrt{s} + a)^{-1}$,

$$f(t) = (\pi\cdot t)^{-1/2} - a\cdot\exp(a^2\cdot t)\cdot\mathrm{erfc}(a\cdot t^{1/2}) \text{ (Oberhettinger and Badii, 1973)} \quad (4.30)$$

The first term in the right side of Eq. 4.26c can be converted to:

$$\frac{a}{b + c\cdot s + \sqrt{d + e\cdot s}} = \frac{k_2}{(\sqrt{s^\tau} + k_3)\cdot(\sqrt{s^\tau} + k_4)} \quad (4.26d)$$

$$= \frac{k_2}{k_4 - k_3} \cdot \left\{ (\sqrt{s'} + k_3)^{-1} - (\sqrt{s'} + k_4)^{-1} \right\} \quad (4.26e)$$

and the original fuction is:

$$f_1(t) = \mathcal{L}^{-1}\left[\frac{k_2}{k_4 - k_3} \cdot \left\{ (\sqrt{s'} + k_3)^{-1} - (\sqrt{s'} + k_4)^{-1} \right\} \right] \quad (4.31a)$$

$$= \frac{k_2 \cdot \exp(-k_1 \cdot t)}{(k_3 - k_4)} \cdot \left[k_3 \cdot e \ \mathrm{erfc}(k_3 \cdot t^{1/2}) - k_4 \cdot e \ \mathrm{erfc}(k_4 \cdot t^{1/2}) \right] \quad (4.31b)$$

$$e \ \mathrm{efrc}(x) = \exp(x^2) \cdot \mathrm{erfc}(x) \quad (2.42)$$

$$\mathcal{L}^{-1}\left\{ s^{-1} \cdot F(s) \right\} = \int_0^t f(u) \, du$$

Thus, the original function of the second Laplace term is:

$$f_2(t) = \mathcal{L}^{-1}\left[s^{-1} \cdot \frac{f}{\left\{ b + c \cdot s + \sqrt{d + e \cdot s} \right\}} \right] \quad (4.32a)$$

$$= \int_0^t \frac{k_5 \cdot \exp(-k_1 \cdot u)}{(k_3 - k_4)} \cdot \left[k_3 \cdot e \ \mathrm{erfc}(k_3 \cdot u^{1/2}) - k_4 \cdot e \ \mathrm{erfc}(k_4 \cdot u^{1/2}) \right] du \quad (4.32b)$$

$$= \frac{k_3 \cdot k_5}{(k_3 - k_4)} \cdot \int_0^t \exp(-k_1 \cdot u) \cdot e \ \mathrm{erfc}(k_3 \cdot u^{1/2}) \, du$$

$$- \frac{k_4 \cdot k_5}{(k_3 - k_4)} \cdot \int_0^t \exp(-k_1 \cdot u) \cdot e \ \mathrm{erfc}(k_4 \cdot u^{1/2}) \, du \quad (4.32c)$$

where $s' = s + k_1$ (4.33a)

$$k_1 = \frac{d}{e} \quad (4.33b)$$

$$k_2 = \frac{a}{c} \quad (4.33c)$$

$$k_3 + k_4 = \frac{\sqrt{e}}{c} \quad (4.33d)$$

$$k_3 \cdot k_4 = \frac{b}{c} - \frac{d}{e} \quad \text{and} \quad (4.33e)$$

$$k_5 = \frac{f}{c} \quad (4.33f)$$

The values of k_3 and k_4 are the roots of the quadratic equation:

$$X^2 - (k_3+k_4)\cdot X + k_3\cdot k_4 = 0 \tag{4.34a}$$

For the two different real values of the roots, the following condition should be satisfied. Under this condition, k_3 and k_4 can be expressed by Eqs. 4.34c and 4.34d.

$$D = (k_3+k_4)^2 - 4\cdot k_3\cdot k_4 > 0 \tag{4.34b}$$

$$k_3 = \frac{1}{2}\left(\frac{\sqrt{e}}{c} + \sqrt{\left(\frac{\sqrt{e}}{c}\right)^2 - 4\cdot\left(\frac{b}{c} - \frac{d}{e}\right)}\right) \tag{4.34c}$$

$$k_4 = \frac{1}{2}\left(\frac{\sqrt{e}}{c} - \sqrt{\left(\frac{\sqrt{e}}{c}\right)^2 - 4\cdot\left(\frac{b}{c} - \frac{d}{e}\right)}\right) \tag{4.34d}$$

Two intergrations in Eq. 4.32c have the same form and can be solved separately. The first integration can be given as follows:

$$\int_0^t \exp(-k_1\cdot u)\cdot e\ \mathrm{erfc}(k_3\cdot u^{1/2})\ du$$

$$= \int_0^t \exp(k_3^2\cdot u - k_1\cdot u)\cdot\mathrm{erfc}(k_3\cdot u^{1/2})\ du \tag{4.35a}$$

$$= \int_0^t \left\{\frac{d}{du}\frac{\exp(k_3^2\cdot u - k_1\cdot u)}{(k_3^2 - k_1)}\right\}\cdot\mathrm{erfc}(k_3\cdot u^{1/2})\ du \tag{4.35b}$$

$$= \frac{\exp(k_3^2\cdot t - k_1\cdot t)}{(k_3^2 - k_1)}\mathrm{erfc}(k_3\cdot t^{1/2}) - \frac{\exp(0)}{(k_3^2 - k_1)}\mathrm{erfc}(0)$$

$$- \int_0^t \frac{\exp(k_3^2\cdot u - k_1\cdot u)}{(k_3^2 - k_1)}\cdot\left\{\frac{d}{du}\mathrm{erfc}(k_3\cdot u^{1/2})\right\} du \tag{4.35c}$$

Based on the definition of the error function (Kreyszig, 1979), the derivative of the complementary error function, erfc, can be derived:

$$\frac{d}{du}\mathrm{erfc}(k_3\cdot u^{1/2}) = \frac{d}{du}\left\{1 - \mathrm{erf}(k_3\cdot u^{1/2})\right\} \tag{4.36a}$$

$$= \frac{d}{du}\left\{1 - \frac{2}{\sqrt{\pi}}\int_0^{k_3 \cdot u^{1/2}} \exp(-x^2)\,dx\right\} \tag{4.36b}$$

since $$\frac{d}{du}\int_0^{k_3 \cdot u^{1/2}} \exp(-x^2)\,dx = \frac{k_3}{2} u^{-1/2} \cdot \exp(-k_3^2 \cdot u) \tag{4.36c}$$

$$\frac{d}{du}\,\mathrm{erfc}(k_3 \cdot u^{1/2}) = -\frac{k_3}{\sqrt{\pi}} u^{-1/2} \cdot \exp(-k_3^2 \cdot u) \tag{4.36d}$$

Inserting Eq. 4.36d into Eq. 4.35c yields:

$$\int_0^t \exp(-k_1 \cdot u) \cdot e\ \mathrm{erfc}(k_3 \cdot u^{1/2})\,du$$

$$= \frac{1}{(k_3^2 - k_1)}\left\{\exp(k_3^2 \cdot t - k_1 \cdot t) \cdot \mathrm{erfc}(k_3 \cdot t^{1/2}) - 1\right\}$$

$$+ \frac{k_3}{\sqrt{\pi} \cdot (k_3^2 - k_1)} \int_0^t \exp(-k_1 \cdot u) \cdot u^{-1/2}\,du \tag{4.35d}$$

Substituting $k_1 \cdot u = x^2$ in the last integration term in Eq. 4.35d yields:

$$\int_0^t \exp(-k_1 \cdot u) \cdot u^{-1/2}\,du = \frac{2}{\sqrt{k_1}} \int_0^{\sqrt{k_1} \cdot t^{1/2}} \exp(-x^2)\,dx = \frac{\sqrt{\pi}}{\sqrt{k_1}}\,\mathrm{erf}\left(\sqrt{k_1} \cdot t^{1/2}\right) \tag{4.37}$$

Thus, Eq. 4.35d becomes:

$$\int_0^t \exp(-k_1 \cdot u) \cdot e\ \mathrm{erfc}(k_3 \cdot u^{1/2})\,du$$

$$= \frac{1}{(k_3^2 - k_1)}\left\{\exp(k_3^2 \cdot t - k_1 \cdot t) \cdot \mathrm{erfc}(k_3 \cdot t^{1/2}) + \frac{k_3}{\sqrt{k_1}} \cdot \mathrm{erf}\left(\sqrt{k_1} \cdot t^{1/2}\right) - 1\right\} \tag{4.35e}$$

By the same procedure, the second intergration of Eq.4.32c can be expressed as follows:

$$\int_0^t \exp(-k_1 \cdot u) \cdot e\ \mathrm{erfc}(k_4 \cdot u^{1/2})\,du$$

$$= \frac{1}{(k_4^2 - k_1)}\left\{\exp(k_4^2 \cdot t - k_1 \cdot t) \cdot \mathrm{erfc}(k_4 \cdot t^{1/2}) + \frac{k_4}{\sqrt{k_1}} \cdot \mathrm{erf}\left(\sqrt{k_1} \cdot t^{1/2}\right) - 1\right\} \tag{4.38}$$

Finally, the concentration in the upper reservoir can be expressed as follows:

$$C_{UR}(t) = f_1(t) + f_2(t) \tag{4.39a}$$

$$= \frac{k_2}{(k_3 - k_4)} \exp(-k_1 \cdot t) \cdot \left\{ k_3 \cdot e \ \mathrm{erfc}(k_3 \cdot t^{1/2}) - k_4 \cdot e \ \mathrm{erfc}(k_4 \cdot t^{1/2}) \right\}$$

$$+ \frac{k_3 \cdot k_5}{(k_3 - k_4) \cdot (k_3^2 - k_1)} \left\{ \exp(-k_1 \cdot t) \cdot e \ \mathrm{erfc}(k_3 \cdot t^{1/2}) + \frac{k_3}{\sqrt{k_1}} \cdot \mathrm{erf}\left(\sqrt{k_1} \cdot t^{1/2}\right) - 1 \right\}$$

$$- \frac{k_4 \cdot k_5}{(k_3 - k_4) \cdot (k_4^2 - k_1)} \left\{ \exp(-k_1 \cdot t) \cdot e \ \mathrm{erfc}(k_4 \cdot t^{1/2}) + \frac{k_4}{\sqrt{k_1}} \cdot \mathrm{erf}\left(\sqrt{k_1} \cdot t^{1/2}\right) - 1 \right\} \tag{4.39b}$$

If there is no advective flow, i.e., $v_z = 0$, it can be called the pure diffusion test. In the case of pure diffusion, the upper reservoir concentration obtained from Eq. 4.39b is identical to the solution of Myrand et al. (1992):

$$C_{UR}(t) = k_2 \cdot e \ \mathrm{erfc}(k_3 \cdot t^{1/2}) \tag{4.40}$$

where $k_2 = C_{UR}(0)$ and (4.33c')

$$k_3 = \frac{n_t \cdot \sqrt{D_h \cdot R_f}}{H_{UR}} \tag{4.33d'}$$

Each analytical solution for the constant and decreasing upper boundary condition can be calculated by using a spread sheet program. Microsoft® Excel serves the error function and complementary error function and was used in this study.

4.5 COLUMN/TANK TEST ANALYSIS II - NUMERICAL SOLUTIONS

In the column and tank tests in this study, reservoirs were installed in the top and bottom of the columns and tanks. This is considered one of the easiest ways to make the permeant flow evenly through the entire exposed surface of the soil specimen. However, it should be noted that the concentrations of a target compound at the inlet and outlet of the

soil specimen could not be measured and the concentrations of the target compound in both reservoirs only can be measured. It means that the exact boundary concentrations cannot be measured directly.

A numerical program must be developed for the boundary conditions present in the column and tank tests so that it will be possible to use the measured reservoir concentration. From a curve fitting method between the model predicted breakthrough curve and measured tracer breakthrough data, the hydrodynamic dispersion coefficient and effective porosity can be estimated. By using the effective porosity obtained from tracer data, the hydrodynamic dispersion coefficients of other transport organic compounds can be obtained.

The governing equation for the one-dimensional mass transport model for advection and diffusion can be expressed as follows:

$$\frac{\partial C}{\partial t} = A \cdot \frac{\partial^2 C}{\partial z^2} - B \cdot \frac{\partial C}{\partial z} \tag{2.19}$$

$$A = \frac{D_h}{R_f} \tag{4.41a}$$

$$B = \frac{v_z}{R_f} \tag{4.41b}$$

and

$$R_f = 1 + \frac{\rho_p \cdot K_p \cdot (1 - n_t)}{n_t} \tag{2.22}$$

where D_h = hydrodynamic dispersion coefficient (cm^2/sec);

v_z = seepage velocity along z direction (cm/sec);

K_p = partition coefficient (g/cm^3);

n_t = total porosity; and

R_f = retardation factor.

If terms like decay, source, and sink are involved, the mass transport model will be

more complicated. In this study, these terms were not included in the mathematical model.

When Δt and Δh have infinitesimal values, the partial differential equation can be converted as follows:

$$\frac{\partial C}{\partial t}(i,t) = \frac{C_{i,t} - C_{i,t-1}}{\Delta t} \tag{4.42a}$$

and

$$\frac{\partial C}{\partial z}(i,t) = \frac{C_{i+1,t} - C_{i,t}}{\Delta h} \tag{4.42b}$$

Then, the governing equation, Eq. 2.19 becomes:

$$\frac{C_{i,t} - C_{i,t-1}}{\Delta t} = A \cdot \frac{C_{i+1,t} - 2 \cdot C_{i,t} + C_{i-1,t}}{(\Delta h)^2} - B \cdot \frac{C_{i+1,t} - C_{i,t}}{\Delta h} \tag{4.43a}$$

Now, the concentration of a position at a certain time step, $C_{i,t-1}$, is expressed in terms of three concentrations of adjacent positions at the next time step, $C_{i-1,t}$, $C_{i,t}$, and $C_{i+1,t}$.

$$C_{i,t-1} = C \cdot C_{i-1,t} + (1-2 \cdot C-D) \cdot C_{i,t} + (C+D) \cdot C_{i+1,t} \tag{4.43b}$$

$$C = -\frac{A \cdot \Delta t}{(\Delta h)^2} \tag{4.44a}$$

and

$$D = \frac{B \cdot \Delta t}{\Delta h} \tag{4.44b}$$

To simplify the system, C and D were considered as constant. The new constants E and F were calculated using the following matrix calculation:

$$(1 - 2 \cdot C - D) = E \tag{4.44c}$$

$$(C + D) = F \tag{4.44d}$$

$$
\begin{array}{llll}
i = 0 & C_{0,t} & = C_{UR,t} & \text{(Upper boundary)} \\
i = 1 & C_{1,t-1} & = C \cdot C_{0,t} + E \cdot C_{1,t} + F \cdot C_{2,t} & \\
i = 2 & C_{2,t-1} & = C \cdot C_{1,t} + E \cdot C_{2,t} + F \cdot C_{3,t} & \text{(4.43c)} \\
\vdots & & \vdots & \\
i = n-1 & C_{n-1,t-1} & = C \cdot C_{n-2,t} + E \cdot C_{n-1,t} + F \cdot C_{n,t} & \\
i = n & C_{n,t-1} & = C \cdot C_{n-1,t} + E \cdot C_{n,t} + F \cdot C_{n+1,t} & \\
i = n+1 & C_{n+1,t} & = C_{LR,t} & \text{(Lower Boundary)}
\end{array}
$$

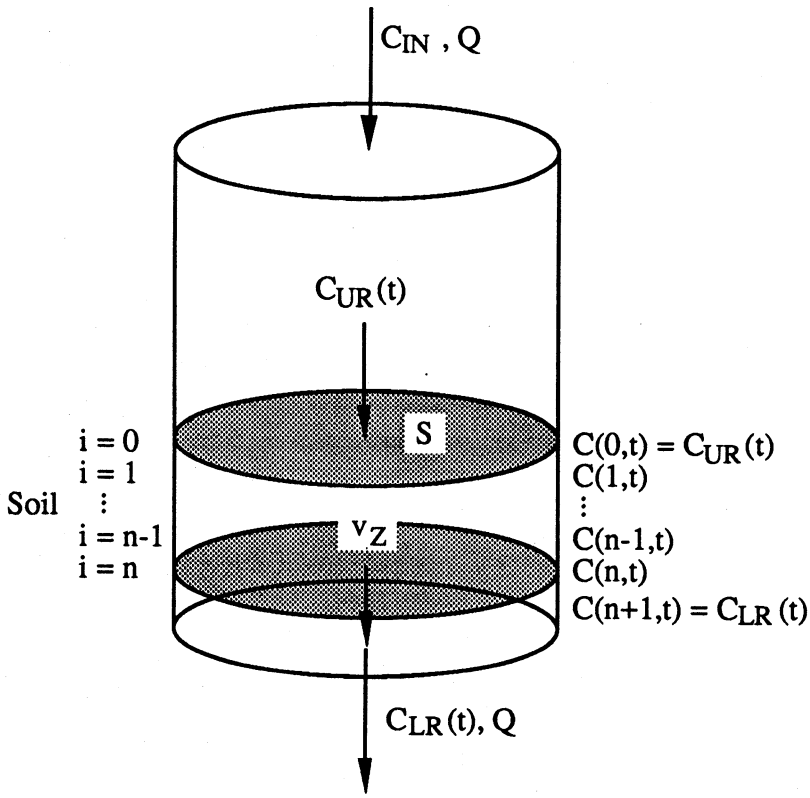

Figure 4.2 Schematic diagram of lower reservoir tank model development.

The mass balance in the upper reservoir can be expressed as follows:

$$H_{UR} \cdot \frac{\partial C_{UR}}{\partial t} = k_h \cdot i \cdot \{C_{IN} - C_{0,t}\} + n_t \cdot D_h \cdot \frac{\partial C}{\partial z}_{z=0} \qquad (4.21b)$$

Then, Eq. 4.21b becomes;

$$H_{UR}\cdot\frac{C_{0,t} - C_{0,t-1}}{\Delta t} = k_h\cdot i\cdot (C_{IN} - C_{0,t}) + n_t\cdot D_h\cdot\frac{C_{1,t} - C_{0,t}}{\Delta h} \qquad (4.21c)$$

Now, the concentration in the upper reservoir at a certain time step, $C_{0,t-1}$, is expressed in terms of two concentrations of adjacent positions at the next time step, $C_{0,t}$ and $C_{1,t}$ and C_{IN}.

$$C_{0,t-1} + G\cdot C_{IN} = (1 + G - H)\cdot C_{0,t} + H\cdot C_{1,t} \qquad (4.21d)$$

$$G = \frac{\Delta t\cdot k_h\cdot i}{H_{UR}} \qquad (4.45a)$$

and

$$H = -\frac{\Delta t\cdot n_t\cdot D_h}{\Delta h\cdot H_{UR}} \qquad (4.45b)$$

Based on the same approach with the upper reservoir mass balance, the lower reservoir can be analyzed. The mass balance is as follows:

$$H_{LR}\cdot\frac{C_{LR,t} - C_{LR,t-1}}{\Delta t} = k_h\cdot i\cdot (C_{n,t} - C_{LR,t}) - n_t\cdot D_h\cdot\frac{C_{LR,t} - C_{n,t}}{\Delta h} \qquad (4.46a)$$

and

$$C_{n+1,t-1} = (G' + H')\cdot C_{n,t} + (1 - G' - H')\cdot C_{n+1,t} \qquad (4.46b)$$

$$G' = -\frac{\Delta t\cdot k_h\cdot i}{H_{LR}} \qquad (4.45a)$$

$$H' = -\frac{\Delta t\cdot n_t\cdot D_h}{\Delta h\cdot H_{LR}} \qquad (4.45b)$$

Thus, the concentration in the upper and lower reservoir at a given time can be estimated by using the concentrations at the previous time step. The linear equations can be

expressed as Eq. 4.46. $C_{0,t}$ and $C_{n+1,t}$ are the concentrations in the upper and lower reservoirs, respectively. The solution of tridiagonal matrix can be calculated easily by using Gauss elimination approach (Conte and Boor, 1980):

$$\begin{bmatrix} C_{0,t-1} - G \cdot C_{IN} \\ C_{1,t-1} \\ C_{2,t-1} \\ \vdots \\ C_{n-1,t-1} \\ C_{n,t-1} \\ C_{n+1,t-1} \end{bmatrix} = \begin{bmatrix} 1+G-H & H & 0 & \cdots & 0 & 0 & 0 \\ C & E & F & & 0 & 0 & 0 \\ 0 & C & E & & 0 & 0 & 0 \\ 0 & 0 & C & \ddots & 0 & 0 & 0 \\ \vdots & \vdots & \vdots & & \vdots & \vdots & \vdots \\ 0 & 0 & 0 & & E & F & 0 \\ 0 & 0 & 0 & \cdots & C & E & F \\ 0 & 0 & 0 & & 0 & G'+H' & 1-G'-H' \end{bmatrix} \cdot \begin{bmatrix} C_{0,t} \\ C_{1,t} \\ C_{2,t} \\ \vdots \\ C_{n-1,t} \\ C_{n,t} \\ C_{n+1,t} \end{bmatrix} \tag{4.46}$$

For the constant upper boundary condition, the linear equations for the concentration at time, t, can be expressed by modifying Eq. 4.46:

$$\begin{bmatrix} C_{0,t-1} \\ C_{1,t-1} \\ C_{2,t-1} \\ \vdots \\ C_{n-1,t-1} \\ C_{n,t-1} \\ C_{n+1,t-1} \end{bmatrix} = \begin{bmatrix} 1 & 0 & 0 & \cdots & 0 & 0 & 0 \\ C & E & F & & 0 & 0 & 0 \\ 0 & C & E & & 0 & 0 & 0 \\ 0 & 0 & C & \ddots & 0 & 0 & 0 \\ \vdots & \vdots & \vdots & & \vdots & \vdots & \vdots \\ 0 & 0 & 0 & & E & F & 0 \\ 0 & 0 & 0 & \cdots & C & E & F \\ 0 & 0 & 0 & & 0 & G'+H' & 1-G'-H' \end{bmatrix} \cdot \begin{bmatrix} C_{0,t} \\ C_{1,t} \\ C_{2,t} \\ \vdots \\ C_{n-1,t} \\ C_{n,t} \\ C_{n+1,t} \end{bmatrix} \tag{4.47}$$

The computer program code which followed the previous approach is listed in Appendix B. The program was written in FORTRAN 77. Also, a verification of the program was conducted. The verification was conducted by comparing the analytical solutions in the previous section. The results are shown in Appendix C.

CHAPTER 5
RESULTS TO DATE

5.1 CONTAMINANT MOVEMENT THROUGH A CLAY LINER

5.1.1 Breakthrough Curves of Organic Compounds

If the boundary conditions of a clay liner are given, the mass transport of contaminants through a clay liner can be predicted by a mathematical analysis. Under the assumptions that the concentration at the upper boundary is constant and the soil below the liner is saturated (i.e., a shallow groundwater level), the analytical solution, which is known as the Ogata and Banks' analytical solution, can be used for the prediction of the mass transport through an earthen barrier. Figure 5.1 shows the breakthrough curves of three typical organic compounds through a clay liner.

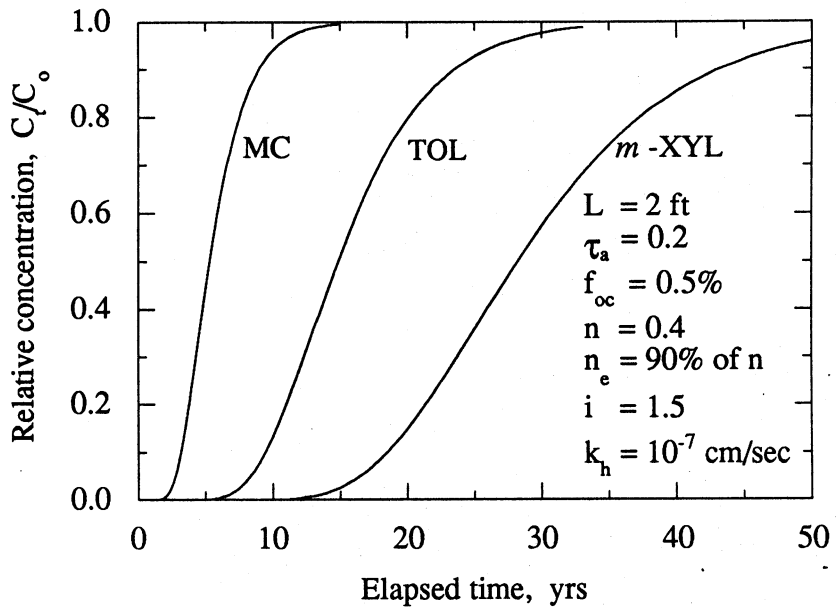

Figure 5.1 Breakthrough curves of organic compounds through a clay liner under typical conditions.

The upper boundary concentrations were assumed to be constant. The total porosity and effective porosity of the clay liner were assumed to be 0.4 and 0.36, respectively. The organic carbon contents of several different clays in Wisconsin were measured (Heim, 1992). The values ranged from 0.21 to 0.97% by weight. The organic carbon content of 0.5% was used to obtain the breakthrough curves. The partition coefficients of organic compounds were estimated by Piwoni and Banerjee's empirical equation (1989). The other conditions were from the design criteria of RCRA Subtitle D regulations, i.e. 30 cm leachate head, minimum 60 cm of earthen liner with less than 10^{-7} cm/sec hydraulic conductivity. Three organic compounds, methylene chloride, toluene, and *m*-xylene were selected based on the frequency of detection in landfill leachates and the range of solubility and molecular weight. The apparent tortuosity of each organic compound was assumed to be identical and 0.2.

Methylene chloride appears in the effluent first, followed by toluene and *m*-xylene. This prediction is essential in conformation with the lower partition coefficient or retardation factor. Methylene chloride has a lower octanol-water partition coefficient than toluene and *m*-xylene. Thus, methylene chloride has a lower partition coefficient and consequently, a lower reatardation factor than the other organic compounds.

The organic carbon content is one of the most important factors that control the contaminant movement through a clay liner. A small decrease in the organic carbon content can make great change in the breakthrough curves of organic compounds. Figure 5.2 shows the effect of the organic carbon content on the breakthrough of *m*-xylene, the most retarded organic compound in the previous simulations.

As the organic carbon content decreases, the effluent concentration of *m*-xylene increases dramatically. It took approximately 6 years for the effluent concentration to reach 10% of the influent concentration for 0.1% organic carbon content, but 34 years for 1% organic carbon content. The difference in the breakthrough times for 0.1 and 1% organic

carbon contents is more distinctive as the breakthrough concentration increases.

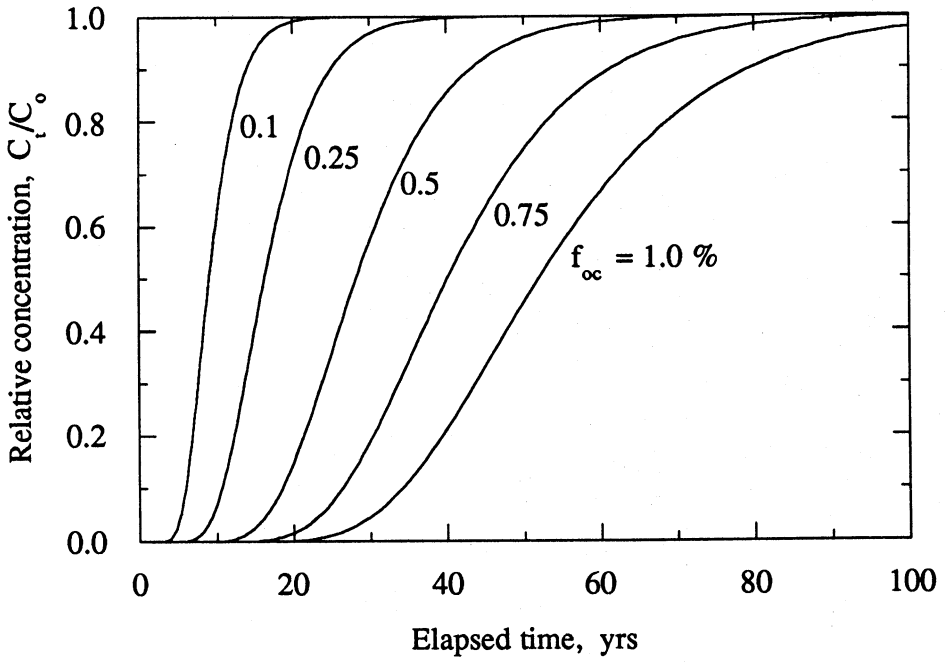

Figure 5.2 Breakthrough curves of *m*-xylene at different organic carbon contents.

5.1.2. Effect of the Concentration at the Upper Boundary

Under the upper and lower boundary conditions used in the Ogata and Banks' analytical solution, the relative concentrations of organic compounds are not affected by the constant upper boundary concentrations. However, in terms of groundwater protection, the effluent concentrations of contaminants are more useful than the relative concentrations of the contaminants. Figures 5.3 and 5.4 show the breakthrough curves of methylene chloride and *m*-xylene under different concentrations at the upper boundary.

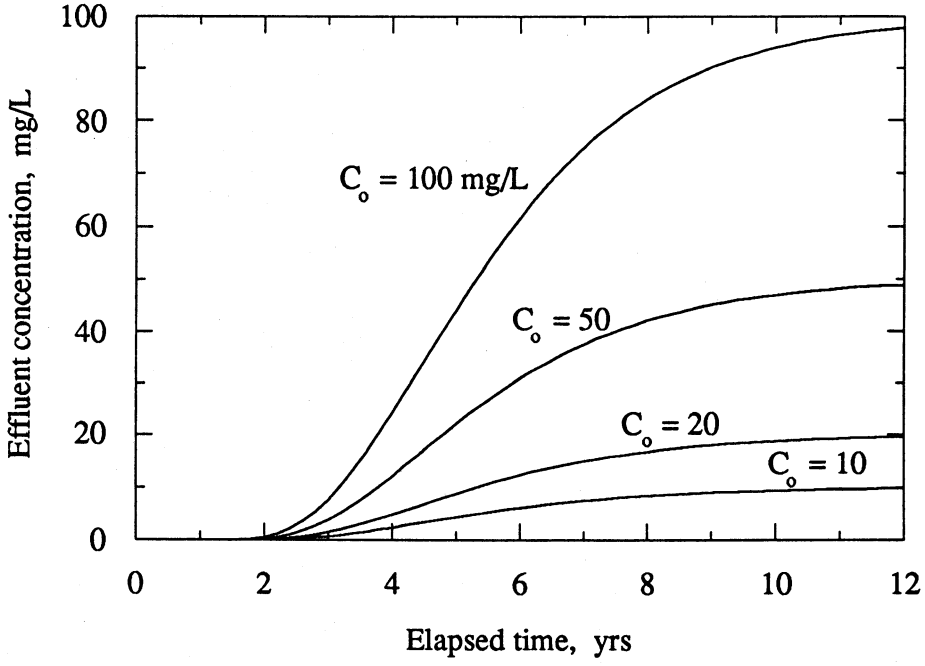

Figure 5.3 The effect of the concentration at the upper boundary on the effluent concentration (MC).

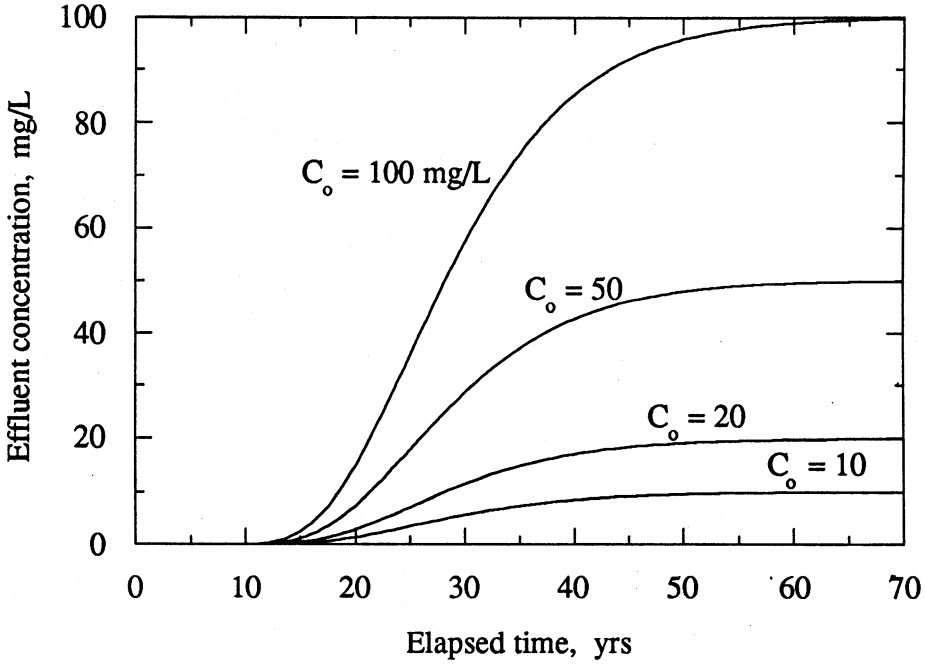

Figure 5.4 The effect of the concentration at the upper boundary on the effluent concentration (*m*-XYL).

The time required for methylene chloride to break through at low concentrations was not significantly affected by the increase in the concentration at the upper boundary. For example, required times for the effluent concentration of methylene chloride to reach 5 ppb for the upper boundary concentrations of 100 and 10 mg/L are 13 and 18 months, respectively. Although the effect of the upper boundary concentration at the upper boundary on the breakthrough time may be considered insignificant, if the upper boundary concentration is controlled within a certain range, the effluent concentration does not increase beyond the controlled upper boundary concentration. Table 5.1 summarizes the required times of methylene chloride and *m*-xylene to break through at different concentrations under the different upper boundary concentrations. As the breakthrough concentration increases from 1 μg/L to 10 mg/L, the difference in the breakthrough times is more distinctive.

Table 5.1 Required times of methylene and *m*-xylene to break through at different concentrations at the upper boundary (months).

Influent conc.	Effluent conc.					
(mg/L)	1 μg/L	10 μg/L	100 μg/L	1 mg/L	10 mg/L	20 mg/L
MC						
10	17	20	26	39	180	N.A.
20	15	19	24	34	65	180
50	15	17	21	29	46	58
100	14	16	20	26	39	46
m-XYL						
10	108	127	160	223	790	N.A.
20	102	120	148	198	336	790
50	96	111	135	174	254	312
100	90	106	127	160	222	254

5.1.3 Effect of the Lower Boundary Condition

The Ogata and Banks' analytical solution is based on the infinitely extended liner assumption (the infinitely extended lower boundary: $C_\infty = 0.0$). If the hydrogeological characteristics of the soil layer below the clay liner is completely different from those of the clay liner, the concept of continuum cannot be accepted. If the groundwater does not flow fast, the assumption that the lower boundary concentration is identical to the effluent concentration (the equal concentration lower boundary: $C_{L.B.} = C_{eff.}$) may be reasonable. On the other hand, a fast groundwater flow flushes the discharged contaminants from the clay liner and may lower the concentration below the liner to zero (the zero concentration lower boundary: $C_{L.B.} = 0.0$). Figure 5.5 shows the comparison between the Ogata and Bank's analytical solution and two numerical solutions under suggested lower boundary conditions. The programs for the numerical solutions are listed in Appendix B.

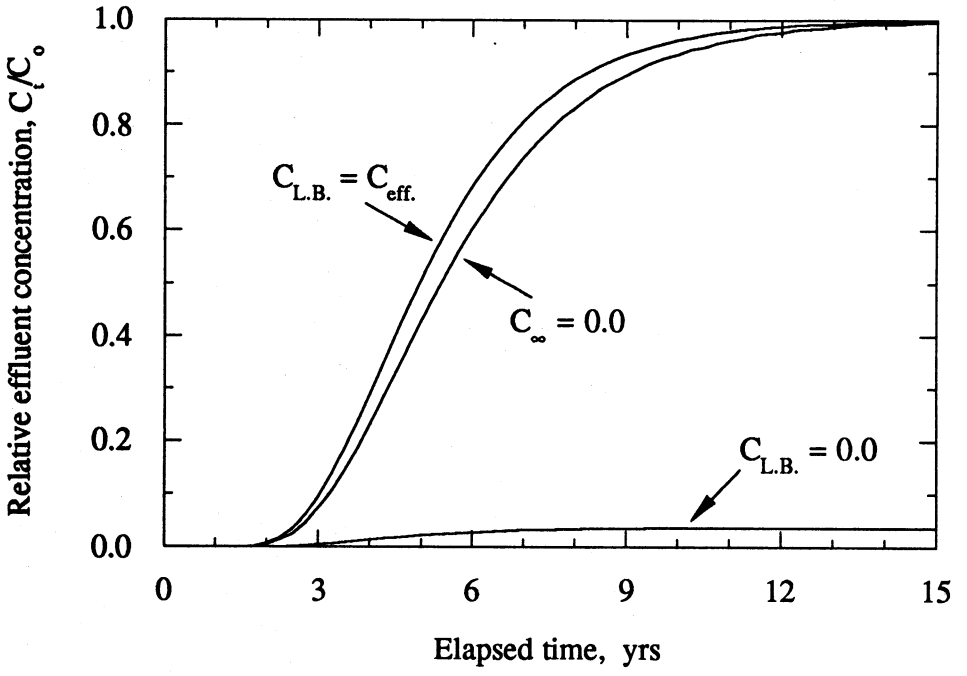

Figure 5.5 The effect of the lower boundary on the breakthrough curve.

In the case of the zero concentration lower boundary condition, the shape of the breakthrough curve is completely different from those of the other two models. Under the zero concentration lower boundary condition, the effluent concentration cannot increase beyond a certain value because of the constantly fixed lower boundary concentration to zero. The breakthrough curve predicted by the equal concentration lower boundary condition is slightly stiffer than that of the infinitely extended lower boundary condition. The breakthrough times of a target contaminant predicted by the three models are identical. The difference of the lower boundary conditions cannot affect the mass transfer of a contaminant until the contaminant breaks through.

The effluent concentration is related to only the advective discharge from the clay liner to the groundwater. The overall mass transfer should include both the advective and diffusive mass transfer. Figures 5.6 and 5.7 show the total discharged amount of methylene chloride and *m*-xylene estimated from three models. Under any lower boundary conditions, the amount of methylene chloride which has been introduced into the clay liner at a given time is identical because of the constant concentration at the upper boundary and the negligible concentration gradient at the top of the clay liner.

Even if the zero concentration lower boundary had the lowest effluent concentration among the three models simulated, it permits the highest discharge of methylene chloride. The highest discharge under the zero concentration lower boundary is caused by higher diffusive mass transfer. Figures 5.8, 5.9, and 5.10 show the concentration profiles of methylene chloride along the depth of the clay liner after three different elapsed times. Before methylene chloride breaks through, the concentration profiles are identical as shown in Figure 5.8.

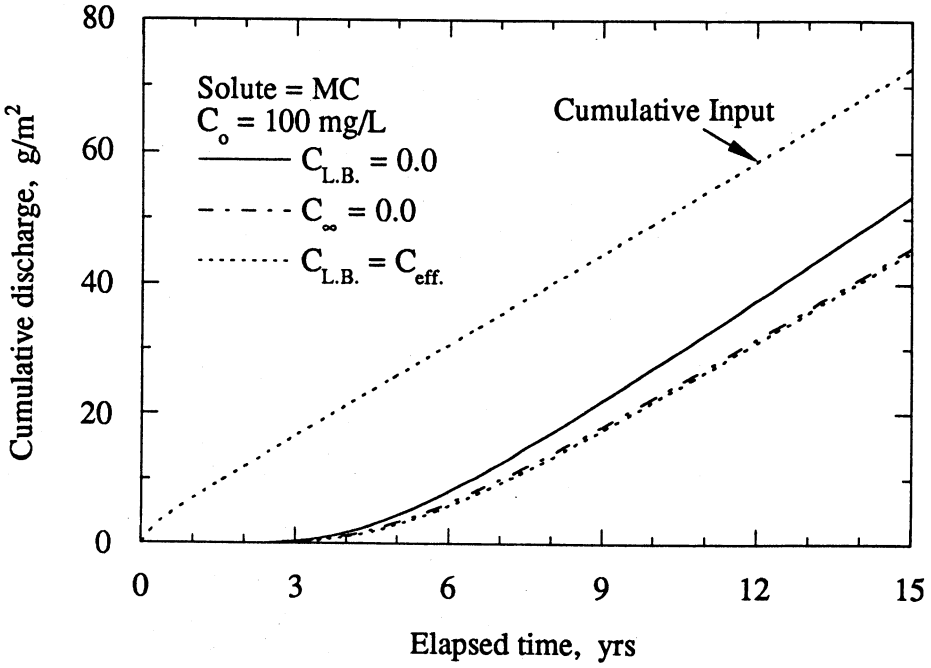

Figure 5.6 The total discharge of methylene chloride.

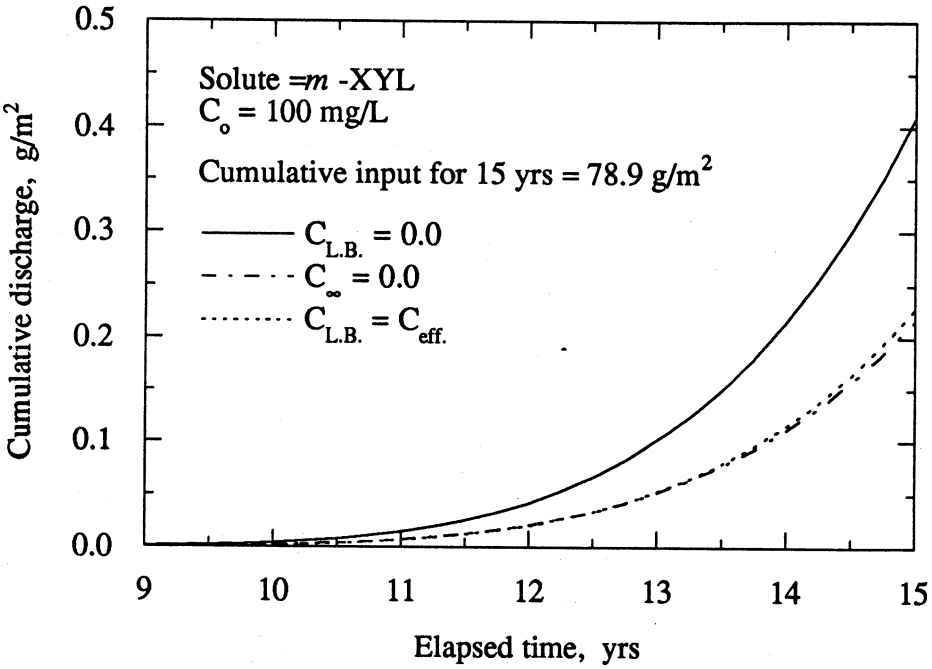

Figure 5.7 The total discharge of *m*-xylene.

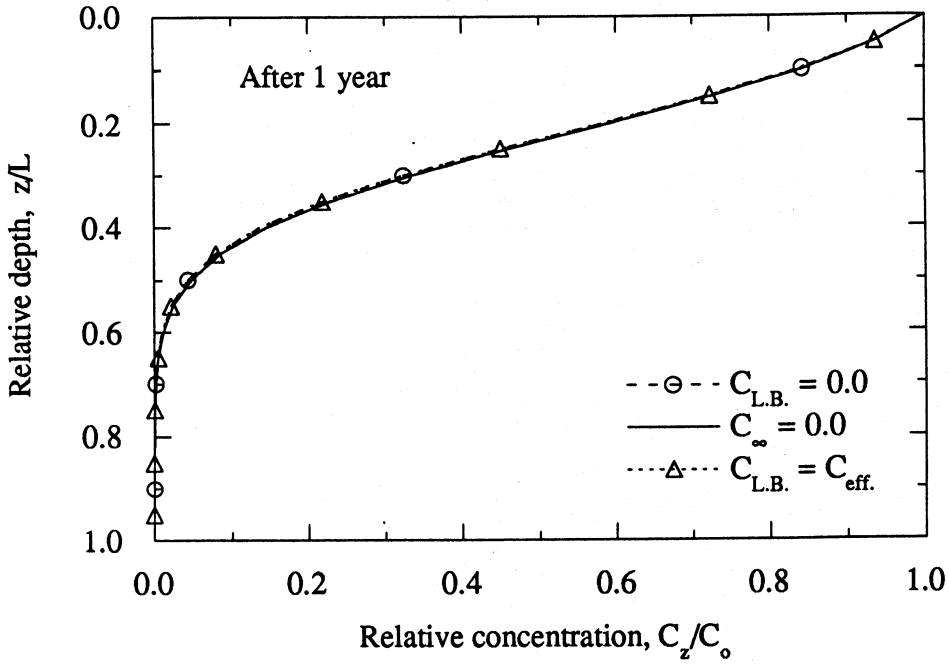

Figure 5.8 Methylene chloride concentration profiles after 1 year.

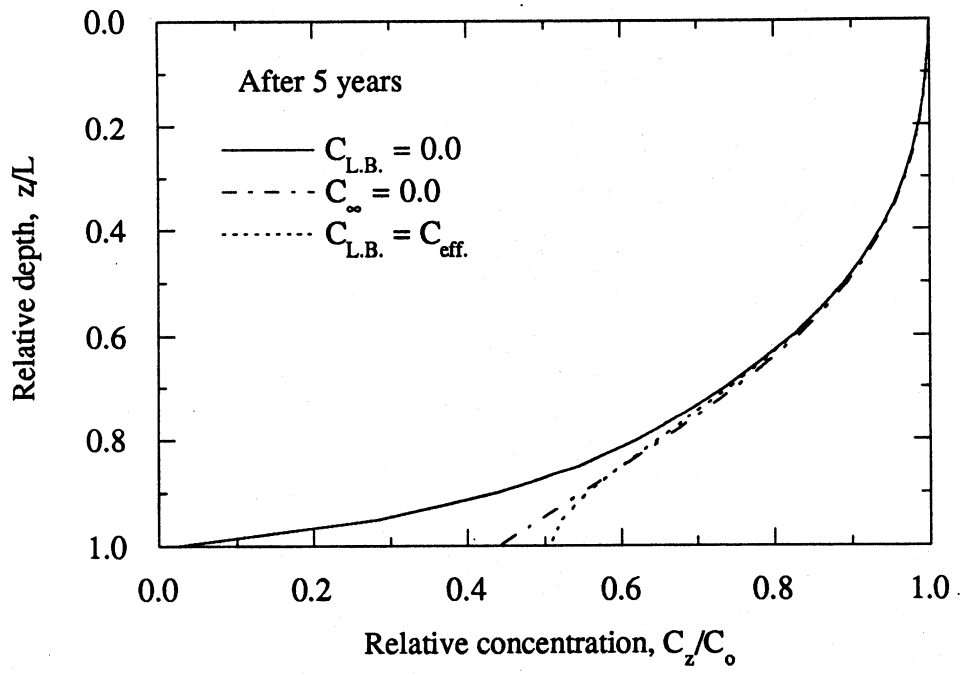

Figure 5.9 Methylene chloride concentration profiles ater 5 years.

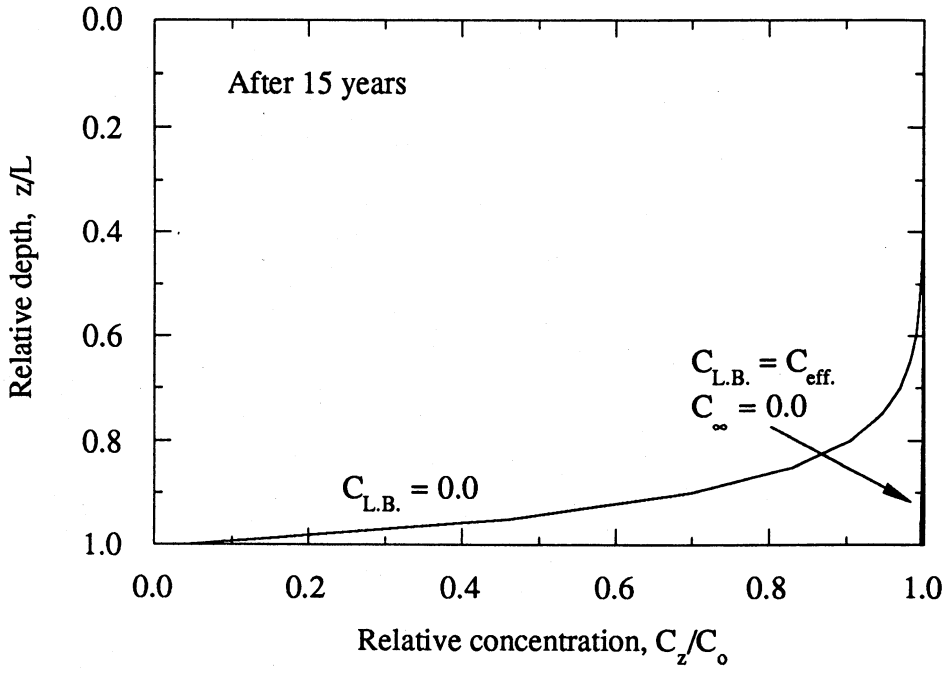

Figure 5.10 Methylene chloride concentration profiles after 15 years.

After the breakthrough of methylene chloride, the zero concentration boundary has a greater concentration gradient at the lower boundary than the other two models. This higher concentration gradient makes higher diffusive mass transfer. The advective and diffusive discharge of methylene chloride predicted under three different lower boundaries after 15 years are shown in Figures 5.11, 5.12, and 5.13.

It is not easy to formulate the boundary conditions. Furthermore, if the soil below the clay liner is not saturated, the mass transport will be more complicated and involve three different phases: solid (soil), liquid (groundwater), and gas (vapor). Depending on the field conditions, proper boundary conditions for the mass transport model should be selected to obtain a representative solution.

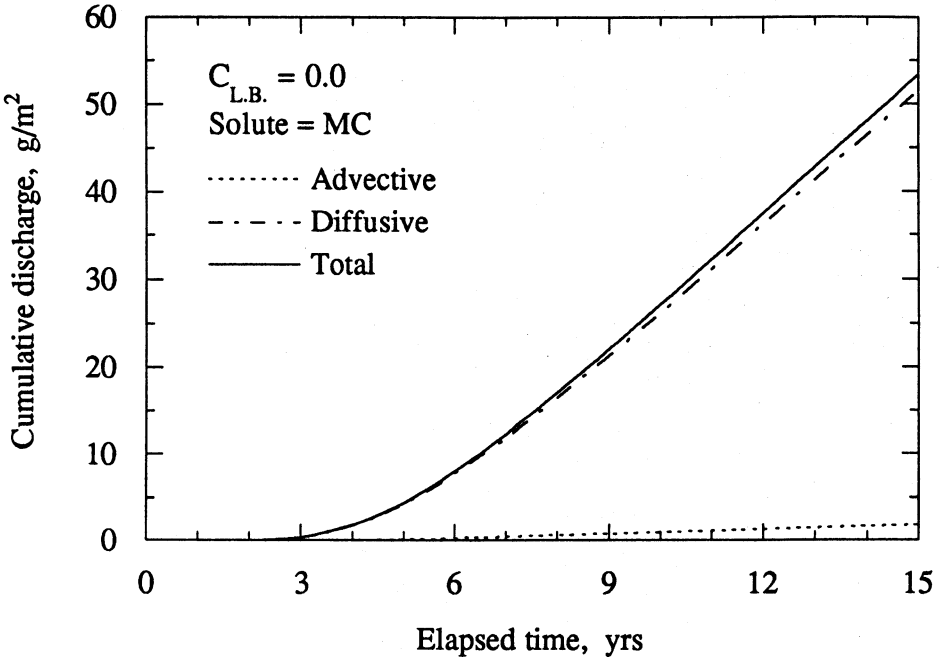

Figure 5.11 Methylene chloride discharge under the zero concentration lower boundary.

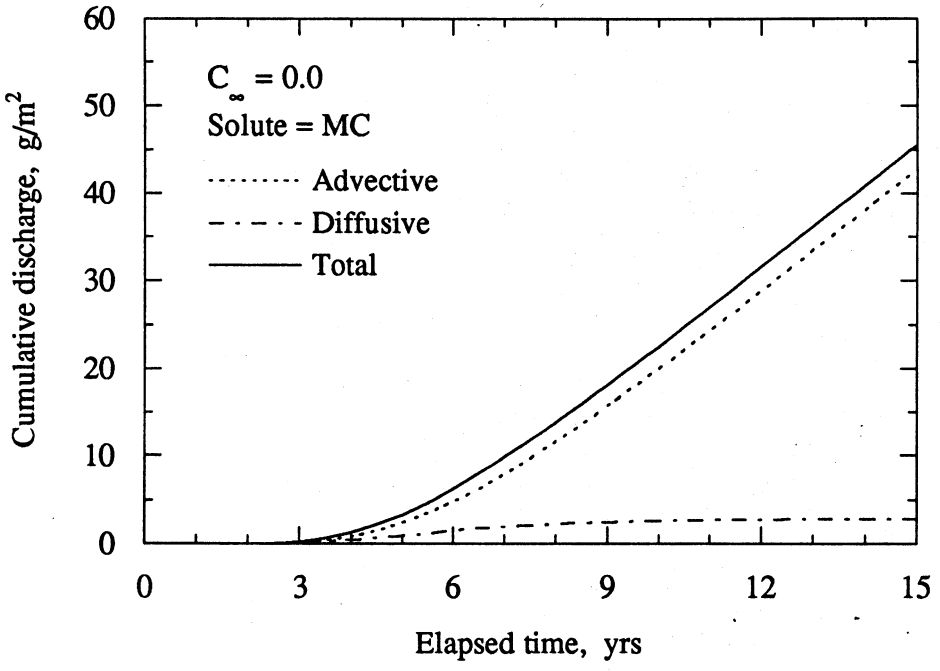

Figure 5.12 Methylene chloride discharge under the Ogata and Banks lower boundary.

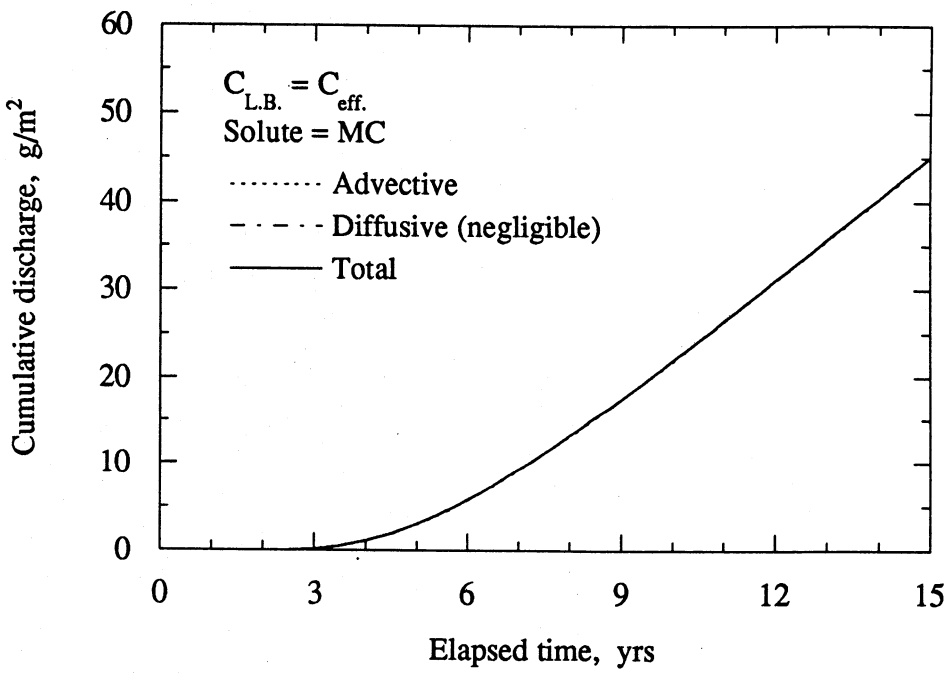

Figure 5.13 Methylene chloride discharge under the equal concentration lower boundary.

5.2 THE SORPTION OF ORGANIC COMPOUNDS ONTO TIRES

5.2.1 Ground Tires

5.2.1.1 Isotherm model

The most frequently used isotherm models are the linear model, Freundlich model, and Langmuir model. The linear model and Freundlich model were compared under the single-component system. The results are listed in Table 5.2.

The parameters in Table 5.2 were obtained by the linear regression with the zero intercept. The two models showed high values of the correlation coefficient except chloroform and methylene chloride within the concentration range tested. For chloroform and methylene chloride, the estimate of the partition coefficient was affected by a small experimental error because those compounds were less sorbed onto ground tires; consequently, the difference between the initial and final aqueous concentration in batch

tests was small.

Table 5.2 Comparison between linear model and Freundlich model.

VOCs	# of tests	Linear model		Freundlich model		
		K_p (L/kg)	R^2	K_f (L/kg)	N_f	R^2
Chloroform	13	51.50	0.3766	53.06	0.984	0.3622
Ethylbenzene	15	978.78	0.9813	1013.45	0.998	0.9917
Methylene chloride	14	11.10	0.5716	3.69	1.304	0.6512
Toluene	15	294.15	0.9825	303.32	0.991	0.9849
1,1,1-Trichloroethane	14	162.95	0.6368	278.23	0.839	0.7560
Trichloroethylene	14	263.27	0.8785	163.34	1.155	0.8935
m -Xylene	14	1046.30	0.9777	1011.35	0.990	0.9832

According to the regression results, the two compared models did not show any significant difference. The Feundlich model parameter, N_f, was very close to unity; thus, for simplicity in mathematical modeling, the linear model was selected to explain the organic compound sorption onto tires.

5.2.1.2 Presence of other organic compounds

The presence of other organic compounds may affect the organic compound sorption onto tires. Theoretically, the partition coefficient is the distribution ratio of activities between two different phases. When two organic compounds are mixed and exist in an aqueous solution, the activities of the two organic compounds are affected. The activity of organic compounds in a mixed solution can be estimated by using the UNIQUAC equation (Prausnitz et al., 1986). In this study, due to complexity and impracticability, the activity coefficient was assumed to be unity.

Batch isotherm tests were conducted to evaluate the effect of the presence of other organic compounds on the sorption of organic compounds onto tires. The results are

summarized in Table 5.3. A t-test was conducted to assess whether the partition coefficients in the single-component and the multi-component systems were different. The results are summarized in Table 5.4.

Table 5.3 Comparison of the partition coefficients obtained in single-component and multi-component systems.

VOCs	Partition coefficient (L/kg)					
	Single-component			Multi-component		
	Average	s[1]	# of tests	Average	s[1]	# of tests
Chloroform	51	11.3	13	54	12.6	13
Ethylbenzene	1,012	68.6	15	852	298.3	11
Methylene chloride	11	1.8	14	12	1.8	11
Toluene	297	21.4	15	290	82.6	13
1,1,1-Trichloroethane	170	27.6	14	199	53.8	13
Trichloroethylene	261	76.5	14	237	69.4	12
m -Xylene	1,000	118.6	14	956	311.8	11

1: Standard deviation.

Table 5.4 Results of t-test between single-component and multi-component sorption tests.

$H_o : K_p$ (single) = K_p (multi)

VOCs	v	$t_{0.025,v}$	|t|	Decision
Chloroform	24	2.064	0.604	Does not reject H_o
Ethylbenzene	24	2.064	2.019	Does not reject H_o
Methylene chloride	23	2.069	2.044	Does not reject H_o
Toluene	26	2.056	0.350	Does not reject H_o
1,1,1-Trichloroethane	25	2.060	1.786	Does not reject H_o
Trichloroethylene	24	2.064	0.557	Does not reject H_o
m -Xylene	23	2.069	0.481	Does not reject H_o

The hypothesis that the mean value of the partition coefficient measured in the single-component system is equal to that in the multi-component system is not rejected. Therefore, within this experimental accuracy and the concentration range tested, organic compounds do not seem to affect each other's sorption significantly. Also, it can be said that the organic compounds do not compete in sorbing onto ground tires in the diluted condition (< 0.6 mM). According to a previous study (Wang and Govind, 1993), the sorption of toxic organic compounds onto wastewater solids was not affected by the presence of competing compounds.

5.2.1.3 Effect of inorganic ions and pH

The presence of inorganic ions may affect the activities of organic compounds. The dissolution of an inorganic salt increases the ionic strength of the solution. Consequently, the activities of inorganics in the solution may change. The activity of an ionic substance can be estimated easily. However, the effect of increased ionic strength by salt addition on the activities of organic substance in a solution has not been studied extensively.

Competition between inorganics and organics may occur. Inorganics are also known to be sorbed onto tires. If the sorption mechanism of orgainc and inorganic compounds is the same, there should be a competition for limited sorption sites in tires. Because of this, the organic sorption capacity of tires may be reduced by the presence of the inorganic substances. The addition of salts may decrease the solubility of the organic solutes in solution (Edil et al., 1991). The organic sorption can be increased by the presence of the inorganic salts.

Batch isotherm tests were conducted to evaluate the effect of inorganic substances and pH on the organic compound sorption onto ground tires. The results are listed in Tables 5.5 and 5.6. These tests were conducted under a multi-component condition.

A t-test was conducted to evaluate the effect of four different factors on the organic

compound sorption onto tires: (1) the presence of inorganic substances, (2) the extremely acidic condition (pH = 2), (3) the slightly basic condition (pH = 9), and (4) the extremely basic condition (pH = 11). Batch tests were performed under the multi-component condition with the deionized water at pH 7 as control tests. The experimental conditions of each factor were given in Tables 2.2, 2.4, and 2.5.

Table 5.5 Results of the effect of inorganic substances on organic sorption.

VOCs	Partition coefficient (L/kg)					
	Distilled water (Control)			Salts containing water		
	Average	s[1]	# of tests	Average	s[1]	# of tests
Chloroform	54	12.6	13	57	3.6	11
Ethylbenzene	852	298.3	11	936	87.4	10
Methylene chloride	14	3.0	13	14	3.0	11
Toluene	290	82.6	13	318	12.9	11
1,1,1-Trichloroethane	199	53.8	13	218	8.3	11
Trichloroethylene	237	69.4	12	265	11.4	11
m -Xylene	956	311.8	11	989	112.8	11

Table 5.6 Results of the effect of pH on organic sorption.

VOCs	Partition coefficient (L/kg)								
	pH = 2			pH = 9			pH = 11		
	Average	s[1]	#	Average	s[1]	#	Average	s[1]	#
CF	53	4.6	7	54	1.4	7	N.A.[2]	N.A.[2]	N.A.[2]
EB	1,036	65.8	7	948	137.9	7	957	116.9	6
MC	15	2.7	7	13	1.7	7	10	1.2	6
TOL	322	16.6	7	317	26.2	7	274	19.2	6
TCA	212	8.8	7	214	10.7	7	185	7.6	6
TCE	259	12.7	7	256	22.3	7	240	13.1	6
XYL	988	89.4	7	975	172.4	7	982	139.7	6

1: Standard deviation.

2: Not avaiable because chloroform was degraded under a high hydroxide condition.

The t-test results are shown in Table 5.7. The hypothesis that the mean values of partition coefficients, except methylene chloride, measured under different conditions are identical to each other was not rejected. Therefore, within this experimental range, the effect of inorganic ions and pH on the organic compound sorption does not seem to be significant. Also, it can be said that the mechanism of organic compound sorption onto tires is not the same as that of inorganic ions, e.g., ion exchange.

Table 5.7 ANOVA table for the data in Tables 5.2, 4, and 5. (upper 5% point).

H_o : Kp (i) = Kp (j) ··· = Kp (k)

	CF	EB	MC	TOL	TCA	TCE	XYL
k	4	5	5	5	5	5	5
N	38	41	42	43	44	43	42
ν_T	3	4	4	4	4	4	4
ν_R	34	36	37	38	39	38	37
ν_D	37	40	41	42	43	42	41
Grand Average	54.92	935.65	12.88	304.74	206.22	251.44	977.05
S_T	101	151,333	88	12,670	5,593	5,759	7,341
S_R	2,166	1,167,087	191	90,815	36,800	59,084	1,423,606
S_D	2,267	1,318,420	279	103,485	42,393	64,844	1,430,947
s^2_T	34	37,833	22	3,167	1,398	1,440	1,835
s^2_R	64	32,419	5	2,390	944	1,555	38,476
F	0.53	1.17	**4.26**	1.33	1.48	0.93	0.05
F(k,40)	2.61	2.61	2.61	2.61	2.61	2.61	2.61
F(k,60)	2.53	2.53	2.53	2.53	2.53	2.53	2.53
Decision	N.R [1]	N.R.	R [2]	N.R.	N.R.	N.R.	N.R.

1 : Does not reject H_o.

2 : Reject H_o.

The experimental data of chloroform batch isotherm tests at pH = 11 were not available since chloroform was completely degraded under extremely high pH conditions.

Thus, the number of treatments, k, in Table 5.7 was 4 instead of 5. For methylene chloride, the partition coefficient values were more scattered, resulting in a higher standard deviation.

5.2.1.4 Effect of particle size

If organic compounds are adsorbed onto only the surface of the tire, the size of the particle will be an important factor. Table 5.8 shows the results of the multi-component sorption isotherm tests by using two different particle sizes.

Smaller ground tires had higher partition coefficients than larger ones since less textiles and steel are contained as the particle size of ground tire decreases. Figures 5.14 and 5.15 show the sorption isotherm results of methylene chloride and toluene. The plots for the other compounds are listed in Appendix E. Due to the low sorption capacity of ground tires and a greater analytical error, methylene chloride had more scattered isotherm results than toluene and other organic compounds.

Table 5.8 Results of the effect of particle size on organic sorption.

VOCs	Partition coefficient (L/kg)					
	2.38 < d < 2.83 mm			1.41 < d < 2.00 mm		
	Mean	s[1]	# of tests	Mean	s[1]	# of tests
Chloroform	68	8.6	6	64	13.3	5
Ethylbenzene	844	166.1	6	1,037	169.8	5
Methylene chloride	17	4.8	6	19	6.1	5
Toluene	301	32.7	6	336	49.3	5
1,1,1-Trichloroethane	223	17.1	6	229	24.6	5
Trichloroethylene	262	24.9	6	276	39.9	5
m -Xylene	835	180.2	6	1,074	177.7	5

1: Standard deviation.

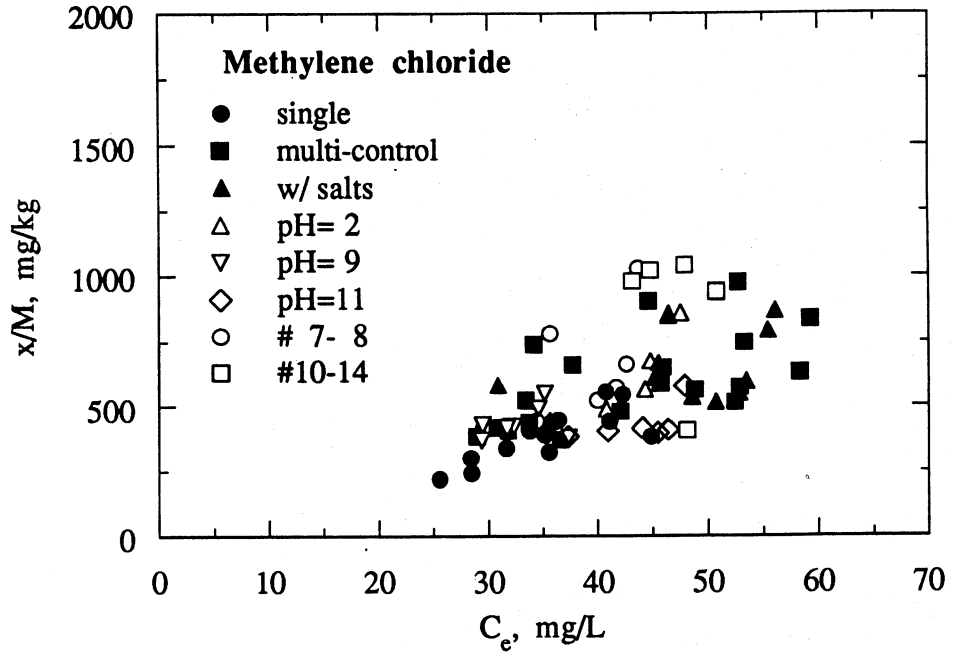

Figure 5.14 Methylene chloride batch isotherm tests.
(# 7- 8 = 2.38 < d < 2.83 mm, and #10-14 = 1.41 < d < 2.00)

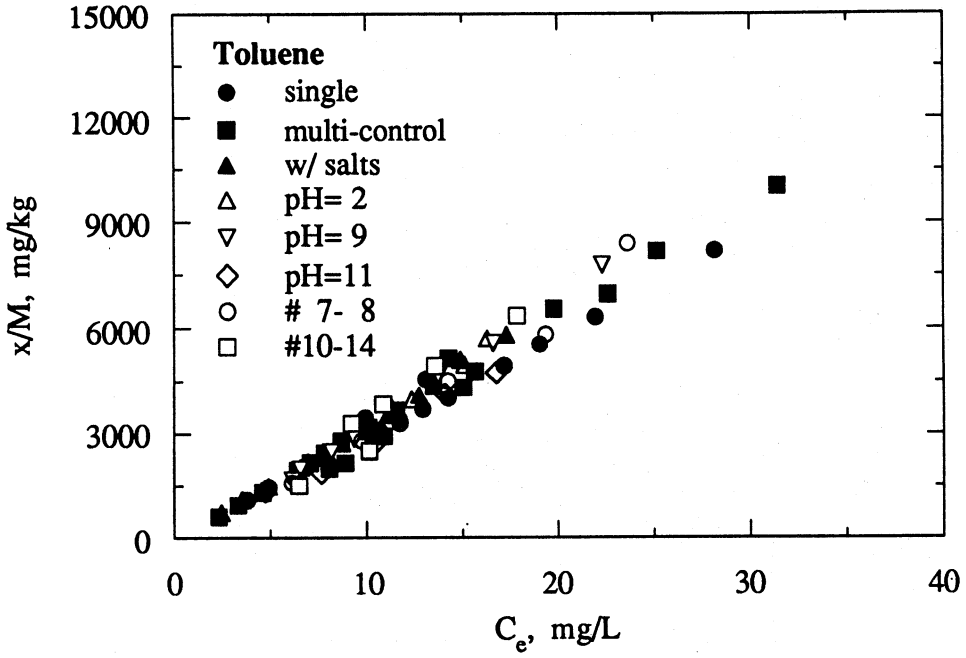

Figure 5.15 Toluene batch isotherm tests.
(# 7- 8 = 2.38 < d < 2.83 mm, and #10-14 = 1.41 < d< 2.00)

5.1.1.5 Effect of temperature

Sorption isotherm tests were conducted at 4°C and 55°C to evaluate the effect of temperature on the organic compound sorption onto tires. The high temperature of 55°C was chosen since the temperature in the landfill is typically 55°C. These tests were not conducted under a rotating condition. The test tubes were kept in a temperature controlled room.

The temperature dependence of equilibrium capacity for sorption can be explained by the heat of solution, ΔH (Weber, 1972). Based on the Arrheunius equation, the partition coefficient at a given temperature can be expressed by the heat of solution, gas constant, and temperature as follows:

$$K_p = \alpha \cdot \exp\left(-\frac{\Delta H}{R \cdot T}\right) \tag{5.1}$$

where α = constant (L/kg);

R = gas constant (= 1.987 cal/mol·K); and

T = absolute temperature, K.

The heat of solution can be obtained by plotting ln K_p versus (1/T). Table 5.9 lists the estimated values of heat of solution of organic compounds in tire.

Table 5.9 Heat of soultions of organic compounds in tire.

VOCs	ΔH (kcal/mol)
Chloroform	- 0.4
Ethylbenzene	- 0.2
Methylene chloride	- 0.6
Toluene	+ 0.3
1,1,1-Trichloroethane	+ 0.7
Trichloroethylene	- 0.1
m-Xylene	- 0.2

All of the organic compounds tested had relatively low heat of solution less than unity. This implies that the sorption of organic compounds tested onto tire is not affected significantly by temperature change. The aqueous phase adsorption has smaller heat effects than the gas phase sorption because water is desorbed from the surface of sorbent when sorption occurs (Weber, 1972). According to a previous study, the heat of solution for toluene vapor in polybutylene was - 9.2 kcal/mol (Park and Bontoux, 1991).

The chemical sorption is known as an exothermic reaction (Weber, 1972). It means the heat of solution is negative. In the case of toluene and trichloroethane, the values of heat of solution of toluene and trichloroethylene were positive. It seems that the heat of solutions of the organic compounds tested are too small to be identified by using the two temperatures tested.

The batch isotherm tests conducted under static conditions showed less loss of organic compounds during tests than those under the rotating condition. Consequently, some of the partition coefficients obtained at 4°C were lower than those obtained under 20°C. Thus, the data obtained at 20°C were not used to estimate the heat of solutions of organic compounds. More batch isotherm tests for the estimation of the temperature effect on the organic compound sorption onto tires will be conducted at a few different temperatures.

5.1.1.6 Structure-activity relationship for partition coefficient

The partition coefficient of the organic compounds has been found to have a good relationship with the solubility of the organic compounds or the octanol-water partition coefficient (Park et al., 1991a). Figure 5.16 shows the relationship between the partition coefficient and octanol-water partition coefficient of the seven organic compounds tested.

The logarithmic values of the partition coefficients of organic compounds onto ground tires were proportional to the logarithmic values of the octanol-water partition

coefficients. The regression equation is given as follows:

$$\log K_p = -0.137 + 0.983 \cdot \log K_{ow} \quad (R^2 = 0.997) \tag{5.2}$$

For most organic compounds, the octanol-water partition coefficient can be obtained in the literature. Therefore, from the above relationship, the partition coefficient of untested organic compounds can be predicted.

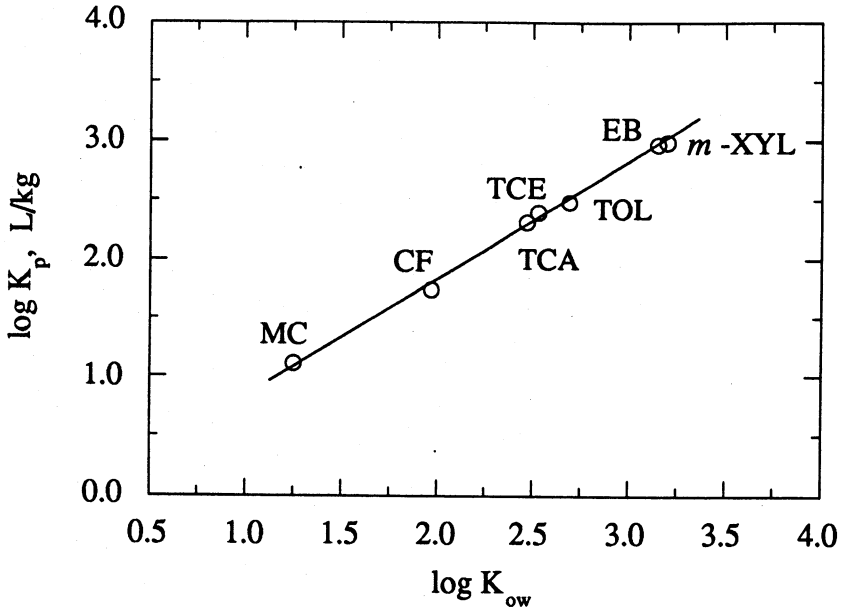

Figure 5.16 Relationship between tire-water partition coefficient and octanol-water partition coefficient of seven organic compounds.

5.1.1.7 Structure-activity relationship for diffusion coefficient

The partiton and diffusion coefficients control the sorption of organic compounds onto tires. With the two key parameters, the required time to reach equilibrium can be assessed. When ground tires are suspended in a well mixed solution, the concentration decrease can be expressed using Eq. 2.44, which contains the partition and diffusion coefficients. The diffusion coefficient was determined by changing the value until finding the best fitting curves which have the least sum of square by trial and error.

One of the best curve fits of the observed data of trichloroethylene is shown in Figure 5.17. The partition coefficient obtained from batch tests was used. The diffusion coefficient was estimated to be 7.9×10^{-8} cm^2/sec. Three organic compounds were tested to obtain the general range of diffusion coefficients of organic compounds through a polymer (Park et al., 1991a).

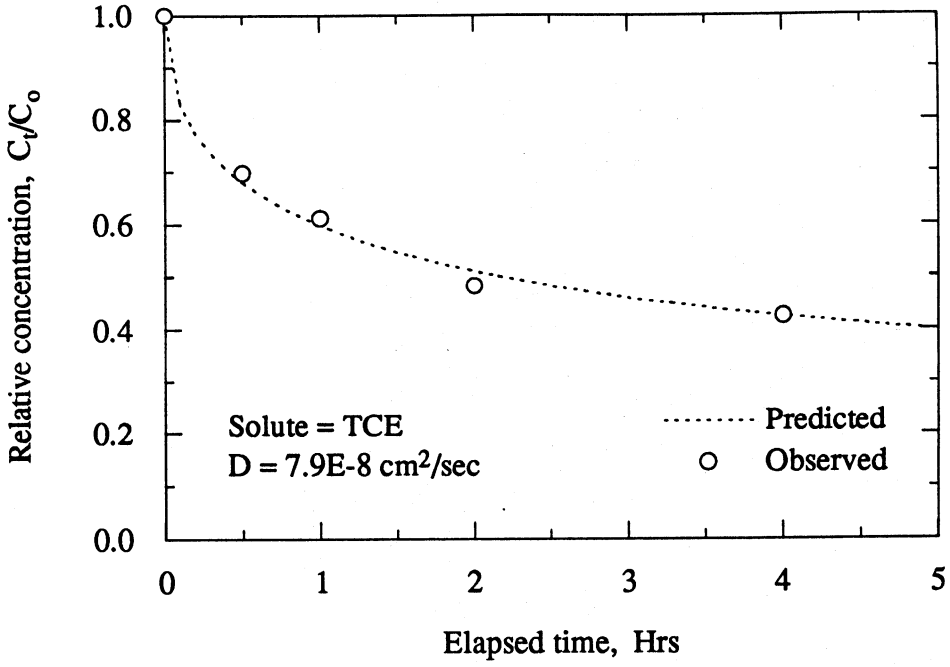

Figure 5.17 Estimation of diffusion coefficient through tire rubber.

It is implicit that as the size of the permeant molecule increases, the activation energy for diffusion through a polymer should increase and the diffusion coefficient should decrease (Glasstone et al., 1941). This phenomenon has been observed by previous studies (Frensdorff, 1964; Berens, 1985; Park et al., 1991a; Park and Nibras, 1993). Figure 5.18 shows the relationship between the diffusion coefficients and the molecular diameters of the three organic compounds listed in Table 3.3.

As expected, the diffusion coefficient of the organic compounds through tires increased with decreasing molecular size. The relationship can be semi-logarithmically

expressed as follows:

$$\log D = -2.747 - 8.259 \cdot d_s \quad (R^2 = 0.908) \tag{5.3}$$

where d_s = molecular diameter (nm).

The difference between the diffusion coefficient in the single and multi-component systems has not yet been investigated. According to a previous study, the diffusion coefficient of an organic compound through HDPE seems to be decreased by the presence of the organic compound which has a greater molecular size or smaller diffusion coefficient (Park and Nibras, 1993). More batch isotherm tests for the estimation of diffusion coefficients will be conducted to assess this effect.

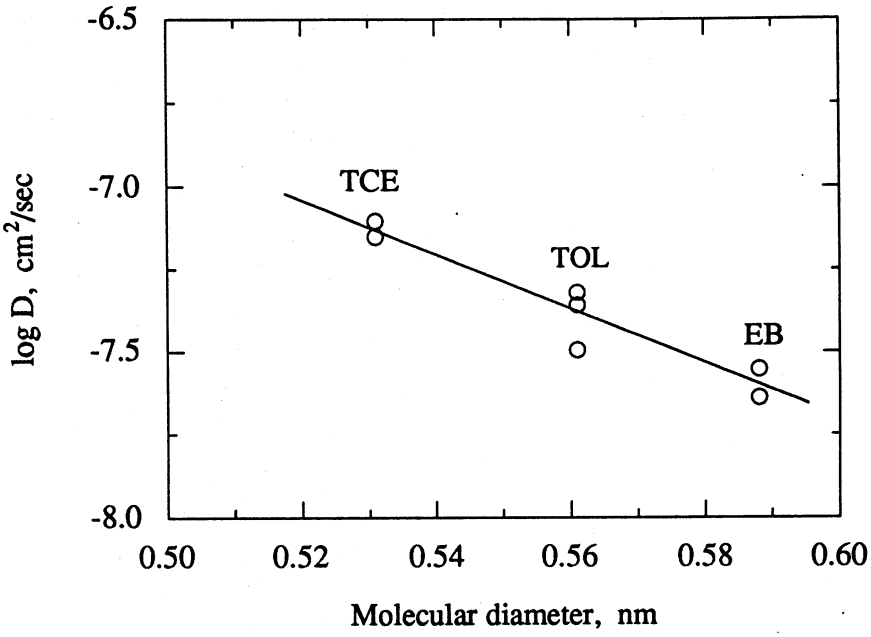

Figure 5.18 Diffusion coefficient and molecular diameter (ground tire).

5.2.2 Tire Chip

The batch isotherm tests with irregularly-shaped tire chips, about 5 × 10 cm were conducted using the 950 mL-Mason jar with a Teflon®-coated cap under a multi-component system. Figure 5.19 shows the comparison between tire chip sorption tests and

ground tire sorption tests.

The slope of the relationship between the partition coefficient versus the octanol-water partition coefficient of tire chips was similar to that of ground tires. The partition coefficient of tire chips was lower in general than that of ground tires because tire chips contain relatively less rubber material, which is the main sorbent. The content of rubber in a tire chip is dependent on the manufacturer or the parts. Manufacturers have their own manufacturing process and formula. Also, within a tire, the sidewall part contains more rubber and less fabric and metal cables than the part which contacts the road surface. In the case of ground tires, the difference of manufacturer or parts should not affect the results of batch isotherm tests significantly because all of the batch sorption tests contained several dozens of ground tires. If the tire chips are applied in the landfill liner system, the effects which can be caused by the difference in tire chips may cancal each other.

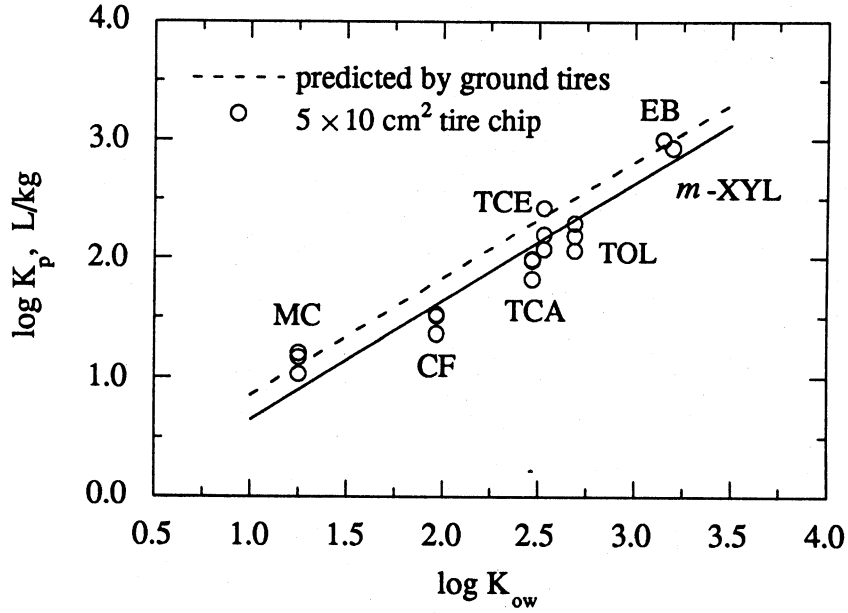

Figure 5.19 Comparision of partition coefficient between tire chips and ground tire.

Since the major sorbent is the rubber materials in tire chips, the partition coefficient of tire chips and ground tires is proportional to the content of the rubber materials. It

means that the regression line of tire chip data has a different intercept but the same slope with that of the ground tire data shown in Eq. 5.2. Then, the following equation can be used to estimate the partition coefficient of tire chips.

$$\log K_p = -0.333 + 0.983 \cdot \log K_{ow} \quad (R^2 = 0.890) \tag{5.4}$$

Eqs. 5.2 and 5.4 indicate that tire chips had approximately a 35% smaller partition coefficient than ground tires. The equilibrium time can be estimated using the partition and diffusion coefficients. Along with Eq. 2.38 subject to the boundary conditions, the concentrations of methylene chloride and *m*-xylene were simulated under a leachate collection system condition. Methylene chloride has the lowest partition coefficient and highest diffusion coefficient among the organic compounds tested. *m*-Xylene has the highest partition coefficient and lowest diffusion coefficient. The partition and diffusion coefficients were estimated by Eq. 5.4 and 5.3, respectively. The porosity of the tire layer was assumed to be 0.5. It was assumed that the tire chips in the tire layer have the same dimension (5 cm in width, 10 cm in length, and 0.5 cm in thickness), and the mass transfer, which occurs perpendicularly to the thickness direction, is negligible. Figures 5.20 and 5.21 show the simulation results for methylene chloride and *m*-xylene.

Methylene chloride and *m*-xylene reached equilibrium within approximately two days and one hour, respectively. Since methylene chloride has a higher diffusion coefficient than *m*-xylene, the mass transfer within tire chips is faster than *m*-xylene under the same concentration gradient. However, the much smaller partition coefficient does not make a high concentration gradient at the interface between the tire surface and the medium solution. For *m*-xylene, the initial mass transfer rate is much faster than methylene chloride because of the high partition coefficient. After a few minutes, due to the lower diffusion coefficient, the mass transfer rate is significantly decreased.

In the leachate collection system, the reaction rate may be increased due to the high

temperature of the landfill. From batch tests, it was found that the effect of temperature on the organic compound sorption onto tires was not significant. However, the diffusion coefficient is affected by temperature. As the temperature increases, the diffusion coefficient increases significantly (Frensdorff, 1964; Park and Bontoux, 1991). The higher diffusion coefficient accelerates the mass transfer and the equilibrium time can be shortened.

Although these simulations may not simulate actual field conditions, it can be said that organic compound sorption onto tires in the leachate collection system reaches equilibrium in a relatively short time. In addition, in a long-term fate study of organic compounds within landfills, the organic compound sorption onto tires can be considered to occur instantaneously.

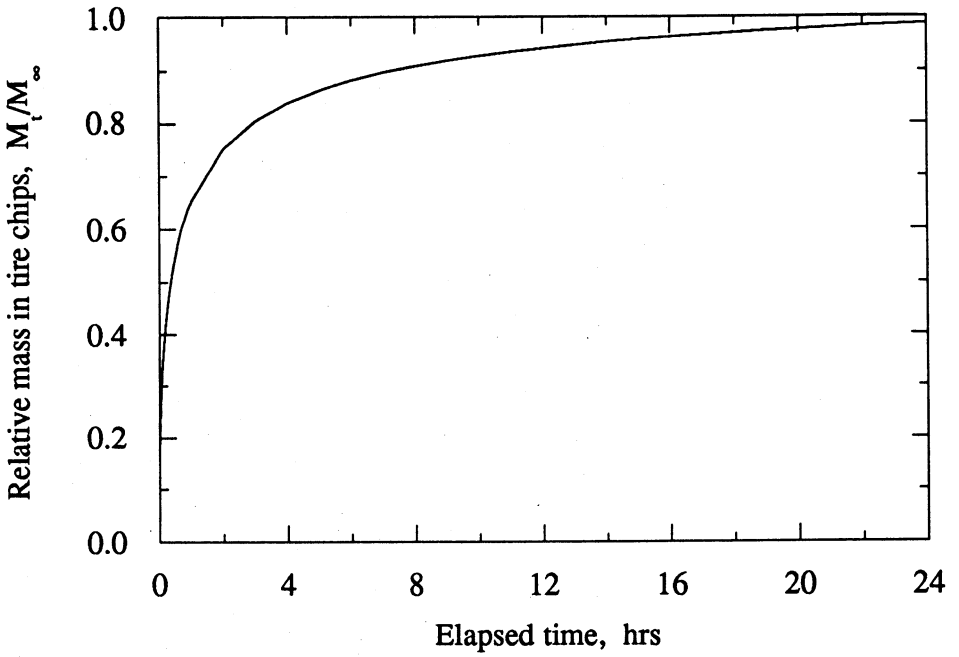

Figure 5.20 The concentration of methylene chloride in the leachate collection system.

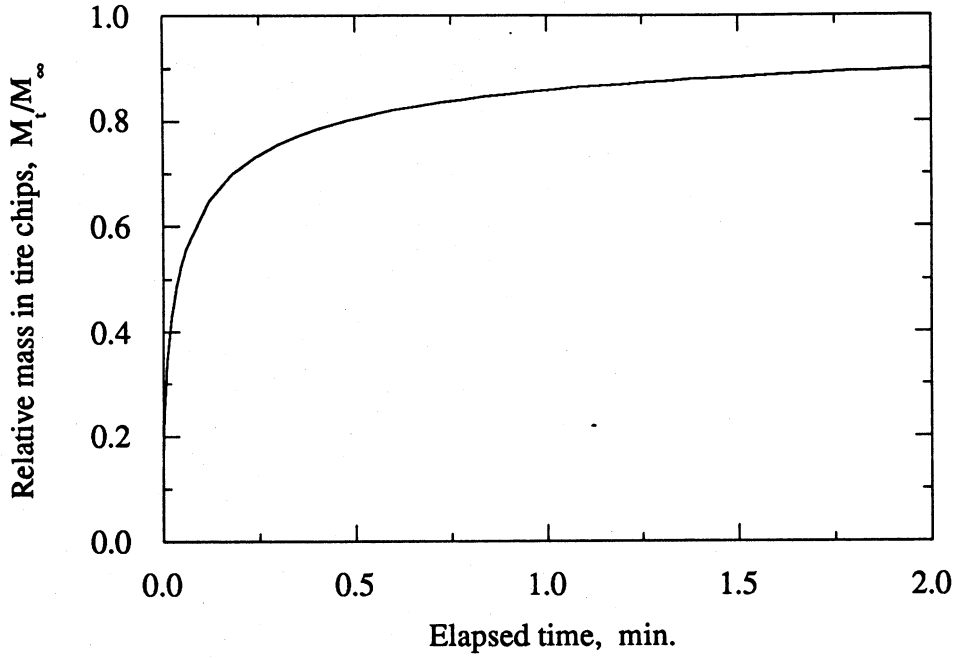

Figure 5.21 The concentration of *m*-xylene in the leachate collection system.

5.3 LONG-TERM TANK TESTS

5.3.1 Tank Compaction

The preparation of tank specimens by compaction was performed following the procedure described in Chapter 3. Water content and lift thickness data are included in Appendix A. The dry density of soil was assumed to be 2.70 g/cm^3 for the estimation of porosity. The volumes of upper and lower reservoirs are approximately 170,000 and 7,300 cm^3, respectively. The properties of tank specimens are listed in Table 5.10.

Table 5.10 Properties of the tank specimens.

	Thickness (cm)	Water content (%)	Dry unit weight (kN/m^3)	Porosity
Tank 2A	12.50	18.7	16.60	0.37
Tank 4	12.00	18.0	17.40	0.34
Tank 5	12.20	18.3	17.07	0.36
Tank 6	12.28	18.5	16.93	0.36

5.3.2 Hydraulic Conductivity

Table 5.11 shows the average and standard deviation of the hydraulic conductivity of the four long-term tank tests. The average and standard deviation data were calculated using the outflow data. There was no significant difference between the inflow and outflow hydraulic conductivities. When the gas in the tanks was vented, a small fraction of the solution in the upper reservoir was lost and the loss of solution was compensated for by the solution in the inflow bag. Due to the incorrect weighing of the amount of the inflow during every weighing period, the hydraulic conductivity was estimated by the outflow.

Table 5.11 Results of hydraulic conductivity in tank tests ($\times 10^{-8}$ cm/sec).

Tank	Hydraulic gradient	Hydraulic conductivity			
		Before VOC spiking		After VOC spiking	
		Average	s[1]	Average	s[1]
Tank 2A	2.86	0.94	0.19	1.25	0.77
Tank 4	2.98	1.54	0.51	1.48	0.53
Tank 5	2.93	1.34	0.27	1.84	0.78
Tank 6	2.91	1.45	0.31	1.93	0.75

1: Standard deviation.

Figure 5.22 shows the trend for the hydraulic conductivity versus time for tank 5. The trend shown for tank 5 is typical of the other tank tests, tank 2A, 4, and 6, shown in Appendix F.

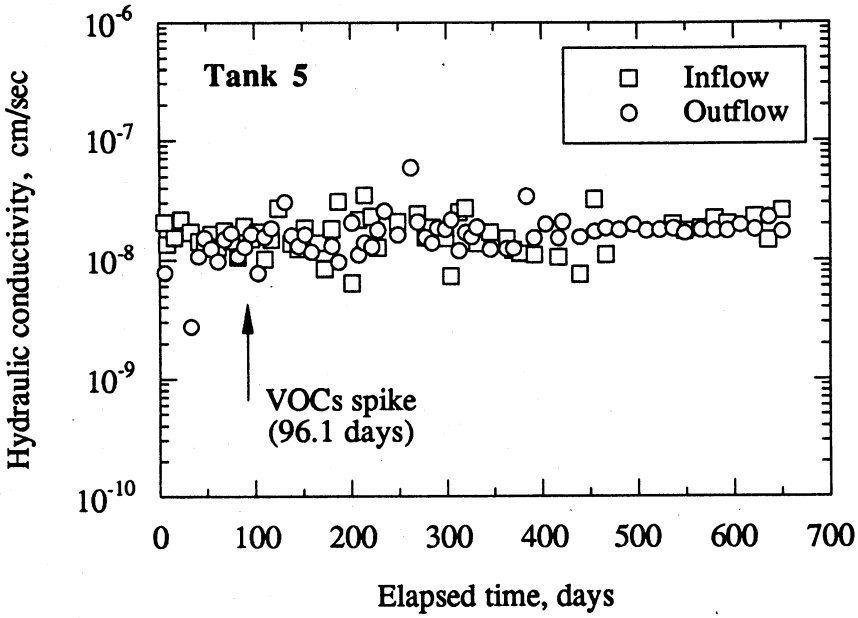

Figure 5.22 Hydraulic conductivity in tank 5.

The hydraulic conductivity was stable in all the tanks. In Table 5.11, the hydraulic conductivity of the three tanks increased slightly after spiking organic compounds. The

organic compounds spiked cannot affect the hydraulic conductivity instantaneously. The increased hydraulic conductivity was not caused by the spiked organic compounds because when organic compounds were spiked, the hydraulic conductivity was still stabilizing and increasing. Also, there was no significant effect of tire chips on the hydraulic conductivity of the clay layer.

The side wall leakage did not seem to occur. In a fixed wall permeability test, if a permeant leaks along the side wall of the permeameter, a dramatically increased hydraulic conductivity was observed (Wambold, 1993).

5.3.3 Tracer

In order to evaluate the stability of a tracer, batch isotherm tests were conducted. The glass tubes containing bromide solution and ground tires or Kirby Lake Till were placed in a constant temperature room (20°C). The concentration after 33 days was considered to be the equilibrium concentration. Table 5.12 lists the results of batch isotherm tests. The equilibrium concentration was nearly always within 2% of the initial concentration. The tracer used in this study, LiBr, showed satisfactory stability during sorption tests.

Table 5.12 Results of tracer (Br^-) sorption tests.

Sorbent	C_e/C_0 - measured				
	Average	Min.	Max.	s[1]	# of tests
Soil	0.99	0.98	1.00	0.008	8
Ground tire	0.99	0.98	1.02	0.015	7
Blank	0.99	0.93	1.01	0.031	6

1: Standard deviation.

In the tank tests, the target concentration of bromide in the upper reservoir was 16

mg/L. Figure 5.23 is the bromide concentrations in the upper reservoirs of the four tanks. As expected by the results of batch isotherm tests, the bromide concentrations in the upper reservoirs were stable and close to 16 mg/L.

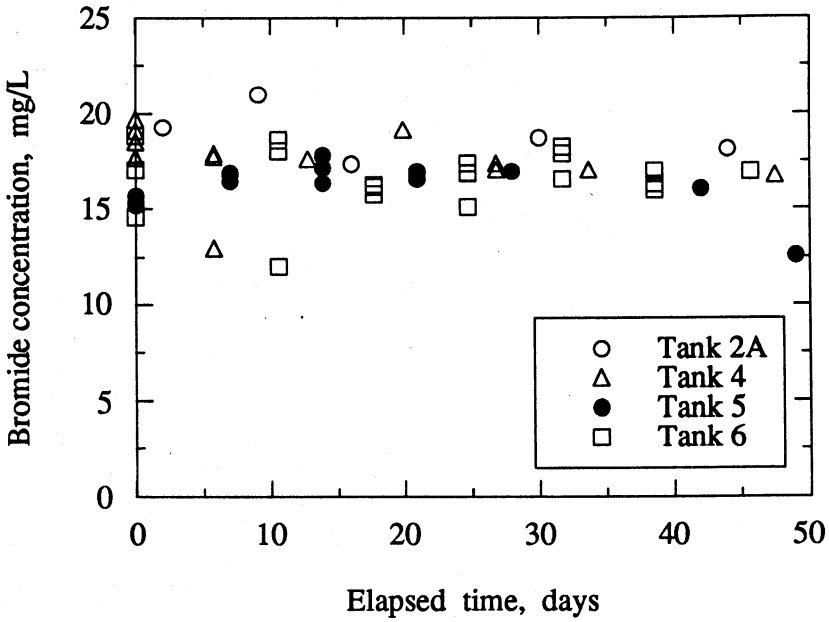

Figure 5.23 Bromide concentration in the upper reservoir.

The apparent tortuosity of bromide was estimated using a numerical model and the observed breakthrough data of bromide. For the numerical solution, the bromide concentration at the upper boundary was considered to be constant as 16 mg/L. The free solution diffusion coefficient of bromide used for the estimation of the apparent tortuosity was 20.8×10^{-6} cm^2/sec (Shackelford and Daniel, 1991a). Figure 5.24 is the observed breakthrough data of bromide versus the best curve obtained by the numerical model. The plots for the other tanks are shown in Appendix G.

The values of the apparent tortuosity of bromide in the four tank specimens ranges from 0.2 to 0.3. The effective porosity was assumed to be 90% of the total porosity of each tank specimen. The effect of the effective porosity was not as significant as that of the

apparent tortuosity. Figure 5.25 shows the effect of the effective porosity on the bromide breakthrough curves under the conditions of tank 2A. More accurate estimation of the apparent tortuosity of bromide will be performed after more data are obtained.

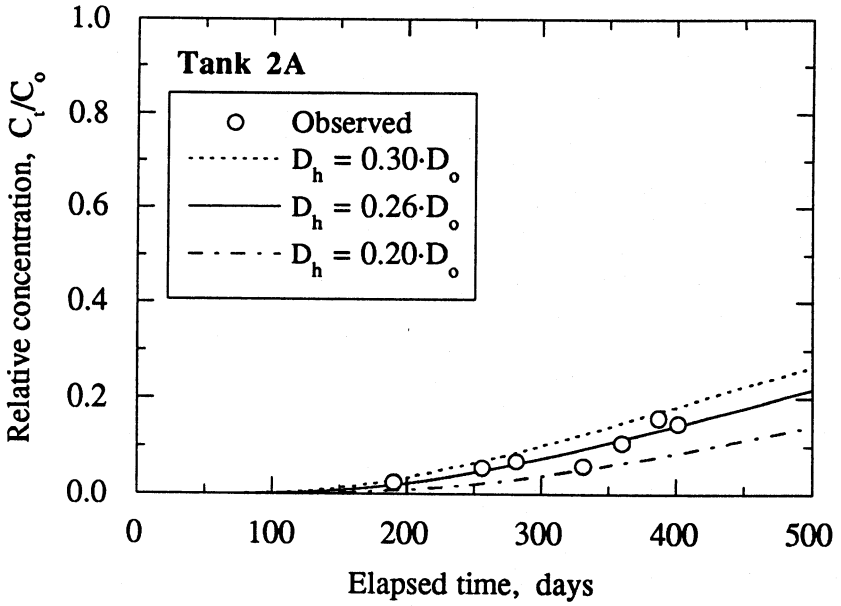

Figure 5.24 Bromide breakthrough curves in tank 2A.

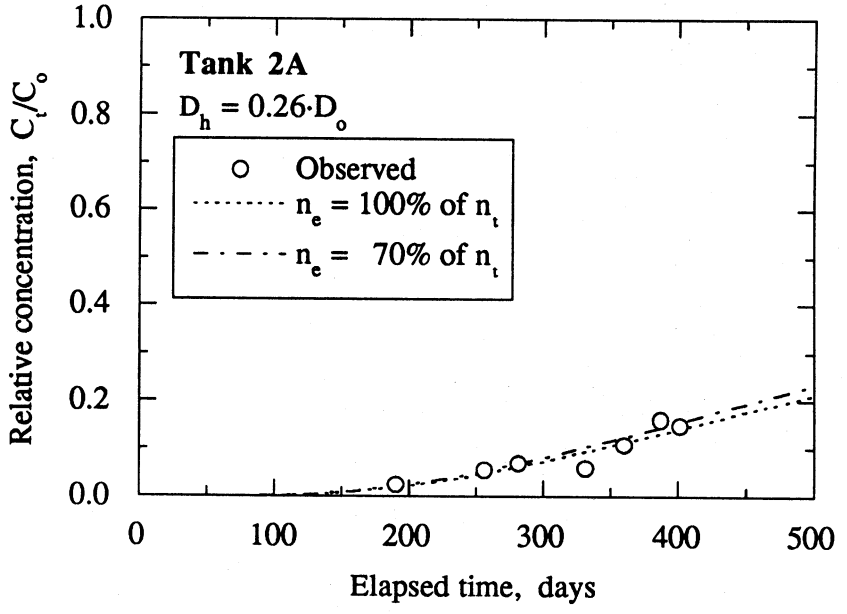

Figure 5.25 The effect of effective porosity on the bromide breakthrough curve.

5.3.4 The Sorption of Organic compounds onto Kirby Lake Till

A few sets of batch isotherm tests using the Kirby Lake Till have been conducted. The partition coefficients of methylene chloride, toluene, and trichloroethylene were estimated. Also, the partition coefficients estimated by emipirical equations were compared with the experimentally obtained values. The comparision is shown in Figure 5.26.

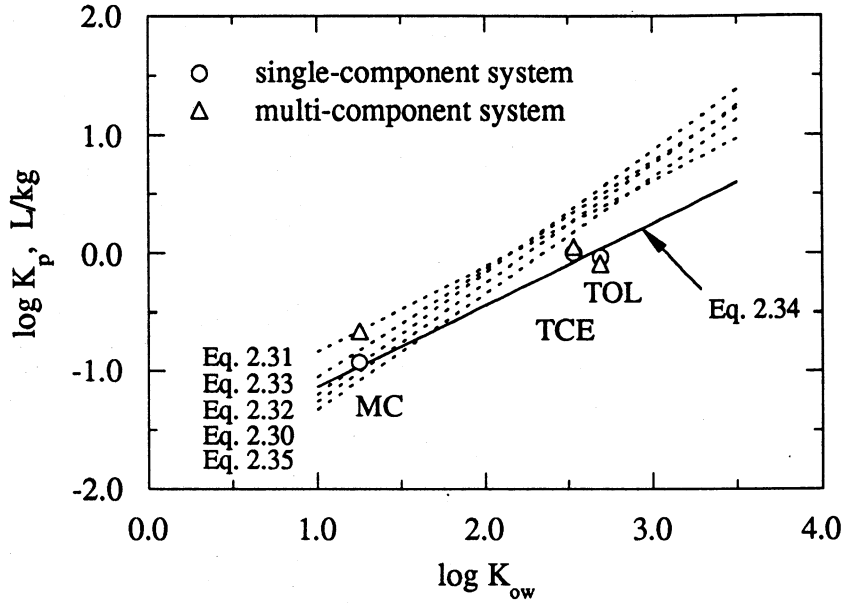

Figure 5.26 Comparison between the experimentally obtained partition coefficients and the predicted values by empirical equations.

For the three organic compounds tested and Kirby Lake Till, the Piwoni and Barnerjee's empirical equation, Eq. 2.34, shows the best agreement with the experimental data. In the case of toluene and trichloroethylene, higher partition coefficients were predicted by the other six equations. The partition coefficients of seven organic compounds estimated by Eq. 2.34 and obtained from laboratory tests are listed in Table 5.13. The K_p values in Table 5.13 are the averages of the single and multi-component batch tests. The tests for other compounds are still in progress and they will be compared with the values in Table 5.13.

Table 5.13 Partition coefficient estimated by Eq. 2.34 (f_{oc} = 9.1%).

Organic compounds	Piwoni and Barnerjee (1989)			Laboratory
	log K_{ow}	log K_{oc}	K_p (L/kg)	K_p (L/kg)
CF	1.97	1.579	0.345	N.A.
EB	3.15	2.394	2.252	N.A.
MC	1.25	1.083	0.110	0.162 ± 0.080
TOL	2.69	2.076	1.084	0.922 ± 0.457
TCA	2.47	1.924	0.764	N.A.
TCE	2.53	1.966	0.841	1.077 ± 0.277
XYL	3.20	2.428	2.438	N.A.

Although there had been some disagreements, several investigators have concluded that the sorption of organic compounds on soils and sediments is not affected by the presence of competing organic compounds (Wang and Govind, 1993). The effect of the presence of other organic compounds will be investigated further.

5.3.5 Organic Compounds in the Upper and Lower Reservoirs

The concentrations of organic compounds in the upper and lower reservoirs have been monitored. The target initial concentrations of methylene chloride, toluene, and trichloroethylene were 16.0 mg/L. The organic compounds were detected at higher concentrations than the target initial concentration. This difference may be caused by analytical error or an incorrect amount of organic compounds injected into tanks. The concentrations in the upper reservoir were shown in Figures 5.24, 5.25, and 5.26.

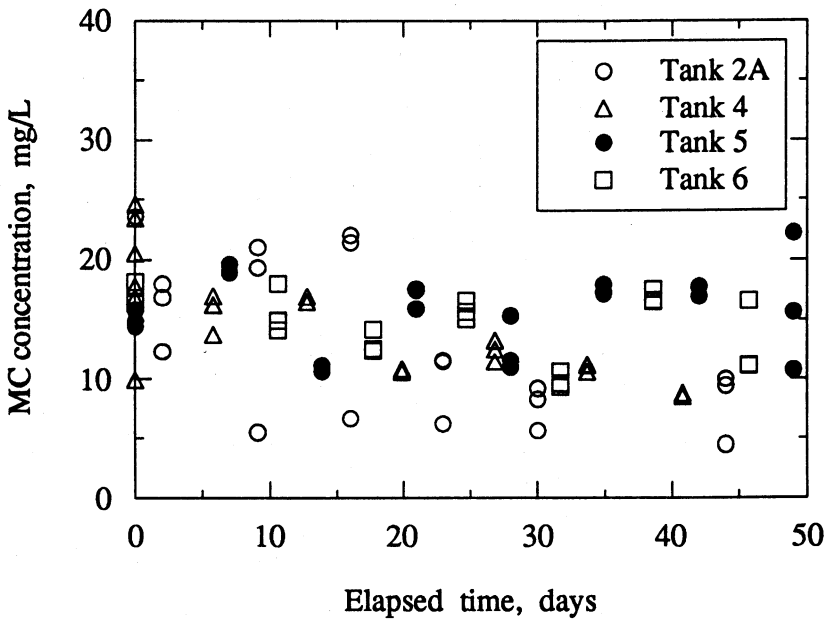

Figure 5.24 Methylene chloride concentration in the upper reservoir.

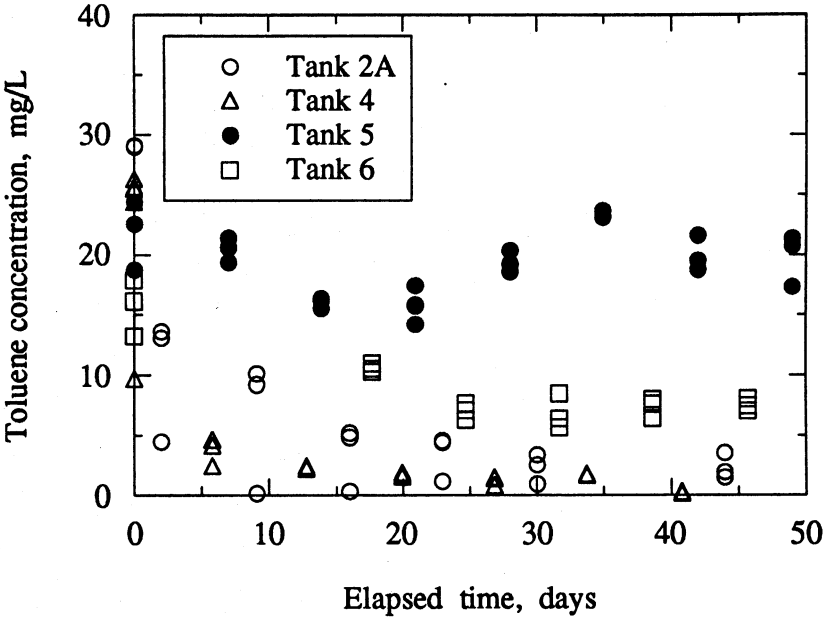

Figure 5.25 Toluene concentration in the upper reservoir.

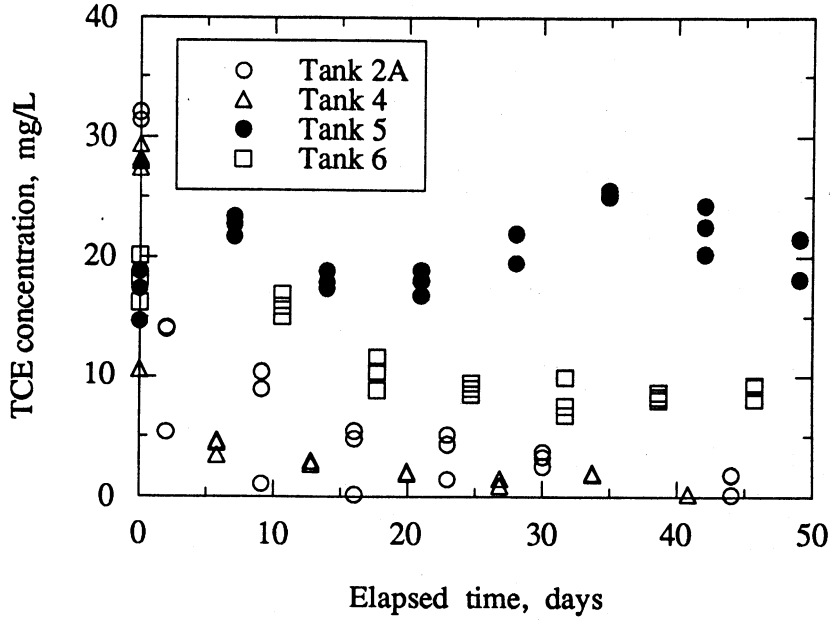

Figure 5.26 TCE concentration in the upper reservoir.

The organic compound concentrations in tank 5, which does not contain tire chips, were relatively constant and higher than those in the three other tanks which contain tire chips because the sorption of organic compounds onto tire chips is much greater and faster than the mass transfer of organic compounds through a clay layer. The concentrations of organic compounds in the upper reservoirs in tanks 2A and 4 were very close. Thus, it can be said that Styroform® does not sorb organic compounds significantly and does not affect the organic compound sorption onto tire chips.

It is impossible to keep the organic compounds within the inflow and outflow bags. The potential losses are caused by volatilization and permeation through Teflon®. Halogenated hydrocarbons can be stored without significant loss in the Teflon® vial within five weeks (Reynolds et al., 1990). The concentrations of methylene chloride, toluene, and trichloroethylene in the Teflon® bag were relatively stable within approximately 20 days (Heim, 1992). Thus, if the solution in the influent bag is totally replaced every two weeks, the losses of organic compounds can be negligible. The losses of seven organic compounds from the Teflon® bag will be tested for the proceeding column tests.

Although approximately 700 days have passed, no organic compounds are detected in the effluent reservoirs of the test tanks. For tanks 2A and 4, since most of toluene and trichloroethylene were sorbed onto tire chips, those organic compounds could not penetrate the clay layer efficiently. Figure 5.27 shows the concentration-depth profiles of organic compounds in tank 5 which were estimated by the numerical model. The apparent tortuosity of each organic compound was assumed to be identical to that of bromide.

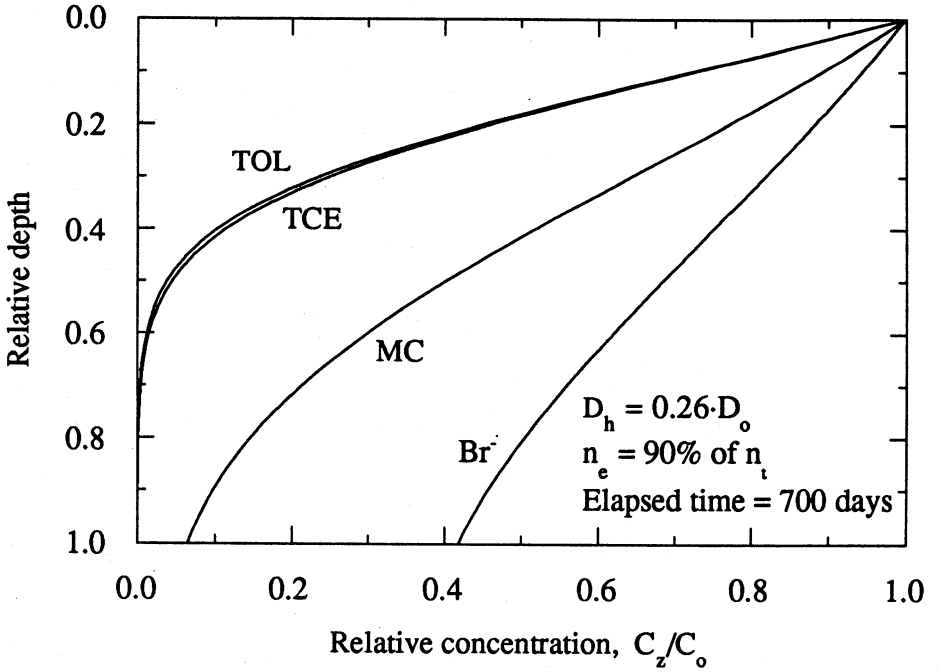

Figure 5.27 Concentration-depth profile of tank 5 specimen after 700 days.

Tank 5 has the highest concentrations of organic compounds in the upper reservoir. According to the results of simulation, after 700 days, toluene and trichloroethylene cannot break through the clay liner. Due to the biodegradation which occurred after 60 days had passed, it is questionable whether methylene chloride will break through the clay layer. According to a previous study (Wambold, 1993), biofilm was found at the surface of the clay liner. It means that the concentration of methylene chloride at the upper boundary may be very low and close to zero.

The long-term tank tests will be terminated in time. The analysis of tire chips and

sectioned soil samples may show the accurate fate of the organic compounds injected in the tanks.

5.4 LONG-TERM COLUMN TESTS

5.4.1 Column Compaction

The compaction of column specimens were performed following the procedure stated in Chapter 3. The properties of the column specimen are listed in Table 5.14. The dry density of soil was assumed to be 2.70 g/cm^3 for the estimation of porosity. Although the column specimens were prepared using the equivalent procedure as the tank specimen, the dry unit weights of the column specimens are higher than those of the tank specimens'. It may be caused by the difference in water contents of specimens.

Table 5.14 Properties of the column specimens.

	Height of specimen (mm)	Water content (%)	Dry unit weight (kN/m^3)	Porosity
Column 1J	122.8	16.36	18.11	0.32
Column 2J	120.8	16.37	18.05	0.32
Column 3J	120.6	16.10	17.78	0.33
Column 4J	115.0	15.58	18.36	0.31
Column 5J	116.8	15.73	18.33	0.31
Column 6J	118.5	15.33	18.49	0.30

Before organic compounds are injected into the upper reservoir, the hydraulic conductivity is being monitored. In order to prevent microbial activity, mercuric chloride has been injected since the hydraulic conductivity monitoring started. Organic compounds and tracer will be injected when the hydraulic conductivity and the ratio of inflow rate to outflow rate is stabilized. The current conditions of the column tests, including hydraulic

conductivity, are listed in Table 5.15.

Table 5.15 Current conditions of column tests.

	Upper reservoir volume (cm^3)	Lower reservoir volume (cm^3)	Hydraulic gradient	Hydraulic conductivity ($\times 10^{-8}$ cm/sec)
Column 1J	3,546	177.63	3.09	2.1
Column 2J	3,761	177.63	3.14	2.2
Column 3J	3,783	177.63	3.14	2.7
Column 4J	4,418	174.33	3.30	1.5
Column 5J	4,208	174.33	3.26	2.1
Column 6J	3,982	174.33	3.24	2.7

CHAPTER 6
SUMMARY AND CONCLUSIONS

The two different issues, the movement of contaminants through clay liner and the sorption of organic compounds onto tires, have been separately investigated in this study for the past three years. The two issues will be combined later to evaluate the effect of scrap tires in landfills on the organic compound movement.

In terms of groundwater protection, it is important to control the concentrations of contaminants at the upper boundary of the barrier if we want to control the effluent concentrations of the contaminants.

The lower boundary of the barrier also affects the contaminant discharge from a liner significantly. The effluent concentration of an organic compound from the liner under the stagnant groundwater condition, where groundwater stands or flows slowly, is higher than that under the condition, where groundwater flows rapidly. The effluent concentration under the fast-moving groundwater condition cannot increase beyond a certain level. However, the total discharge from the liner under the fast-moving groundwater condition is more than that under the stagnant groundwater condition because of the higher concentration gradient at the lower boundary.

Under the rapidly-flowing groundwater condition, the diffusive mass transfer at the lower boundary of the barrier contributes to the total discharge more than the advective mass transfer. On the other hand, under the stagnant groundwater condition, the diffusive mass transfer is negligible compared to the advective mass transfer.

The work accomplished to date that relate to the movement of organic contaminants through clay liner are as follows:

1. Since the mass transport of a solute in the column and tank tests influences the

concentration of the solute in the upper reservoir, an analytical solution of the advective-diffusive mass transport equation was derived to evaluate the mass transport parameters in terms of the concentration of the solute in the upper reservoir versus time data. Furthermore, a numerical solution based on the concentration of the solute in the lower reservoir was developed for the same purpose.

2. Batch isotherm tests on Kirby Lake Till have been completed for three organic compounds.
3. Six long-term column and four tank tests have been initiated.

The findings to date related to the sorption of organic compounds onto tires are as follows:

1. The sorption of organic compounds onto tires were not significantly affected by the presence of other organic or inorganic compounds. The effect of pH and temperature did not seem to be the significant. Thus, it is anticipated that tires sorb organic compounds in landfills as observed in laboratory.
2. The sorption capacity of tire chips is approximately 35% of the sorption capacity of ground tires because tire chips contain less rubber materials than ground tires. The sorption capacity of tire chips may be estimated by the ratio of the weight fraction of rubber materials in tire chips versus that in ground tires.
3. The two key parameters of the mass transfer through tires, the partition and diffusion coefficients, can be estimated using available characteristics of the organic compounds. The tire-water partition and diffusion coefficient of an organic compound can be estimated using the octanol-water partition coefficient and the molecular diameter of the organic compound. The partition and diffusion coefficients of the organic compounds tested are enough high for them to penetrate through tires in a short time period.

CHAPTER 7
FUTURE WORK

More batch isotherm tests need to be conducted to evaluate the effect of temperature on the sorption of organic compounds onto tires, and to estimate the diffusion coefficient of organic compounds in tires and the partition coefficient of Kirby Lake Till.

Long-term tank tests need to be terminated and tank specimens cored and sectioned to obtain the concentration-depth profiles of the injected organic compounds. For the analysis of the concentration-depth profiles, the numerical model under changing lower boundary should be applied.

Seven organic compounds and tracer are planned to be injected into the column specimens for the long-term column tests. The hydraulic conductivity and the ratio between the amount of influent and effluent for each column need to be monitored until organic compounds are injected. In the case of the long-term column tests, the analytical solution under decreasing upper boundary condition developed in this study should be applied to analyze the concentration in the upper reservoir in a relatively short time period. Also, the breakthrough curves, if available, should be analyzed by a numerical model under the changing upper and lower boundary conditions. The results from two models should be compared.

Finally, based on the findings from the experiments, the use of scrap tires as a landfill leachate collection system should be evaluated using the mathematical model. Design guidelines then can be proposed for applying shredded tires to landfills for the purpose of retardation of the movement of organic compounds.

REFERENCES

Acar, Y. B., and Haider, L. (1990), "Transport of Low-Concentration Contaminants in Saturated Earthen Barriers," *J. of Geotechnical Engineering*, ASCE, Vol. 116, No. 7, pp. 1031-1052.

ASCE (1994), "Cold Regions Lab Studies Use of Tire Chips as Insulation under Gravel Road," *ASCE News*, Vol. 19, No. 2, p. 9.

ASTM (1992a), "Standard Test Method for Particle-Size analysis of Soils," *1992 Annual Book of ASTM Standards*, Vol. 04.08, D 422-63.

ASTM (1992b), "Standard Test Method for Laboratory Compaction Characteristics of Soil Using Standard Effort (12,400 ft-lbf/ft^3 (600 kN-m/m^3))," *1992 Annual Book of ASTM Standards*, Vol. 04.08, D 698-91.

ASTM (1992c), "Standard Test Method for Permeability of Granular Soils (Constant Head)," *1992 Annual Book of ASTM Standards*, Vol. 04.08, D 2434-68.

ASTM (1992d), "Standard Test Method for Pore Water Extraction and Determination of the Soluble Salt Content of Soils by Refractometer," *1992 Annual Book of ASTM Standards*, Vol. 04.08, D 4542-85.

ASTM (1992e), "Standard Test Method for Measurement of Hydraulic Conductivity of Saturated Porous Materials Using a Flexible Wall Permeameter," *1992 Annual Book of ASTM Standards*, Vol. 04.08, D 5084-90.

Bahr, J. M. (1989), "Analysis of nonequilibrium desorption of volatile organics during field test of aquifer decontamination," *J. of Contaminant Hydrology*, Vol. 4, pp. 205-222.

Barone, F. S., Rowe, R. K., and Quigley, R. M. (1992), "A laboratory estimation of diffusion and adsorption coefficients for several volatile organics in a natural clayey soil," *J. of Contaminant Hydrology*, Vol. 10, No. 3, pp. 225-250.

Bear, J. (1972), *Dynamics of Fluids in Porous Media*, New York, American Elsevier, p. 661, p. 764.

Beck, R. E. and Schultz, J. S. (1970), "Hindered Diffusion in Microporous Membranes with Known Pore Geometry," *Science*, Vol. 170, p. 1302.

Beckman, J. A., Crane, G., Kay, E. L., and Laman, J. R. (1974), "Scrap Tire Disposal," *Rubber Chemistry and Technology*, Vol. 47, No. 3, pp. 597-624.

Benson, C. H. and Daniel, D. E. (1990), "The Influence of Clods on the Hydraulic Conductivity of Compacted Clay," *J. of Geotechnical Engineering*, ASCE, Vol. 116, No. 8, pp. 1031-1052.

Bonoli, L. and Witherspoon, P. A. (1968), "Diffusion of Aromatic and Cycloparaffin Hydrocarbons in Water from 2 to 60°C," *The Journal of Physical Chemistry*, Vol. 72, No. 7, pp. 2532-2534.

Box, G. E. P., Hunter, W. G., and Hunter, J. S. (1978), Sta ics for Experimenters, John Wiley & Sons, Inc.

Carman, P. C., and Haul, R. A. (1954), "Measurement of Diffusion Coefficients," *Proc. Roy. Soc.* Vol. 222-A, pp. 109-118.

Chantong, A., and Massoth, F. E. (1983), "Restrictive Diffusion in Aluminas," *AIChE J.*, Vol. 29, No. 5, pp. 725-731.

Conte, S. D., and Boor, C. D. (1980), *Elementary Numerical Analysis - An Algorithmic Approach*, 3rd ed., New York, MacGraw-Hill, inc., p. 155.

Crank, J. (1964), *The Mathematics of Diffusion*, 2nd Edition, Clarendon Press, Oxford, U.K.

Curtis, G. P., Robert, P. V., and Reinhard, M. (1986), "A natural gradient tracer experiment on solute transport in a sand aquifer: 4. Sorption of organic solutes and its influence on mobility," *Water Resources Research*, Vol. 22, pp. 2059-2067.

Davis, S. N., Campbell, D. J., Bentley, H. W., and Flynn, T. J. (1985), *Ground-Water Tracers*, U.S. EPA., Office of Research and Development, Ada, OK.

Davis, S. N., Thompson, G. M., Bentley, H. W., and Stiles, G. (1980), "Ground-Water Tracers - A Short Review," *Ground Water*, Vol. 18, No. 1, pp. 14-23.

Dodds, J., Domenico, W. F., Evans, D. R., Fish, L. W., Lassahn, P. L., and Toth, W. J. (1983), *Scrap Tires: a Resource and Technology Evaluation of Tire Pyrolysis and Other Selected Alternatives Technologies*, Prepared for the U.S. Department of Energy Report, EGG-2241, Prepared by EG & G Idaho, Inc., November, Idaho Falls, ID.

Dostal, K. A. (1990), *WERL Treatability Data Base, Risk Reduction Engineering Laboratory*, U.S. EPA., Cincinnati, OH.

Domenico, P. A., and Schwartz, F. W. (1990), *Physical and Chemical Hydrogeology*, New York, John Wiley & Sons, Inc., pp. 358-377, p. 640.

Edil, T. B., Berthouex, P. M., Park, J. K., Hargett, D. L., Standstorm, L., and Zelmanowitz, S. (1991), "Effect of Volatile Organic Compounds on Clay Landfill Liner Performance," *Waste Management & Research*, vol. 9, pp. 171-187.

Edil, T. B., and Bosscher, P. J. (1992), "Development of Engineering Criteria for Shredded Waste Tires in Highway Applications," Final Report to Wisconsin Department of Transportation and Wisconsin Department of Natural Resources, September, 1992.

Edil, T. B., Fox, P. J., and Ahl, S. W. (1992), " Hydraulic Conductivity and Compressibility of Waste Tire Chips," *Proc. of 15th Annual Madison Waste Conference*, pp. 49-61, September, 1992.

Ehrig, H. J. (1983), "Quality and Quantity of Sanitary Landfill Leachate," *Waste Management and Research*, Vol. 1, pp. 53-68.

Eldin, N. N., and Piekarski, J. A. (1993), "Scrap Tires: Management and Economics," *J. of Environmental Engineering*, ASCE, Vol. 119, No. 6, pp. 1217-1232.

EPA (1986), *Test Methods for Evaluating Solid Wastes*, SW-846, U.S.EPA., Office of Solid Waste and Emergency Response, Washington, D.C.

EPA (1991), *Markets for Scrap Tires*, EPA/530-SW-90-074A, U.S.EPA., Office of Solid Waste, October, Washington, D.C.

Farrell, J., and Reinhard, M. (1994), "Desorption of Halogenated Organics from Model Solids, Sediments, and Soil under Unsaturated Conditions. 2. Kinetics," *Environmental Science & Technology*, Vol. 28, No. 1, pp. 63-72.

Frensdorff, H. K. (1964), "Diffusion and Sorption of Vapors in Ethylene-Propylene Copolymers. II. Diffusion," *J. of Polymer Science: Part A*, Vol. 2, pp. 341-355.

Gibbons, R. D., Dolan, D., Keough, H., O'Leary, K., and O'Hara, R. (1992), "A Comparison of Chemical Constituents in Leachate from Industrial Hazardous Waste & Municipal Solid Waste Landfills," *Proc. of 15th Annual Madison Waste Conference*, Madison, WI., pp. 251-276, September, 1992.

Gillham R. W. and O'Hannesin, S. F. (1990), "Sorption of Aromatic Hydrocarbons by Materials Used in Construction Ground-Water Sampling Wells," Ground Water and Vadose Zone Monitoring, ASTM STD 1053, pp. 108-122.

Gillham, R. W., Robin, M., J., L. Dytynyshyn, D. J., and John, H. M. (1984), "Diffusion and Nonreactive and Reactive Solutes through Fine-grained Barrier Materials," *Canadian Geotechnical J.*, Vol. 21, No. 3, pp. 541-550.

Glade, M. J., Bollmann, D. D., and Tagawa, L. T. (1993), "Beneficial Use of Shredded Tires at the Lowry Landfill Superfund Site: A Case Study," *Proc. of 16th Annual Madison Waste Conference*, Madison, WI., pp. 442-459, September, 1993.

Glasstone, S., Laidler, K. J., and Eyring, H. (1941), *The Theory of Rate Processes*, MacGraw-Hill, New York, N.Y.

Goudey, J. S., and Barton, B. A. (1992), "The Toxicity of Scrap Tire Materials to Selected Aquatic Organisms," Prepared for Souris Basin Development Authority, Prepared by Hydroqual Laboratories Limited, Calgary, Alberta.

Greenkorn, R. A., and Kessler, D. P. (1972), *Transfer Operations*, New York, MacGraw-Hill, p. 548.

Griffith, G. P. (1975), "Removal of Ionic Mercury from Waste Water Using Modified Scrap Rubber," *Removal of Soluble Mercury from Waste Water complexing Techniques*, Bulletin 74, Virginia Water Resources Research Center.

Hall, Dana, and Allen, E. (1972), *Chemistry*, Vol. 45, No. 6, pp. 6-12.

Hall, T. J. (1991), "Reuse of Shredded Tire Material for Leachate Collection Systems," *Proc. of 14th Annual Madison Waste Conference*, Madison, WI., pp. 367-376, September, 1991.

Hassett, J. J., Banwart, W. L., and Griffin, R. A. (1983), *Environment and Solid Wastes: Characterization , Treatment and Disposal*, ed. C. W. Francis and S. I. Auerbach, Stoneham, Mass., Butterworth, pp. 161-178.

Heim, D., P. (1992), "Advective and Diffusive Transport of Three Volatile Organic Compounds Through a Compacted Clay," Thesis of Master Degree, Dept. of Civil & Environmental Eng., University of Wisconsin-Madison.

Helfferich, F. (1966), *In Ion Exchange, A Series of Advances*, ed. J. A. Marinsky, New York, Marcel Dekker, pp. 65-100, p. 424.

Henderson, W. H., Lightsey G. R., and Poonawala, N. A. (1977), "Competitive Adsorption of Metal Ions by Low Cost Organic Materials," *Bulletin of Environmental Contamination and Toxicology*, Vol. 13, pp. 340-344.

Higgins, A. J., Singley, M. E., Nocitra, N., Callanan, K., Whitson, B., and Singh, A. (1980), "Shredded Rubber Tires as a Bulking Agent," *Compost Science/Land Utilization*, Nov./Dec. pp. 20-23.

House of Representatives (1990), "Scrap Tire Management and Recycling Opportunities," Committee on Small Business, U.S. House of Representatives, Washington, D.C., April, 1990.

Hudson, J. F., and Lake, E. E. (1977), "A Planning Bibliography on Tire Reuse and Disposal," prepared by Urban System Research & Engineering, Inc., Cambridge, Mass., p.50.

Jaca Corporation (1988), "Shredded Tires for Landfills as Flow-Zone Material," Prepared for Domino Salvage Inc., April.

Johnson, R. L., Cherry, J. A., and Pankow, J. F. (1989), "Diffusive Contaminant Transport in Natural Clay: A Field Example and Implications for Clay-lined Waste Disposal Sites," *Environmental Science & Technologies*, Vol. 23, No. 3., pp. 340-349.

Kan, A. T., and Tomson, M. B. (1990), "Effect of pH concentration on the Transport of Naphthalene in Saturated Aquifer Media,' *J. of Contaminant Hydrology*, Vol. 5, No. 3, pp. 235-251.

Karickhoff, S. W., Brown, D. S., and Scott, T. A. (1979), "Sorption of Hydrophobic Pollutants on Natural Sediments," *Water Research*, Vol. 13, pp. 241-248.

Karickhoff, S. W. (1984), "Organic Pollutant Sorption in Aquatic Systems," *J. of Hydraulic Engineering*, ASCE, Vol. 110, No. 6, pp. 707-735.

Kenaga, E. E. (1980), "Predicted bioconcentration factors and soil sorption coefficients of pesticides and other chemicals," *Ecotoxicology and Environmental Safety,* Vol. 4, pp. 26-38.

Knocke, W. R. and Hemphill, L. H. (1981), "Mercury (II) Sorption by Waste Rubber," *Water Research*, Vol. 15, pp. 275-282.

Kreyszig, E. (1979), *Advanced Engineering Mathematics*, 4th ed., John Wiley & Sons, Inc., p. 830.

Kurt, A., C., and Wagner, J., F. (1991), "Cation transport and retardation processes in view of the toxic waste deposition problem in clay rocks and clay liner encapsulation," *Engineering Geology*, Vol. 30, pp. 103-113.

Minnesota Pollution Control Agency (1990), "Waste Tires in Sub-grade Road Beds," Prepared by Twin City Testing Corporation, St. Paul, MN, February, St. Paul, MN.

Lee, G. Fred, and Jones, R. Anne (1991), *Municipal Solid Waste Management: Long-Term Public Health and Environmental Protection*, prepared for Short course "Landfill and Groundwater Quality", University Extension, University of California-Davis.

Lin, T., Little, J. C., and Nazaroff, W. W. (1994), "Transport and Sorption of Volatile Organic Compounds and Water Vapor within Dry Soil Grains," *Environmental Science & Technologies*, Vol. 28, No. 2., pp. 322-330.

Mackay, D., *Multimedia Environmental Models - The Fugacity Approach*, Lewis Publishers, Chelsea, MI., 1991, pp. 69-70.

Myrand, D., and Gillham, R. W., Sudicky, E. A., O'Hannesin, S. F., and Johnson, R. L. (1992), "Diffusion of Volatile Organic Compounds in Natural Clay Deposits: Laboratory Tests," *J. of Contaminant Hydrology*, Vol. 10, pp. 159-177.

Nelson, B. R., and Book, P. R. (1986), "Monitoring of Volatile Organic Hydrocarbons at Minnesota Sanitary Landfills, *Proc. of 9th Madison Waste Conference*, Madison, WI., pp. 72-84, September, 1986.

Nkedi-Kizza, P., Rao, P. S. C., Jessup, R. E., and Davidson, J. M. (1982), "Ion exchange and diffusive mass transfer during miscible displacement through an aggregated Oxisol," *J. of Soil Sci. Soc. Am.*, Vol. 46, pp. 471-476.

Netzer, A., and Wilkinson, P. (1974), "Removal of Heavy Metals from Waste Water Utilizing Discarded Automotive Tyres," *J. of Water Pollution Control*, Vol. 9, pp. 62-66.

Nkedi-Kizza, P., Biggar, J. W., van Genuchten, M. Th., Wierenga, P. J., Selim, H. M., Davidson, J. M., and Nielsen, D. R. (1983), "Modeling tritium and chloride 36 transport through an aggregated Oxisol," *Water Resources Research*, Vol. 19, pp. 691-700.

Oberhettinger, F. and Badii, L. (1973), *Table of Laplace Transforms*, Springer-Verlag, New York, p. 229.

Ogata A., and Banks, R. B. (1961), "A Solution of the Differential Equation of Longitudinal Dispersion in Porous Media," U.S. Geological Survey Professional Paper 411-A.

Park, J. K., Bontoux, L., Holsen, T. M., Jenkins, D., and Selleck, R. E. (1991a), "Permeation of Polybutylene Pipe and Gasket Material by organic Chemicals," *J. of American Water Works Association,* Vol. 83, pp. 71-78.

Park, J. K. and Bontoux, L. (1991), "Effects of Temperature, Repeated Exposure, and Aging on Polybutylene Permeation by Organic Chemicals," *J. of Applied Polymer Science*, Vol. 42, pp. 2989-2995.

Park, J. K., Edil, T. B., and Berthouex, P.M. (1991b), "Transport of Volatile organic Compounds (VOCs) through a Clay Liner," *Proc. of the Special Conference* Sponsored by the Environmental Eng. Div. of the Amer. Soc. of Civil Engr, Edited by Krenkel, Reno, Nevada, pp. 6-11, July, 1991.

Park, J. K., and Nibras, M. (1993), "Mass Flux of Organic Chemicals through Polyethylene Geomembranes," *Water Environment Research*, Vol. 65, pp. 227-237.

Park, N. B. (1992), "Evaluation of the Potential Toxicity of Automobile Tires in the Aquatic Environment," Prepared for Environment Canada National Water Research Institute, Burlington, Ontario, Prepared by B.A.R. Environmental Inc., August, Guelph, Ontario.

Piwoni, M. D. and Banerjee, P. (1989), "Sorption of Volatile Organic Solvents from Aquifer Solution onto Subsurface Solids," *J. of Contaminant Hydrology,* Vol. 4, No. 5, pp. 163-179.

Plumb, R. H., and Pitchford A. M. (1985), "Volatile Organic Scans: Implications for Ground Water Monitoring," *Proc. of NWWA/API Conference Petroleum Hydrocarbons and Organic Chemicals in Ground Water - Prevention, Detection, and Restoration*, Houston, TX., pp. 207-222, November, 1985.

Prausnitz, J. M., Lichtentthaler, R. N., and de Azevedo, E. G. (1986), *Molecular Thermodynamics of Fluid-Phase Equilibria*, 2nd Edition, Prentice-Hall, Inc., Englewood Cliffs, N.J.

Priddle, M. W., and Jackson, R. E. (1991), "Laboratory column measurement of VOC retardation factors and comparison with field values," *Ground water*, Vol. 29, pp. 260-266.

Rao, P. S. C., and Davidson, J. M. (1979), "Adsorption and movement of selected pesticides at high concentrations in soils," *Water Research*, Vol. 13, No. 4, pp. 375-380.

Rao, P. S. C., Davidson, J. M., Berkheiser, V. E., Ou, L. T., Street, J. J., Wheeler, W. B., and Yuan, T. L. (1982), *Retardation and Transformation of Selected Pesticides and Phosphorus in Soil-Water Systems: A Critical Review*, U.S.EPA., EPA-600/3-82-060, Athens, GA., 1982.

Rebhun, M., Kalabo, R., Grossman, L., Manka, J., and Rav-Acha, C. (1992), "Sorption of Organics on Clay and Synthetic Humic-Clay Complexes Simulating Aquifer Processes," *Water Research*, Vol. 26, No. 1, pp. 79-84.

Reisch, M. S. (1993), "Rubber - Slow Growth Ahead," *Chemistry & Engineering News*, May, 10, pp. 24-33.

Reynold, G. W., Hoff, J. T., and Gillham, R. W. (1990), "Sampling Bias Caused by Materials Used to Monitor Halocarbons in Groundwater," *Environmental Science and Technology*, Vol. 24, No. 1, pp. 135-142.

Renkin, E. M. (1954), "Filtration, Diffusion and Molecular Sieving Through Porous Cellulose Membranes," *J. Gen. Physiol.*, Vol. 38, p. 225.

Roberts, P. V., Goltz, M. N., and Mackay, D. M. (1986), "A natural gradient experiment on solute transport in a sand aquifer, 3. Retardation estimates and mass balances for organic solutes," *Water Resources Research*, Vol. 22, pp. 2047-2058.

Rowe, R. K. (1987), "Pollutant Transport Through Barriers," *Geotechnical Practice for Waste Disposal '87*, ed. R. D. Woods, ASCE Special Publication, No. 1, pp. 159-181.

Rowley, A. G., Husband, F. M., and Cunningham, A. B. (1984), "Mechanisms of Metal Adsorption from Aqueous by Waste Tyre Rubber," *Water Research*, Vol. 18, No. 8, pp. 981-984.

Rubber Manufacturers Association (1989), "A Report on the RMT TCLP Assessment Project," September, Washington, D.C.

Sakti, J. P., Park, J. K., and Hoopes, J. A. (1992), "Permeation of Organic Chemicals through HDPE Geomembranes," *Proc. of the Environmental Eng.* Sessions at "Water Forum '92," Baltimore, MA, pp. 201-207, July, 1992.

Satterfield, C. N., and Pitcher, W. H., Jr. (1973), "Restricted Diffusion in Liquids within Fine Pores," *AIChE J.*, Vol. 19, No. 3, pp. 628-635.

Scheels, N. E. (1993), "Removal of Digester Sludge Odors Using Ground Rubber Tires," Thesis of Master Degree, Dept. of Civil & Environmental Eng., University of Wisconsin-Madison.

Schwarzenbach, F. W., and Westall, J. (1981), "Transport of nonpolar organic compounds from surface water to groundwater - Laboratory studies," *Environmental Science & Technology*, Vol. 15, pp. 1300-1367.

Shackelford, C. D. (1990), "Transit-time Design of Earthen Barriers," *Engineering Geology*, Vol. 29, pp. 79-94.

Shackelford, C. D. (1991), "Laboratory Diffusion testing for Waste Disposal - A Review," *J. of Contaminant Hydrology*, Vol. 7, No. 3, pp. 177-217.

Shackelford, C. D. and Daniel, D. E. (1991a), "Diffusion in Saturated Soil, I. Background," *J of Geotechnical Eng.*, ASCE., Vol. 117, No. 3, pp. 467-484.

Shackelford, C. D. and Daniel, D. E. (1991b), "Diffusion in Saturated Soil, II. Results for Compacted Clay," *J of Geotechnical Eng.*, ASCE., Vol. 117, No. 3, pp. 485-506.

Shimizu, Y. Takei, N., and Terashima, Y. "Sorption of Organic Pollutants from Vapor Phase: The effects of Natural Solid Characteristics and Moisture Content," Water Science Technologies, Vol. 26, No. 1, pp. 79-87.

Snoeyink, V. L., and W. J. Jr. Weber (1967), "The Surface Chemistry of Active Carbon," *Environmental Science and Technologies*, Vol. 1, pp. 228-234.

Standard Methods for the Examination of Water and Wastewater, 17th ed., APHA, AWWA, and WEF, Washington, DC., 4-168 p..

Stone, R. B., Caston, L. C., Hoss, D. E., and Cross, F. A. (1975), "Experiments on Some Possible Effects of Tire Reefs on Pinfish (Lagodon rhomboides) and Black Sea Bass (Centropristis striata)," *Marine Fisheries Review*, Vol. 37, No. 3.

Tchobanoglous, G., Theisen, H., and Vigil, S. (1993), *Integrated Solid Waste Management*, New York, MacGraw-Hill, Inc., p. 394.

Tharin, D. W. (1974), "Tire Rubber Removes Mercury from Process Stream," Presented at the 4th Annual Environmental Engineering and Science Conference, Louisville, KY.

Tuma, J., J. (1970), *Engineering Mathematics Handbook*, MacGraw-Hill, Inc., pp. 154-155.

Verschueren, K. (1983), *Handbook of Environmental Data on Organic Chemicals*, New York, Van Nostrand Reinhold Company, Inc.

Voice, T. C., Rice, C. P., and Weber, W. J. (1983), "Effect of Solids Concentration on the Sorptive Partitioning of Hydrophobic Pollutants in Aquatic Systems, *Environmental Science and Technologies*, Vol. 17, pp. 513-518.

Wang, L, and Govind, R. (1993), "Sorption of Toxic Organic Compounds on Wastewater Soils: Mechanism and Modeling," *Environmental Science and Technologies*, Vol. 27, No. 1, pp. 152-164.

Wambold, W. S. (1993), "Large and Small Laboratory Tests of VOC Transport through Compacted Clay," Thesis of Master Degree, Dept. of Civil & Environmental Eng., University of Wisconsin-Madison.

Waste Management of Pennsylvania (1990), "Use of Tire Chips in Liner Protective Cover," Prepared by J & L testing Company Inc., Canonsburg, PA, June, Morrisville, PA.

Weber, J. W. Jr. (1972), *Physicochemical Processes for Water quality Control*, Wiley-interscience, New York, N.Y., p. 236.

Wilke, C. R., and Chang, R. N. (1955), "Correlation of diffusion coefficients in dilute solutions," *AIChE J.*, Vol. 1, No. 2, pp. 264-270.

Yiacoumi, S. and Tien, C. (1994), "A Method of Organic Solute Uptake from Aqueous Solution by Soils," *Water Resources Research*, Vol. 30, No. 2. pp. 571-580.

APPENDIX A

TANK TESTS COMPACTION DATA

Soil weight applied: 31.03 kg/lift (=68.4 lb/lift)
Dry density of soil particle = 2.70 g/cm^3
Density of water = 1.0 g/cm^3

Tank 2A

Volume of Top reservoir: 168 L

Lift	Thickness (cm)	Water content (%)	Volume (cm^3)	Dry Unit Weight (kN/m^3)	Porosity	Saturation (%)
1	5.91	18.86	17,236	14.86	0.439	65.0
2	4.83	17.72	14,085	18.36	0.307	108.0
3	5.59	16.57	16,309	16.01	0.396	68.3
4	4.89	19.20	14,271	17.89	0.324	107.9
5	5.02	20.43	14,641	17.26	0.348	103.2
6	5.53	19.46	16,124	15.80	0.403	77.7
Overall	31.75	18.71	92,667	16.60	0.373	84.8

Tank 4

Volume of Top reservoir: 170 L

Lift	Thickness (cm)	Water content (%)	Volume (cm^3)	Dry Unit Weight (kN/m^3)	Porosity	Saturation (%)
1	5.08	18.16	14,827	17.37	0.344	93.5
2	4.95	17.70	14,456	17.89	0.325	99.4
3	5.40	17.59	15,753	16.43	0.380	77.6
4	5.21	17.00	15,197	17.12	0.354	83.9
5	4.83	17.95	14,085	18.32	0.308	108.7
6	5.02	19.48	14,641	17.40	0.343	100.7
Overall	30.48	17.98	88,960	17.40	0.343	92.9

Tank 5

Volume of Top reservoir: 169 L

Lift	Thickness (cm)	Water content (%)	Volume (cm^3)	Dry Unit Weight (kN/m^3)	Porosity	Saturation (%)
1	4.89	17.92	14271	18.09	0.317	104.2
2	4.64	17.98	13529	19.07	0.280	124.8
3	5.84	17.57	17051	15.18	0.427	63.7
4	5.02	17.86	14641	17.64	0.334	96.1
5	5.46	19.42	15939	15.99	0.396	79.9
6	5.14	19.17	15012	17.01	0.358	93.0
Overall	30.99	18.32	90443	17.07	0.356	89.6

Tank 6

Volume of Top reservoir: 169 L

Lift	Thickness (cm)	Water content (%)	Volume (cm^3)	Dry Unit Weight (kN/m^3)	Porosity	Saturation (%)
1	4.76	17.75	13,900	18.61	0.298	112.9
2	5.40	20.06	15,753	16.09	0.392	83.8
3	5.84	19.57	17,051	14.93	0.436	68.3
4	4.51	17.10	13,159	19.75	0.254	135.4
5	5.46	18.22	15,939	16.15	0.390	76.9
6	5.21	18.57	15,197	16.89	0.362	88.2
Overall	31.18	18.54	90,999	16.93	0.361	88.7

APPENDIX B

CODES FOR COMPUTER PROGRAMS

B.1 Code for the Analytical Solution of

$$\frac{\partial C}{\partial t} = A \cdot \frac{\partial^2 C}{\partial z^2} - B \cdot \frac{\partial C}{\partial z}$$

where $C(z,0) = 0.0$;

$C(0,t) = C_o$; and

$C(\infty,t) = 0.0$.

```
C**********  CONSTANT UPPER BOUNDARY  **********
C**********  OGATA & BANKS BOUNDARY  **********
C**********    LIST OF INPUT DATA     **********

C      DH: HYDRODYNAMIC DISPERSION COEFFICIENT, CM^2/SEC
C      KP: SOIL-WATER PARTITION COEFFICIENT, CM^3/G
C      DT: UNIT TIME INTERVAL, DAY
C      N : # OF LINER SEGMENTS
C      M : # OF ELAPSED UNIT TIME
C      K : # OF SIMULATIONS
C      CONC: CONC. IN LINER(1-N), MG/L
C      CO: INTIAL CONC,  MG/L
C      RCE: RELATIVE CONC. OF EFFLUENT
C      LL: TOTAL DEPTH OF LINER, CM
C      DD: DIAMETER OF TANK, CM
C      KH: HYDAULIC CONDUCTICITY, CM/SEC
C      HG: HYDRAULIC GRADIENT
C      TP: TOTAL POROSITY
C      EP: EFFECTIVE POROSITY
C      DS: DRY DENSITY OF LINER, G/CM^3
C      BD: BULK DENSITY, G/CM^3
C      VT: VOLUME OF TOP RESERVOIR,  CM^3
C      RF: RETARDATION FACTOR
C      SV: SEEPAGE VELOCITY, CM/DAY
C      QD: DARCY'S FLOW RATE, CM^3/DAY
C      PC: PECLET NUMBER
C      DL: UNIT DEPTH OF LINER, CM
C      XA: CROSS-SECTIONAL AREA OF LINER, CM^2
C      FLUX: MASS FLUX, MG/M^2,DAY
C      MASS: ACCUMULATIVE MASS,  MG/M^2
C      ET: TOTAL ELAPSED TIME, DAY
C      TIME: ELAPSED TIME, DAY
C      A,B,C,E,F,G,H: INTERMEDIATE PARAMETERS
C      S : OUTPUT SPACE INTERVAL
C      T : OUTPUT TIME INTERVAL

      REAL  LL,DD,KH,HG,TP,DS,VT,VB,DT,RF,SV,DL,XA,ET,BD,QD,RCO,RCE,PC,
     +    RC,X,ERFCX,TIME,DEPTH,U,AEFLX,DEFLX,AEMASS,DEMASS,TEMASS,
     +    AIFLX,DIFLX,AIMASS,DIMASS,TIMASS,TMASS,MASS,SMASS,LMASS
      INTEGER  N,M,L,I,J,K,S,T,V,W
      REAL  CONC(505),DH(10),KP(10),EP(10),CO(10)
```

```
C** OPEN OUTPUT FILE
      OPEN (UNIT=11, FILE='VOC 5:UNIT1.DAT')
      OPEN (UNIT=12, FILE='VOC 5:UNIT2.DAT')
      OPEN (UNIT=10, FILE='VOC 5:O&B.OUT')

C** INPUT DATA
      READ (11,4) LL,DD
      READ (11,5) KH,HG
      READ (11,5) TP,DS
      READ (11,3) DT
00003 FORMAT (1X,E10.4)
00004 FORMAT (4(1X,E10.4))
00005 FORMAT (2(1X,E10.4))
      READ (11,*) N
      READ (11,*) M
      READ (11,*) L
      READ (11,*) S
      READ (11,*) T

      DO  1  K = 1, L

      READ (12,7) DH(K),KP(K),EP(K),CO(K)
00007 FORMAT (5(1X,E10.4))

C** CALCULATED PARAMETERS
      RF = 1 + (( DS * KP(K) * (1 - TP))/TP)
      SV = (KH * HG * 60 * 60 *24) / EP(K)
      DL = LL/N
      XA = 3.141592/4 * (DD**2)
      ET = M * DT
      PV = (XA * LL) * TP
      EPV = (XA * LL) * EP(K)
      BD = (1-TP) * DS
      QD = KH*60*60*24*HG*10000
      PC = SV*L/(DH(K)*60*60*24)

C** OUTPUT
      WRITE (10,900)
     +    '**** CONSTANT  UPPER   BOUNDARY ****'
      WRITE(10,901)
     +    '****   OGATA & BANKS  BOUNDARY  ****'
      WRITE (10,1010)  'UPPER BOUNDARY  = ',CO(K),' MG/L'
      WRITE (10,1000)  'HYDRODYNAMIC DISPERSION COEFF.  = ',DH(K),
     +                 ' CM^2/SEC'
      WRITE (10,1000)  'PARTITION COEFFICIENT  = ',KP(K),' L/KG'
      WRITE (10,1000)  'PECLET NUMBER  = ',PC
      WRITE (10,1010)  'INITIAL UPPER RESERVOIR CONC.  = ',CO(K),' MG/L'
      WRITE (10,1000)  'LENGTH OF LINER  = ',LL,' CM'
      WRITE (10,1010)  'UNIT TIME INTERVAL  = ',DT,' DAY'
      WRITE (10,1010)  'UNIT LENGTH INTERVAL  = ', DL,' CM'
      WRITE (10,1000)  'HYDRAULIC CONDUCTIVITY  = ',KH,' CM/SEC'
      WRITE (10,1010)  'HYDRAULIC GRADIENT  = ',HG
      WRITE (10,1010)  'TOTAL POROSITY  = ',TP
      WRITE (10,1010)  'EFFECTIVE POROSITY  = ',EP(K)
      WRITE (10,1010)  'DRY DENSITY  = ',DS,' G/CM^3'
      WRITE (10,1010)  'BULK DENSITY  = ',BD,' G/CM^3'
      WRITE (10,1020)  'PORE VOLUME  = ',PV,' CM^3'
```

```
      WRITE (10,1020)  'EFFECTIVE PORE VOLUME  = ',EPV,' CM^3'
      WRITE (10,1020)  'EFFLUENT FLOW RATE  = ',QD,' CM^3/M^2,DAY'
      WRITE (10,1010)  'SPECIFIC GRAVITY  = ',DS
      WRITE (10,1010)  'RETARDATION FACTOR  = ',RF
      WRITE (10,1000)  'SEEPAGE VELOCITY  = ',SV, ' CM/DAY'
      WRITE (10,1020)  'ELAPSED TIME  = ',ET,' DAY'
00900 FORMAT (/,A47)
00901 FORMAT (A47,/)
01000 FORMAT (A35,E10.4,A14)
01010 FORMAT (A35,F10.4,A14)
01020 FORMAT (A35,F10.2,A14)

      WRITE (10,1110) 'TIME','EFF. CONC','INPUT','OUTPUT','LINER'
01110 FORMAT(//,A6,A16,A30,A52,A30)
      WRITE (10,1120) 'ADV.FLUX','DIF.FLUX','ADV.MASS','DIF.MASS',
     + 'TOTAL M','ADV.FLUX','DIF.FLUX','ADV.MASS','DIF.MASS','TOTAL M'
01120 FORMAT (24X,4(2X,A8),2X,A7,2X,4(2X,A8),3X,A7)
      WRITE (10,1200) '(DAYS)','(MG/L)    RC','(MG/M^2,DAY)',
     +       '(MG/M^2)','(MG/M^2, DAY)','(MG/M^2)','(MG/M^2)'
01200 FORMAT (A7,A15,5X,A14,13X,A10,15X,A14,13X,A10,11X,8A)

C** INITIAL CONDITION
      W = 0.0
      J = 0.0
      DO 10  I = 2, N+2
        CONC(I) = 0.0
00010 CONTINUE

      CONC(1) = CO(K)
      RCE = 0.0
      RC = 0.0
      AIFLX = QD*CONC(1)*10**(-3)
      DIFLX = 0.0
      AIMASS = 0.0
      DIMASS = 0.0
      TIMASS = 0.0
      TMASS = 0.0
      AEFLX = 0.0
      DEFLX = 0.0
      AEMASS = 0.0
      DEMASS = 0.0
      TEMASS = 0.0

      GO TO 90

00030 W = W + 1
00040 J = J + 1

      CONC(1) = CO(K)

      DO 50 I = 2,N+2
          X = (RF*DL*(I-1) - SV*DT*J)/(2*SQRT(RF*DH(K)*24*60*60*DT*J))
        CALL ERFC (X,ERFCX)
          A = ERFCX
          X = (RF*DL*(I-1) + SV*DT*J)/(2*SQRT(RF*DH(K)*24*60*60*DT*J))
        CALL ERFC (X,ERFCX)
          B = ERFCX
```

```
        CONC(I) = CO(K)/2*(A+B*EXP(SV*DL*(I-1)/(DH(K)*24*60*60)))
00050 CONTINUE

      AIFLX = AIFLX
      AIMASS = AIMASS + AIFLX*DT
      DIFLX = TP*DH(K)*60*60*24*10*(CONC(1)-CONC(2))/DL
      DIMASS = DIMASS + DIFLX*DT
      TIMASS = AIMASS + DIMASS

      AEFLX = QD*CONC(N+1)*10**(-3)
      AEMASS = AEMASS + AEFLX*DT
      DEFLX = TP*DH(K)*60*60*24*10*(CONC(N+1)-CONC(N+2))/DL
      DEMASS = DEMASS + DEFLX*DT
      TEMASS = AEMASS + DEMASS

      TMASS = TIMASS - TEMASS

      Q = J/T

     IF (W.EQ.Q)  THEN
        GO TO 90
     ELSE
       GO TO 40
      END IF

00090 TIME = J * DT
      RCE = CONC(N+1)/CO(K)
      WRITE (10,1400)  TIME,CONC(N+1),RCE,AIFLX,DIFLX,AIMASS,
     +   DIMASS,TIMASS,AEFLX,DEFLX,AEMASS,DEMASS,TEMASS,TMASS
01400 FORMAT(F7.1,1X,F8.3,1X,F6.4,2(2X,E9.3,4(1X,E9.3),2X,E9.3))

      IF (J.EQ.M)  THEN
        GO TO 100
      ELSE
        GO TO 30
      END IF

00100 WRITE (10,1500)  'DEPTH','CONC. PROFILE','RELATIVE CONC.'
01500 FORMAT(/,1X,A8,A17,A16)
      WRITE (10,1600)  '(CM)','(MG/L)'
01600 FORMAT(A9,4X,A10,/)

      LMASS = 0.0
      SMASS = 0.0
      MASS = 0.0

      DO 160 I = 1, N
        LMASS = LMASS + (CONC(I)+CONC(I+1))/2*DL*TP*10
00160 CONTINUE
      SMASS = LMASS*KP(K)*DS*(1-TP)/TP
      MASS = LMASS + SMASS
      RATIO = TMASS/MASS*100

      V = 0
      I = 1
      DEPTH = 0.0
      RCO = 1.0
```

```
      WRITE (10,1700) DEPTH, CONC(1), RCO

00130 V = V+1
00140 I = I+1
00150 U = (I-1)/S

      IF (U.EQ.V) THEN
        GO TO 120
      ELSE
        GO TO 140
      END IF

00120 DEPTH = (I-1)*DL
      RC = CONC(I)/CO(K)
      WRITE (10,1700) DEPTH,CONC(I),RC
01700 FORMAT(F9.3,F13.3,F14.4)

      IF (I.EQ.N+1) THEN
        WRITE (10,1800) 'TOTAL MASS OF CONTAMINANT IN LINER = ',
     +                  MASS,' MG/M^2'
        WRITE (10,1900) 'TOTAL MASS IN PORE WATER = ',LMASS,' MG/M^2'
        WRITE (10,1900) 'TOTAL MASS SORBED ONTO SOIL = ',SMASS,
     +                  ' MG/M^2'
        WRITE (10,1910) 'MASS RATIO (BTC/PROFILE) = ',RATIO,' %'
01800 FORMAT(/,A39,E9.3,A7)
01900 FORMAT(A39,E9.3,A7)
01910 FORMAT(A39,F9.3,A7)
        GO TO 1
      ELSE
        GO TO 130
      END IF

00001 CONTINUE

      STOP
      END

C********** SUBROUTINE COMPLEMENTARY ERROR FUNCTION ********

      SUBROUTINE ERFC (X,ERFCX)

      INTEGER  I
      REAL X,T,TT,ERFX,ERFCX

      I = 0.0
      IF(X.LT.0.0)  I=1.0
        X = ABS(X)
        T = 1.0/(1.0+0.3275911*X)
        TT = 0.254829592*T - 0.284496736*T**2 + 1.421413741*T**3
     +     - 1.453152027*T**4 + 1.061405429*T**5
        ERFX = 1.0 - TT*EXP(-1.0*X**2)

      IF (I.EQ.0) ERFCX = 1.0 - ERFX
      IF (I.EQ.1) ERFCX = 1.0 + ERFX

      RETURN
      END
```

B.2 Code for the Numerical Solution of

$$\frac{\partial C}{\partial t} = A \cdot \frac{\partial^2 C}{\partial z^2} - B \cdot \frac{\partial C}{\partial z}$$

where $C(z,0) = 0.0$;

$C(0,t) = C_0$; and

$C(L^+,t) = 0.0$.

```
C**********  CONSTANT UPPER BOUNDARY  **********
C**********    ZERO LOWER BOUNDARY    **********
C**********    LIST OF INPUT DATA     **********

C      DH: HYDRODYNAMIC DISPERSION COEFFICIENT, CM^2/SEC
C      KP: SOIL-WATER PARTITION COEFFICIENT, CM^3/G
C      DT: UNIT TIME INTERVAL, DAY
C      N : # OF LINER SEGMENTS
C      M : # OF ELAPSED UNIT TIME
C      K : # OF SIMULATIONS
C      CONC: CONC. IN LINER(1-N), MG/L
C      CO: INTIAL CONC,  MG/L
C      RCE: RELATIVE CONC. OF EFFLUENT
C      LL: TOTAL DEPTH OF LINER, CM
C      DD: DIAMETER OF TANK, CM
C      KH: HYDAULIC CONDUCTICITY, CM/SEC
C      HG: HYDRAULIC GRADIENT
C      TP: TOTAL POROSITY
C      EP: EFFECTIVE POROSITY
C      DS: DRY DENSITY OF LINER, G/CM^3
C      BD: BULK DENSITY, G/CM^3
C      VT: VOLUME OF TOP RESERVOIR,  CM^3
C      RF: RETARDATION FACTOR
C      SV: SEEPAGE VELOCITY, CM/DAY
C      QD: DARCY'S FLOW RATE, CM^3/DAY
C      DL: UNIT DEPTH OF LINER, CM
C      XA: CROSS-SECTIONAL AREA OF LINER, CM^2
C      FLUX: MASS FLUX, MG/M^2,DAY
C      MASS: ACCUMULATIVE MASS,  MG/M^2
C      ET: TOTAL ELAPSED TIME, DAY
C      TIME: ELAPSED TIME, DAY
C      A,B,C,E,F,G,H: INTERMEDIATE PARAMETERS
C      S : OUTPUT SPACE INTERVAL
C      T : OUTPUT TIME INTERVAL

       REAL  LL,DD,KH,HG,TP,DS,VT,VB,DT,RF,SV,DL,XA,ET,BD,QD,RCO,RCE,
     +    RC,A,B,C,E,F,Q,TIME,DEPTH,U,AEFLX,DEFLX,AEMASS,DEMASS,TEMASS,
     +    AIFLX,DIFLX,AIMASS,DIMASS,TIMASS,TMASS,MASS,SMASS,LMASS
       INTEGER  N,M,L,I,J,K,S,T,V,W
       REAL  CONC(505),DH(10),KP(10),EP(10),CO(10)

C** OPEN OUTPUT FILE
```

```
      OPEN (UNIT=11, FILE='VOC 5:UNIT1.DAT')
      OPEN (UNIT=12, FILE='VOC 5:UNIT2.DAT')
      OPEN (UNIT=10, FILE='VOC 5:LB=O.OUT')

C** INPUT DATA
      READ (11,4) LL,DD
      READ (11,5) KH,HG
      READ (11,5) TP,DS
      READ (11,3) DT
00003 FORMAT (1X,E10.4)
00004 FORMAT (4(1X,E10.4))
00005 FORMAT (2(1X,E10.4))
      READ (11,*) N
      READ (11,*) M
      READ (11,*) L
      READ (11,*) S
      READ (11,*) T

      DO  1  K = 1, L

      READ (12,7) DH(K),KP(K),EP(K),CO(K)
00007 FORMAT (5(1X,E10.4))

C** CALCULATED PARAMETERS
      RF = 1 + (( DS * KP(K) * (1 - TP))/TP)
      SV = (KH * HG * 60 * 60 *24) / EP(K)
      DL = LL/N
      XA = 3.141592/4 * (DD**2)
      ET = M * DT
      PV = (XA * LL) * TP
      EPV = (XA * LL) * EP(K)
      BD = (1-TP) * DS
      QD = KH*60*60*24*HG*10000
      A = DH(K)*24*60*60/RF
      B = SV/RF
      C = - (A * DT)/(DL**2)
      E = 1 - (2 * C) - (B*DT/DL)
      F = C + (B*DT/DL)

C** OUTPUT
      WRITE (10,900)
     +    '**** CONSTANT  UPPER   BOUNDARY ****'
      WRITE(10,901)
     +    '********   C(L.B.) = 0.0   *********'
      WRITE (10,1010)  'UPPER BOUNDARY  = ',CO(K),' MG/L'
      WRITE (10,1000)  'HYDRODYNAMIC DISPERSION COEFF.  = ',DH(K),
     +                 ' CM^2/SEC'
      WRITE (10,1000)  'PARTITION COEFFICIENT  = ',KP(K),' L/KG'
      WRITE (10,1010)  'INITIAL UPPER RESERVOIR CONC.  = ',CO(K),' MG/L'
      WRITE (10,1000)  'LENGTH OF LINER  = ',LL,' CM'
      WRITE (10,1010)  'UNIT TIME INTERVAL  = ',DT,' DAY'
      WRITE (10,1010)  'UNIT LENGTH INTERVAL  = ', DL,' CM'
      WRITE (10,1000)  'HYDRAULIC CONDUCTIVITY  = ',KH,' CM/SEC'
      WRITE (10,1010)  'HYDRAULIC GRADIENT  = ',HG
      WRITE (10,1010)  'TOTAL POROSITY  = ',TP
      WRITE (10,1010)  'EFFECTIVE POROSITY  = ',EP(K)
      WRITE (10,1010)  'DRY DENSITY  = ',DS,' G/CM^3'
```

```
      WRITE (10,1010)  'BULK DENSITY  = ',BD,' G/CM^3'
      WRITE (10,1020)  'PORE VOLUME  = ',PV,' CM^3'
      WRITE (10,1020)  'EFFECTIVE PORE VOLUME  = ',EPV,' CM^3'
      WRITE (10,1020)  'EFFLUENT FLOW RATE  = ',QD,' CM^3/M^2,DAY'
      WRITE (10,1010)  'SPECIFIC GRAVITY  = ',DS
      WRITE (10,1010)  'RETARDATION FACTOR  = ',RF
      WRITE (10,1000)  'SEEPAGE VELOCITY  = ',SV, ' CM/DAY'
      WRITE (10,1020)  'ELAPSED TIME  = ',ET,' DAY'
00900 FORMAT (/,A47)
00901 FORMAT (A47,/)
01000 FORMAT (A35,E10.4,A14)
01010 FORMAT (A35,F10.4,A14)
01020 FORMAT (A35,F10.2,A14)
      WRITE (10,1110) 'TIME','EFF. CONC','INPUT','OUTPUT','LINER'
01110 FORMAT(//,A6,A16,A30,A52,A30)
      WRITE (10,1120) 'ADV.FLUX','DIF.FLUX','ADV.MASS','DIF.MASS',
     + 'TOTAL M','ADV.FLUX','DIF.FLUX','ADV.MASS','DIF.MASS','TOTAL M'
01120 FORMAT (24X,4(2X,A8),2X,A7,2X,4(2X,A8),3X,A7)
      WRITE (10,1200) '(DAYS)','(MG/L)    RC','(MG/M^2,DAY)',
     +       '(MG/M^2)','(MG/M^2, DAY)','(MG/M^2)','(MG/M^2)'
01200 FORMAT (A7,A15,5X,A14,13X,A10,15X,A14,13X,A10,11X,8A)

C** INITIAL CONDITION
      W = 0.0
      J = 0.0

      DO 10  I = 2, N+1
        CONC(I) = 0.0
00010 CONTINUE

      CONC(1) = CO(K)
      RCE = 0.0
      RC = 0.0
      AIFLX = QD*CONC(1)*10**(-3)
      DIFLX = 0.0
      AIMASS = 0.0
      DIMASS = 0.0
      TIMASS = 0.0
      TMASS = 0.0
      AEFLX = 0.0
      DEFLX = 0.0
      AEMASS = 0.0
      DEMASS = 0.0
      TEMASS = 0.0

      GO TO 90

00030 W = W + 1
00040 J = J + 1

      CALL TRIDIA (C,E,F,CONC,N)

      AIFLX = QD*CONC(1)*10**(-3)
      AIMASS = AIMASS + AIFLX*DT
      DIFLX = TP*DH(K)*60*60*24*10*(CONC(1)-CONC(2))/DL
      DIMASS = DIMASS + DIFLX*DT
      TIMASS = AIMASS + DIMASS
```

```
      AEFLX = QD*CONC(N+1)*10**(-3)
      AEMASS = AEMASS + AEFLX*DT
      DEFLX = TP*DH(K)*60*60*24*10*CONC(N)/(2*DL)
      DEMASS = DEMASS + DEFLX*DT
      TEMASS = AEMASS + DEMASS

      TMASS = TIMASS - TEMASS

      Q = J/T

      IF (W.EQ.Q)  THEN
        GO TO 90
      ELSE
        GO TO 40
      END IF

00090 TIME = J * DT
      RCE = CONC(N+1)/CO(K)
      WRITE (10,1400)  TIME,CONC(N+1),RCE,AIFLX,DIFLX,AIMASS,
     +   DIMASS,TIMASS,AEFLX,DEFLX,AEMASS,DEMASS,TEMASS,TMASS
01400 FORMAT(F7.1,1X,F8.3,1X,F6.4,2(2X,E9.3,4(1X,E9.3),2X,E9.3))

      IF (J.EQ.M)  THEN
        GO TO 100
      ELSE
        GO TO 30
      END IF

00100 WRITE (10,1500)  'DEPTH','CONC. PROFILE','RELATIVE CONC.'
01500 FORMAT(/,1X,A8,A17,A16)
      WRITE (10,1600)  '(CM)','(MG/L)'
01600 FORMAT(A9,4X,A10,/)

      LMASS = 0.0
      SMASS = 0.0
      MASS = 0.0

      DO 160 I = 1, N
        LMASS = LMASS + (CONC(I)+CONC(I+1))/2*DL*TP*10
00160 CONTINUE
      SMASS = LMASS *KP(K)*DS*(1-TP)/TP
      MASS = LMASS + SMASS
      RATIO = TMASS/MASS*100

      V = 0
      I = 1
      DEPTH = (I-1)*DL
      RCO = 1.0
      WRITE (10,1700) DEPTH, CONC(1), RCO

00130 V = V+1
00140 I = I+1
00150 U = (I-1)/S
      IF (U.EQ.V) THEN
        GO TO 120
      ELSE
```

```
        GO TO 140
       END IF

00120 DEPTH = (I-1)*DL
       RC = CONC(I)/CO(K)
       WRITE (10,1700) DEPTH,CONC(I),RC
01700 FORMAT(F9.3,F13.3,F14.4)

       IF (I.EQ.N+1) THEN
         WRITE (10,1800) 'TOTAL MASS OF CONTAMINANT IN LINER = ',
     +                    MASS,' MG/M^2'
         WRITE (10,1900) 'TOTAL MASS IN PORE WATER = ',LMASS,' MG/M^2'
         WRITE (10,1900) 'TOTAL MASS SORBED ONTO SOIL = ',SMASS,
     +                   ' MG/M^2'
         WRITE (10,1910) 'MASS RATIO (BTC/PROFILE) = ',RATIO,' %'
01800 FORMAT(/,A39,E9.3,A7)
01900 FORMAT(A39,E9.3,A7)
01910 FORMAT(A39,F9.3,A7)
         GO TO 1
       ELSE
         GO TO 130
       END IF

00001 CONTINUE

       STOP
       END
       C********** SUBROUTINE TRIDIAGONAL MATRIX ********

       SUBROUTINE TRIDIA (C,E,F,CONC,N)

       INTEGER I
       REAL SUB(305),DIAG(305),SUP(305),CONC(305)

       DIAG(1) = 1
       SUP(1) = 0

       DO 11 I = 2, N+1
         SUB(I) = C
         DIAG(I) = E
         SUP(I) = F
00011 CONTINUE

       DO 12  I = 2, N+1
         SUB(I) = SUB(I)/DIAG(I-1)
         DIAG(I) = DIAG(I) - SUB(I) * SUP(I-1)
         CONC(I) = CONC(I) - SUB(I) * CONC(I-1)
00012 CONTINUE

       CONC(N+1) = CONC(N+1)/DIAG(N+1)

       DO 13  I = N,1,-1
         CONC(I) = (CONC(I) - SUP(I) * CONC(I+1))/DIAG(I)
00013 CONTINUE

       RETURN
       END
```

B.3 Code for the Numerical Solution of

$$\frac{\partial C}{\partial t} = A \cdot \frac{\partial^2 C}{\partial z^2} - B \cdot \frac{\partial C}{\partial z}$$

where $C(z,0) = 0.0$;

$C(0,t) = C_0$; and

$C(L^+,t) = C(L^-,t)$.

```
C**********  CONSTANT UPPER BOUNDARY  **********
C**********  C(LB) = C(EFF) BOUNDARY  **********
C**********    LIST OF INPUT DATA     **********
C      DH: HYDRODYNAMIC DISPERSION COEFFICIENT, CM^2/SEC
C      KP: SOIL-WATER PARTITION COEFFICIENT, CM^3/G
C      DT: UNIT TIME INTERVAL, DAY
C      N : # OF LINER SEGMENTS
C      M : # OF ELAPSED UNIT TIME
C      K : # OF SIMULATIONS
C      CONC: CONC. IN LINER(1-N), MG/L
C      CO: INTIAL CONC,  MG/L
C      RCE: RELATIVE CONC. OF EFFLUENT
C      LL: TOTAL DEPTH OF LINER, CM
C      DD: DIAMETER OF TANK, CM
C      KH: HYDAULIC CONDUCTICITY, CM/SEC
C      HG: HYDRAULIC GRADIENT
C      TP: TOTAL POROSITY
C      EP: EFFECTIVE POROSITY
C      DS: DRY DENSITY OF LINER, G/CM^3
C      BD: BULK DENSITY, G/CM^3
C      VT: VOLUME OF TOP RESERVOIR,  CM^3
C      RF: RETARDATION FACTOR
C      SV: SEEPAGE VELOCITY, CM/DAY
C      QD: DARCY'S FLOW RATE, CM^3/DAY
C      DL: UNIT DEPTH OF LINER, CM
C      XA: CROSS-SECTIONAL AREA OF LINER, CM^2
C      FLUX: MASS FLUX, MG/M^2,DAY
C      MASS: ACCUMULATIVE MASS,  MG/M^2
C      ET: TOTAL ELAPSED TIME, DAY
C      TIME: ELAPSED TIME, DAY
C      A,B,C,E,F,G,H: INTERMEDIATE PARAMETERS
C      S : OUTPUT SPACE INTERVAL
C      T : OUTPUT TIME INTERVAL

       REAL  LL,DD,KH,HG,TP,DS,VT,VB,DT,RF,SV,DL,XA,ET,BD,QD,RCO,RCE,
     +    RC,A,B,C,E,F,Q,TIME,DEPTH,U,AEFLX,DEFLX,AEMASS,DEMASS,TEMASS,
     +    AIFLX,DIFLX,AIMASS,DIMASS,TIMASS,TMASS,MASS,SMASS,LMASS
       INTEGER  N,M,L,I,J,K,S,T,V,W
       REAL  CONC(505),DH(10),KP(10),EP(10),CO(10)
C** OPEN OUTPUT FILE
       OPEN (UNIT=11, FILE='VOC 5:UNIT1.DAT')
       OPEN (UNIT=12, FILE='VOC 5:UNIT2.DAT')
```

```
      OPEN (UNIT=10, FILE='VOC 5:LB=EFF.OUT')
C** INPUT DATA
      READ (11,4) LL,DD
      READ (11,5) KH,HG
      READ (11,5) TP,DS
      READ (11,3) DT
00003 FORMAT (1X,E10.4)
00004 FORMAT (4(1X,E10.4))
00005 FORMAT (2(1X,E10.4))
      READ (11,*) N
      READ (11,*) M
      READ (11,*) L
      READ (11,*) S
      READ (11,*) T

      DO  1  K = 1, L

      READ (12,7) DH(K),KP(K),EP(K),CO(K)
00007 FORMAT (5(1X,E10.4))
C** CALCULATED PARAMETERS
      RF = 1 + (( DS * KP(K) * (1 - TP))/TP)
      SV = (KH * HG * 60 * 60 *24) / EP(K)
      DL = LL/N
      XA = 3.141592/4 * (DD**2)
      ET = M * DT
      PV = (XA * LL) * TP
      EPV = (XA * LL) * EP(K)
      BD = (1-TP) * DS
      QD = KH*60*60*24*HG*10000
      A = DH(K)*24*60*60/RF
      B = SV/RF
      C = - (A * DT)/(DL**2)
      E = 1 - (2 * C) - (B*DT/DL)
      F = C + (B*DT/DL)
C** OUTPUT
      WRITE (10,900)
     +    '**** CONSTANT  UPPER   BOUNDARY ****'
      WRITE(10,901)
     +    '*******   C(LB) = C(EFF)   *******'
      WRITE (10,1010)  'UPPER BOUNDARY  = ',CO(K),' MG/L'
      WRITE (10,1000)  'HYDRODYNAMIC DISPERSION COEFF.  = ',DH(K),
     +                 ' CM^2/SEC'
      WRITE (10,1000)  'PARTITION COEFFICIENT  = ',KP(K),' L/KG'
      WRITE (10,1010)  'INITIAL UPPER RESERVOIR CONC.  = ',CO(K),' MG/L'
      WRITE (10,1000)  'LENGTH OF LINER  = ',LL,' CM'
      WRITE (10,1010)  'UNIT TIME INTERVAL  = ',DT,' DAY'
      WRITE (10,1010)  'UNIT LENGTH INTERVAL  = ', DL,' CM'
      WRITE (10,1000)  'HYDRAULIC CONDUCTIVITY  = ',KH,' CM/SEC'
      WRITE (10,1010)  'HYDRAULIC GRADIENT  = ',HG
      WRITE (10,1010)  'TOTAL POROSITY  = ',TP
      WRITE (10,1010)  'EFFECTIVE POROSITY  = ',EP(K)
      WRITE (10,1010)  'DRY DENSITY  = ',DS,' G/CM^3'
      WRITE (10,1010)  'BULK DENSITY  = ',BD,' G/CM^3'
      WRITE (10,1020)  'PORE VOLUME  = ',PV,' CM^3'
      WRITE (10,1020)  'EFFECTIVE PORE VOLUME  = ',EPV,' CM^3'
      WRITE (10,1020)  'EFFLUENT FLOW RATE  = ',QD,' CM^3/M^2,DAY'
      WRITE (10,1010)  'SPECIFIC GRAVITY  = ',DS
```

```
      WRITE (10,1010)  'RETARDATION FACTOR  = ',RF
      WRITE (10,1000)  'SEEPAGE VELOCITY  = ',SV, ' CM/DAY'
      WRITE (10,1020)  'ELAPSED TIME  = ',ET,' DAY'
00900 FORMAT (/,A47)
00901 FORMAT (A47,/)
01000 FORMAT (A35,E10.4,A14)
01010 FORMAT (A35,F10.4,A14)
01020 FORMAT (A35,F10.2,A14)
      WRITE (10,1110) 'TIME','EFF. CONC','INPUT','OUTPUT','LINER'
01110 FORMAT(//,A6,A16,A30,A52,A30)
      WRITE (10,1120) 'ADV.FLUX','DIF.FLUX','ADV.MASS','DIF.MASS',
     + 'TOTAL M','ADV.FLUX','DIF.FLUX','ADV.MASS','DIF.MASS','TOTAL M'
01120 FORMAT (24X,4(2X,A8),2X,A7,2X,4(2X,A8),3X,A7)
      WRITE (10,1200) '(DAYS)','(MG/L)    RC','(MG/M^2,DAY)',
     +       '(MG/M^2)','(MG/M^2, DAY)','(MG/M^2)','(MG/M^2)'
01200 FORMAT (A7,A15,5X,A14,13X,A10,15X,A14,13X,A10,11X,8A)

C** INITIAL CONDITION
      W = 0.0
      J = 0.0

      DO 10  I = 2, N+1
        CONC(I) = 0.0
00010 CONTINUE

      CONC(1) = CO(K)
      RCE = 0.0
      RC = 0.0
      AIFLX = QD*CONC(1)*10**(-3)
      DIFLX = 0.0
      AIMASS = 0.0
      DIMASS = 0.0
      TIMASS = 0.0
      TMASS = 0.0
      AEFLX = 0.0
      DEFLX = 0.0
      AEMASS = 0.0
      DEMASS = 0.0
      TEMASS = 0.0

      GO TO 90

00030 W = W + 1
00040 J = J + 1

      CALL TRIDIA (C,E,F,CONC,N)

      AIFLX = QD*CONC(1)*10**(-3)
      AIMASS = AIMASS + AIFLX*DT
      DIFLX = TP*DH(K)*60*60*24*10*(CONC(1)-CONC(2))/DL
      DIMASS = DIMASS + DIFLX*DT
      TIMASS = AIMASS + DIMASS

      AEFLX = QD*CONC(N+1)*10**(-3)
      AEMASS = AEMASS + AEFLX*DT
      DEFLX = TP*DH(K)*60*60*24*10*(CONC(N)-CONC(N+1))/(2*DL)
      DEMASS = DEMASS + DEFLX*DT
```

```
      TEMASS = AEMASS + DEMASS

      TMASS = TIMASS - TEMASS

      Q = J/T

      IF (W.EQ.Q)  THEN
        GO TO 90
      ELSE
        GO TO 40
      END IF

00090 TIME = J * DT
      RCE = CONC(N+1)/CO(K)
      WRITE (10,1400)  TIME,CONC(N+1),RCE,AIFLX,DIFLX,AIMASS,
     +   DIMASS,TIMASS,AEFLX,DEFLX,AEMASS,DEMASS,TEMASS,TMASS
01400 FORMAT(F7.1,1X,F8.3,1X,F6.4,2(2X,E9.3,4(1X,E9.3),2X,E9.3))

      IF (J.EQ.M)  THEN
        GO TO 100
      ELSE
        GO TO 30
      END IF
00100 WRITE (10,1500)  'DEPTH','CONC. PROFILE','RELATIVE CONC.'
01500 FORMAT(/,1X,A8,A17,A16)
      WRITE (10,1600)  '(CM)','(MG/L)'
01600 FORMAT(A9,4X,A10,/)

      LMASS = 0.0
      SMASS = 0.0
      MASS = 0.0

      DO 160 I = 1, N
        LMASS = LMASS + (CONC(I)+CONC(I+1))/2*DL*TP*10
00160 CONTINUE
      SMASS = LMASS *KP(K)*DS*(1-TP)/TP
      MASS = LMASS + SMASS
      RATIO = TMASS/MASS*100

      V = 0
      I = 1
      DEPTH = (I-1)*DL
      RCO = 1.0
      WRITE (10,1700) DEPTH, CONC(1), RCO

00130 V = V+1
00140 I = I+1
00150 U = (I-1)/S

      IF (U.EQ.V) THEN
        GO TO 120
      ELSE
        GO TO 140
      END IF

00120 DEPTH = (I-1)*DL
      RC = CONC(I)/CO(K)
```

```
      WRITE (10,1700) DEPTH,CONC(I),RC
01700 FORMAT(F9.3,F13.3,F14.4)

      IF (I.EQ.N+1) THEN
        WRITE (10,1800) 'TOTAL MASS OF CONTAMINANT IN LINER = ',
     +                  MASS,' MG/M^2'
        WRITE (10,1900) 'TOTAL MASS IN PORE WATER = ',LMASS,' MG/M^2'
        WRITE (10,1900) 'TOTAL MASS SORBED ONTO SOIL = ',SMASS,
     +                  ' MG/M^2'
        WRITE (10,1910) 'MASS RATIO (BTC/PROFILE) = ',RATIO,' %'
01800 FORMAT(/,A39,E9.3,A7)
01900 FORMAT(A39,E9.3,A7)
01910 FORMAT(A39,F9.3,A7)
        GO TO 1
      ELSE
        GO TO 130
      END IF

00001 CONTINUE

      STOP
      END

C********** SUBROUTINE TRIDIAGONAL MATRIX ********

      SUBROUTINE TRIDIA (C,E,F,CONC,N)

      INTEGER  N,I
      REAL SUB(305),DIAG(305),SUP(305),CONC(305)

      DIAG(1) = 1
      SUP(1) = 0

      DO 11 I = 2, N+1
        SUB(I) = C
        DIAG(I) = E
        SUP(I) = F
00011 CONTINUE
      DIAG(N+1) = E+F

      DO 12  I = 2, N+1
        SUB(I) = SUB(I)/DIAG(I-1)
        DIAG(I) = DIAG(I) - SUB(I) * SUP(I-1)
        CONC(I) = CONC(I) - SUB(I) * CONC(I-1)
00012 CONTINUE

      CONC(N+1) = CONC(N+1)/DIAG(N+1)

      DO 13  I = N,1,-1
        CONC(I) = (CONC(I) - SUP(I) * CONC(I+1))/DIAG(I)
00013 CONTINUE

      RETURN
      END
```

B.4 Code for the Numerical Solution of

$$\frac{\partial C}{\partial t} = A \cdot \frac{\partial^2 C}{\partial z^2} - B \cdot \frac{\partial C}{\partial z}$$

where $C(z,0) = 0.0$;

$C(0,t) = C_0$; and

Completely mixed bower boundary.

```
C**********  CONSTANT UPPER BOUNDARY  **********
C******  COMPLETELY MIXED LOWER BOUNDARY *******
C**********  LIST OF INPUT DATA  **********

C      DH: HYDRODYNAMIC DISPERSION COEFFICIENT, CM^2/SEC
C      KP: SOIL-WATER PARTITION COEFFICIENT, CM^3/G
C      DT: UNIT TIME INTERVAL, DAY
C      N : # OF LINER SEGMENTS
C      M : # OF ELAPSED UNIT TIME
C      K : # OF SIMULATIONS
C      CIN: CONC. OF INFLUENT, MG/L
C      CONC: CONC. IN LINER(1-N), MG/L
C      CUR: CONC. IN UPPER RESERVOIR, MG/L
C      CLR: CONC. IN LOWER RESERVOIR, MG/L
C      CO: INTIAL CUR,  MG/L
C      RCUR: RELATIVE CONC. OF CUR
C      RCLR: RELATIVE CONC. OF CLR
C      RCE: RELATIVE CONC. OF EFFLUENT
C      LL: TOTAL DEPTH OF LINER, CM
C      DD: DIAMETER OF TANK, CM
C      KH: HYDAULIC CONDUCTICITY, CM/SEC
C      HG: HYDRAULIC GRADIENT
C      PVT: REQUIRED TIME FOR ONE PORE VOLUME, DAY
C      EPVT: REQUIRED TIME FOR ONE EFFECTIVE PORE VOLUME, DAY
C      PPV: PASSED PORE VOLUME
C      TP: TOTAL POROSITY
C      EP: EFFECTIVE POROSITY
C      PV: PORE VOLUME, CM^3
C      EPV: EFFECTIVE PORE VOLUME, CM^3
C      DS: DRY DENSITY OF LINER, G/CM^3
C      BD: BULK DENSITY, G/CM^3
C      VT: VOLUME OF TOP RESERVOIR,  CM^3
C      RF: RETARDATION FACTOR
C      SV: SEEPAGE VELOCITY, CM/DAY
C      DL: UNIT DEPTH OF LINER, CM
C      XA: CROSS-SECTIONAL AREA OF LINER, CM^2
C      ET: TOTAL ELAPSED TIME, DAY
C      TIME: ELAPSED TIME, DAY
C      A,B,C,E,F,G,H: INTERMEDIATE PARAMETERS
C      S : OUTPUT SPACE INTERVAL
C      T : OUTPUT TIME INTERVAL
```

```
      REAL  LL,DD,KH,HG,TP,DS,VT,VB,DT,RF,SV,DL,XA,ET,PV,EPV,BD,QD,
     +      RCLR,RCUR,RCE,RC,PVT,EPVT,A,B,C,E,F,HA,HB,HC,HD,Q,
     +      TIME,DEPTH,U,PPV,HLR
      INTEGER  N,M,L,I,J,K,S,T,V,W
      REAL  CONC(305),DH(10),KP(10),EP(10),CO(10),CIN(10)

C** OPEN OUTPUT FILE
      OPEN (UNIT=11, FILE='VOC 5:UNIT1.DAT')
      OPEN (UNIT=12, FILE='VOC 5:UNIT2.DAT')
      OPEN (UNIT=10, FILE='VOC 5:LOWER RES.OUT')

C** INPUT DATA
      READ (11,4) LL,DD,VB,VT
      READ (11,5) KH,HG
      READ (11,5) TP,DS
      READ (11,3) DT
00003 FORMAT (1X,E10.4)
00004 FORMAT (4(1X,E10.4))
00005 FORMAT (2(1X,E10.4))
      READ (11,*) N
      READ (11,*) M
      READ (11,*) L
      READ (11,*) S
      READ (11,*) T

      DO  1  K = 1, L

      READ (12,7) DH(K),KP(K),EP(K),CO(K),CIN(K)
00007 FORMAT (5(1X,E10.4))

C** CALCULATED PARAMETERS
      RF = 1 + (( DS * KP(K) * (1 - TP))/TP)
      SV = (KH * HG * 60 * 60 *24) / EP(K)
      DL = LL/N
      XA = 3.141592/4 * (DD**2)
      ET = M * DT
      PV = (XA * LL) * TP
      EPV = (XA * LL) * EP(K)
      BD = (1-TP) * DS
      QD = (KH*60*60*24*HG*XA)
      HLR = VB/XA

      IF (QD.EQ.0)  THEN
        PVT = 0.0
        EPVT = 0.0
      ELSE
        PVT = PV/QD
        EPVT = EPV/QD
      END IF

      A = DH(K)*24*60*60/RF
      B = SV/RF
      C = - (A * DT)/(DL**2)
      E = 1 - (2 * C) - (B*DT/DL)
      F = C + (B*DT/DL)
      HA = - DT*KH*24*60*60*HG/HLR -(DT*TP*DH(K)*24*60*60)/(HLR*DL)
      HB = 1 - HA
```

```
C** OUTPUT
      WRITE (10,900)
     +    '**** CONSTANT  UPPER   BOUNDARY ****'
      WRITE(10,901)
     +    '**** COMPLETELY MIXED LOWER BOUNDARY ****'
      WRITE (10,1000)  'HYDRODYNAMIC DISPERSION COEFF.  = ',DH(K),
     +                 ' CM^2/SEC'
      WRITE (10,1010)  'PARTITION COEFFICIENT  = ',KP(K),' L/KG'
      WRITE (10,1010)  'INITIAL UPPER RESERVOIR CONC.  = ',CO(K),' MG/L'
      WRITE (10,1010)  'INFLUENT CONC.  = ',CIN(K),' MG/L'
      WRITE (10,1000)  'LENGTH OF LINER  = ',LL,' CM'
      WRITE (10,1000)  'DIAMETER OF TANK  = ',DD, ' CM'
      WRITE (10,1000)  'CROSS-SECTIONAL AREA  = ',XA,' CM^2'
      WRITE (10,1000)  'VOLUME OF LOWER RESERVOIR  = ',VB,' CM^3'
      WRITE (10,1000)  'HEIGHT OF LOWER RESERVOIR  = ',HLR,' CM'
      WRITE (10,1010)  'UNIT TIME INTERVAL  = ',DT,' DAY'
      WRITE (10,1010)  'UNIT LENGTH INTERVAL  = ', DL,' CM'
      WRITE (10,1000)  'HYDRAULIC CONDUCTIVITY  = ',KH,' CM/SEC'
      WRITE (10,1010)  'HYDRAULIC GRADIENT  = ',HG
      WRITE (10,1010)  'TOTAL POROSITY  = ',TP
      WRITE (10,1010)  'EFFECTIVE POROSITY  = ',EP(K)
      WRITE (10,1010)  'DRY DENSITY  = ',DS,' G/CM^3'
      WRITE (10,1010)  'BULK DENSITY  = ',BD,' G/CM^3'
      WRITE (10,1000)  'PORE VOLUME  = ',PV,' CM^3'
      WRITE (10,1000)  'EFFECTIVE PORE VOLUME  = ',EPV,' CM^3'
      WRITE (10,1000)  'EFFLUENT FLOWRATE  = ',QD,' CM^3/DAY'
      WRITE (10,1010)  'SPECIFIC GRAVITY  = ',DS
      WRITE (10,1010)  'RETARDATION FACTOR  = ',RF
      WRITE (10,1000)  'SEEPAGE VELOCITY  = ',SV, ' CM/DAY'
      WRITE (10,1000)  'ELAPSED TIME  = ',ET,' DAY'
      WRITE (10,1000)  'ONE PORE VOLUME  = ',PVT,' DAY'
      WRITE (10,1000)  'ONE EFFECTIVE PORE VOLUME  = ',EPVT,' DAY'
00900 FORMAT (/,A47)
00901 FORMAT (A49,/)
01000 FORMAT (A35,E10.4,A10)
01010 FORMAT (A35,F10.3,A10)

      WRITE (10,1110) 'ELAPSED TIME','PORE VOLUME',
     +     'UPPER CONC','LOWER CONC','EFFLUENT CONC'
01110 FORMAT (//,A12,A15,A15,A18,A19)
      WRITE (10,1200)   '(DAYS)','(MG/L) C(T)/C(0)',
     +      '(MG/L) C(T)/C(0)','(MG/L) C(T)/C(0)'
01200 FORMAT (3X,A6,17X,A19,1X,A17,1X,A17,/)

C** INITIAL CONDITION
      W = 0.0
      J = 0.0

      DO 10  I = 2, N+2
        CONC(I) = 0.0
00010 CONTINUE

      CONC(1) = CO(K)
      RCUR = CONC(1)/CO(K)
      RCLR = CONC(N+2)/CO(K)
      RCE = CONC(N+1)/CO(K)
```

```
      RC = 0.0

      GO TO 90

00030 W = W + 1
00040 J = J + 1

      CALL TRIDIA (C,E,F,HA,HB,CONC,N)

      Q = J/T

      IF (W.EQ.Q)  THEN
        GO TO 90
      ELSE
        GO TO 40
      END IF

00090 TIME = J * DT
      RCUR = CONC(1)/CO(K)
      RCLR = CONC(N+2)/CO(K)
      RCE = CONC(N+1)/CO(K)

      IF (QD.EQ.0)  THEN
        PPV = 0.0
      ELSE
        PPV = TIME/PVT
      END IF

      WRITE (10,1400)  TIME,PPV,CONC(1),RCUR,CONC(N+2),RCLR,
     +                 CONC(N+1),RCE
01400 FORMAT(F9.2,E17.3,F10.3,F7.4,F10.3,F7.4,F11.3,F7.4)

      IF (J.EQ.M)  THEN
        GO TO 100
      ELSE
        GO TO 30
      END IF

00100 WRITE (10,1500)  'DEPTH','CONC. PROFILE','RELATIVE CONC.'
01500 FORMAT(/,1X,A8,A17,A16)
      WRITE (10,1600)  '(CM)','(MG/L)'
01600 FORMAT(A9,4X,A10,/)

      V = 0
      I = 1
      DEPTH = (I-1)*DL
      WRITE (10,1700) DEPTH, CONC(1), RCUR

00130 V = V+1
00140 I = I+1
00150 U = (I-1)/S

      IF (U.EQ.V) THEN
        GO TO 120
      ELSE
        GO TO 140
      END IF
```

```
00120 DEPTH = (I-1)*DL
      RC = CONC(I)/CO(K)
      WRITE (10,1700) DEPTH,CONC(I),RC
01700 FORMAT(F9.3,F13.3,F14.4)

      IF (I.EQ.N+1) THEN
        GO TO 1
      ELSE
        GO TO 130
      END IF

00001 CONTINUE

      STOP
      END

C********** SUBROUTINE TRIDIAGONAL MATRIX ********

      SUBROUTINE TRIDIA (C,E,F,HA,HB,CONC,N)

      INTEGER  N,I
      REAL SUB(305),DIAG(305),SUP(305),CONC(305)

      DIAG(1) = 1
      SUP(1) = 0

      DO 10 I = 2, N+1
        SUB(I) = C
        DIAG(I) = E
        SUP(I) = F
00010 CONTINUE

      DIAG(N+2) = HB
      SUB(N+2) = HA

      DO 11  I = 2, N+2
        SUB(I) = SUB(I)/DIAG(I-1)
        DIAG(I) = DIAG(I) - SUB(I) * SUP(I-1)
        CONC(I) = CONC(I) - SUB(I) * CONC(I-1)
00011 CONTINUE

      CONC(N+2) = CONC(N+2)/DIAG(N+2)

      DO 12  I = N+1,1,-1
        CONC(I) = (CONC(I) - SUP(I) * CONC(I+1))/DIAG(I)
00012 CONTINUE

      RETURN
      END
```

B.5 Code for the Numerical Solution of

$$\frac{\partial C}{\partial t} = A \cdot \frac{\partial^2 C}{\partial z^2} - B \cdot \frac{\partial C}{\partial z}$$

where $C(z,0) = 0.0$;

Completely mixed upper boundary; and

Completely mixed lower boundary.

```
C**********  CONSTANT UPPER BOUNDARY  **********
C******  COMPLETELY MIXED LOWER BOUNDARY *******
C**********  LIST OF INPUT DATA  **********

C       DH: HYDRODYNAMIC DISPERSION COEFFICIENT, CM^2/SEC
C       KP: SOIL-WATER PARTITION COEFFICIENT, CM^3/G
C       DT: UNIT TIME INTERVAL, DAY
C       N : # OF LINER SEGMENTS
C       M : # OF ELAPSED UNIT TIME
C       K : # OF SIMULATIONS
C       CIN: CONC. OF INFLUENT, MG/L
C       CONC: CONC. IN LINER(1-N), MG/L
C       CUR: CONC. IN UPPER RESERVOIR, MG/L
C       CLR: CONC. IN LOWER RESERVOIR, MG/L
C       CO: INTIAL CUR,  MG/L
C       RCUR: RELATIVE CONC. OF CUR
C       RCLR: RELATIVE CONC. OF CLR
C       RCE: RELATIVE CONC. OF EFFLUENT
C       LL: TOTAL DEPTH OF LINER, CM
C       DD: DIAMETER OF TANK, CM
C       KH: HYDAULIC CONDUCTICITY, CM/SEC
C       HG: HYDRAULIC GRADIENT
C       PVT: REQUIRED TIME FOR ONE PORE VOLUME, DAY
C       EPVT: REQUIRED TIME FOR ONE EFFECTIVE PORE VOLUME, DAY
C       PPV: PASSED PORE VOLUME
C       TP: TOTAL POROSITY
C       EP: EFFECTIVE POROSITY
C       PV: PORE VOLUME, CM^3
C       EPV: EFFECTIVE PORE VOLUME, CM^3
C       DS: DRY DENSITY OF LINER, G/CM^3
C       BD: BULK DENSITY, G/CM^3
C       VT: VOLUME OF TOP RESERVOIR,  CM^3
C       RF: RETARDATION FACTOR
C       SV: SEEPAGE VELOCITY, CM/DAY
C       DL: UNIT DEPTH OF LINER, CM
C       XA: CROSS-SECTIONAL AREA OF LINER, CM^2
C       ET: TOTAL ELAPSED TIME, DAY
C       TIME: ELAPSED TIME, DAY
C       A,B,C,E,F,G,H: INTERMEDIATE PARAMETERS
C       S : OUTPUT SPACE INTERVAL
C       T : OUTPUT TIME INTERVAL
```

```
      REAL  LL,DD,KH,HG,TP,DS,VT,VB,DT,RF,SV,DL,XA,ET,PV,EPV,BD,QD,
     +      RCLR,RCUR,RCE,RC,PVT,EPVT,HUR,HLR,
     +      A,B,C,E,F,HA,HB,HC,HD,HE,Q,TIME,DEPTH,U,PPV
      INTEGER  N,M,L,I,J,K,S,T,V,W
      REAL  CONC(305),DH(10),KP(10),EP(10),CO(10),CIN(10)
C** OPEN OUTPUT FILE

      OPEN (UNIT=11, FILE='VOC 5:UNIT1.DAT')
      OPEN (UNIT=12, FILE='VOC 5:UNIT2.DAT')
      OPEN (UNIT=10, FILE='VOC 5:UPPER & LOWER.OUT')
C** INPUT DATA
      READ (11,4) LL,DD,VB,VT
      READ (11,5) KH,HG
      READ (11,5) TP,DS
      READ (11,3) DT
00003 FORMAT (1X,E10.4)
00004 FORMAT (4(1X,E10.4))
00005 FORMAT (2(1X,E10.4))
      READ (11,*) N
      READ (11,*) M
      READ (11,*) L
      READ (11,*) S
      READ (11,*) T

      DO  1  K = 1, L

      READ (12,7) DH(K),KP(K),EP(K),CO(K),CIN(K)
00007 FORMAT (5(1X,E10.4))
C** CALCULATED PARAMETERS
      RF = 1 + (( DS * KP(K) * (1 - TP))/TP)
      SV = (KH * HG * 60 * 60 *24) / EP(K)
      DL = LL/N
      XA = 3.141592/4 * (DD**2)
      ET = M * DT
      PV = (XA * LL) * TP
      EPV = (XA * LL) * EP(K)
      BD = (1-TP) * DS
      QD = (KH*60*60*24*HG*XA)
      HLR = VB/XA
      HUR = VT/XA

      IF (QD.EQ.0)  THEN
        PVT = 0.0
        EPVT = 0.0
      ELSE
        PVT = PV/QD
        EPVT = EPV/QD
      END IF

      A = DH(K)*24*60*60/RF
      B = SV/RF
      C = - (A * DT)/(DL**2)
      E = 1 - (2 * C) - (B*DT/DL)
      F = C + (B*DT/DL)
      HA = - DT*KH*24*60*60*HG/HLR -(DT*TP*DH(K)*24*60*60)/(HLR*DL)
      HB = 1 - HA
      HC = DT*KH*24*60*60*HG/HUR
```

```
      HD = -(DT*TP*DH(K)*24*60*60)/(HUR*DL)
      HE = 1 + HC - HD
C** OUTPUT
      WRITE (10,900)
     +    '**** CONSTANT  UPPER   BOUNDARY ****'
      WRITE(10,901)
     +    '**** COMPLETELY MIXED LOWER BOUNDARY ****'
      WRITE (10,1000)  'HYDRODYNAMIC DISPERSION COEFF.  = ',DH(K),
     +                 ' CM^2/SEC'
      WRITE (10,1010)  'PARTITION COEFFICIENT  = ',KP(K),' L/KG'
      WRITE (10,1010)  'INITIAL UPPER RESERVOIR CONC.  = ',CO(K),' MG/L'
      WRITE (10,1010)  'INFLUENT CONC.  = ',CIN(K),' MG/L'
      WRITE (10,1000)  'LENGTH OF LINER  = ',LL,' CM'
      WRITE (10,1000)  'DIAMETER OF TANK  = ',DD, ' CM'
      WRITE (10,1000)  'CROSS-SECTIONAL AREA  = ',XA,' CM^2'
      WRITE (10,1000)  'VOLUME OF UPPER RESERVOIR  = ',VT,' CM^3'
      WRITE (10,1000)  'HEIGHT OF UPPER RESERVOIR  = ',HUR,' CM'
      WRITE (10,1000)  'VOLUME OF LOWER RESERVOIR  = ',VB,' CM^3'
      WRITE (10,1000)  'HEIGHT OF LOWER RESERVOIR  = ',HLR,' CM'
      WRITE (10,1010)  'UNIT TIME INTERVAL  = ',DT,' DAY'
      WRITE (10,1010)  'UNIT LENGTH INTERVAL  = ', DL,' CM'
      WRITE (10,1000)  'HYDRAULIC CONDUCTIVITY  = ',KH,' CM/SEC'
      WRITE (10,1010)  'HYDRAULIC GRADIENT  = ',HG
      WRITE (10,1010)  'TOTAL POROSITY  = ',TP
      WRITE (10,1010)  'EFFECTIVE POROSITY  = ',EP(K)
      WRITE (10,1010)  'DRY DENSITY  = ',DS,' G/CM^3'
      WRITE (10,1010)  'BULK DENSITY  = ',BD,' G/CM^3'
      WRITE (10,1000)  'PORE VOLUME  = ',PV,' CM^3'
      WRITE (10,1000)  'EFFECTIVE PORE VOLUME  = ',EPV,' CM^3'
      WRITE (10,1000)  'EFFLUENT FLOWRATE  = ',QD,' CM^3/DAY'
      WRITE (10,1010)  'SPECIFIC GRAVITY  = ',DS
      WRITE (10,1010)  'RETARDATION FACTOR  = ',RF
      WRITE (10,1000)  'SEEPAGE VELOCITY  = ',SV, ' CM/DAY'
      WRITE (10,1000)  'ELAPSED TIME  = ',ET,' DAY'
      WRITE (10,1000)  'ONE PORE VOLUME  = ',PVT,' DAY'
      WRITE (10,1000)  'ONE EFFECTIVE PORE VOLUME  = ',EPVT,' DAY'
00900 FORMAT (/,A47)
00901 FORMAT (A49,/)
01000 FORMAT (A35,E10.4,A10)
01010 FORMAT (A35,F10.3,A10)

      WRITE (10,1110) 'ELAPSED TIME','PORE VOLUME',
     +     'UPPER CONC','LOWER CONC','EFFLUENT CONC'
01110 FORMAT (//,A12,A15,A15,A18,A19)
      WRITE (10,1200)   '(DAYS)','(MG/L) C(T)/C(0)',
     +      '(MG/L) C(T)/C(0)','(MG/L) C(T)/C(0)'
01200 FORMAT (3X,A6,17X,A19,1X,A17,1X,A17,/)

C** INITIAL CONDITION
      W = 0.0
      J = 0.0

      DO 10  I = 2, N+2
        CONC(I) = 0.0
00010 CONTINUE

      CONC(1) = CO(K)
```

```
      RCUR = CONC(1)/CO(K)
      RCLR = CONC(N+2)/CO(K)
      RCE = CONC(N+1)/CO(K)
      RC = 0.0

      GO TO 90

00030 W = W + 1
00040 J = J + 1

      CONC(1) = CONC(1) - HC*CIN(K)

      CALL TRIDIA (C,E,F,HA,HB,HD,HE,CONC,N)

      Q = J/T

      IF (W.EQ.Q)  THEN
        GO TO 90
      ELSE
        GO TO 40
      END IF

00090 TIME = J * DT
      RCUR = CONC(1)/CO(K)
      RCLR = CONC(N+2)/CO(K)
      RCE = CONC(N+1)/CO(K)

      IF (QD.EQ.0)  THEN
        PPV = 0.0
      ELSE
        PPV = TIME/PVT
      END IF

     WRITE (10,1400)  TIME,PPV,CONC(1),RCUR,CONC(N+2),RCLR,
    +                 CONC(N+1),RCE
01400 FORMAT(F9.2,E17.3,F10.3,F7.4,F10.3,F7.4,F11.3,F7.4)

      IF (J.EQ.M)  THEN
        GO TO 100
      ELSE
        GO TO 30
      END IF

00100 WRITE (10,1500)  'DEPTH','CONC. PROFILE','RELATIVE CONC.'
01500 FORMAT(/,1X,A8,A17,A16)
      WRITE (10,1600)  '(CM)','(MG/L)'
01600 FORMAT(A9,4X,A10,/)

      V = 0
      I = 1
      DEPTH = (I-1)*DL
      WRITE (10,1700) DEPTH, CONC(1), RCUR

00130 V = V+1
00140 I = I+1
00150 U = (I-1)/S
```

```
      IF (U.EQ.V) THEN
        GO TO 120
      ELSE
        GO TO 140
      END IF

00120 DEPTH = (I-1)*DL
      RC = CONC(I)/CO(K)
      WRITE (10,1700) DEPTH,CONC(I),RC
01700 FORMAT(F9.3,F13.3,F14.4)

      IF (I.EQ.N+1) THEN
        GO TO 1
      ELSE
        GO TO 130
      END IF

00001 CONTINUE

      STOP
      END

C********** SUBROUTINE TRIDIAGONAL MATRIX ********

      SUBROUTINE TRIDIA (C,E,F,HA,HB,HD,HE,CONC,N)

      INTEGER  N,I
      REAL SUB(305),DIAG(305),SUP(305),CONC(305)

      DIAG(1) = HE
      SUP(1) = HD

      DO 10 I = 2, N+1
        SUB(I) = C
        DIAG(I) = E
        SUP(I) = F
00010 CONTINUE

      DIAG(N+2) = HB
      SUB(N+2) = HA

      DO 11  I = 2, N+2
        SUB(I) = SUB(I)/DIAG(I-1)
        DIAG(I) = DIAG(I) - SUB(I) * SUP(I-1)
        CONC(I) = CONC(I) - SUB(I) * CONC(I-1)
00011 CONTINUE

      CONC(N+2) = CONC(N+2)/DIAG(N+2)

      DO 12  I = N+1,1,-1
        CONC(I) = (CONC(I) - SUP(I) * CONC(I+1))/DIAG(I)
00012 CONTINUE

      RETURN
      END
```

APPENDIX C

NUMERICAL MODEL VERIFICATION

The numerical models developed in this study were verified using analytical solutions. The analytical solutions have limitations when they are used. The solutions obtained from both analytical and numerical approaches should be identical within the limitation. For example, before a solute breaks through a barrier, the concentration-depth profile of the solute obtained from the numerical solution for the tank test with a lower reservoir should be the same with that from Ogata and Banks' analytical solution. Also, before a solute breaks through a barrier, the concentration change of the solute in the upper reservoir in column tests estimated by the numerical solution should have the same trend with that estimated by the analytical solution derived in this study.

The comparison between the analytical and the numerical solutions were conducted under two different conditions, the pure diffusion case (no advection) and the advection-diffusion case.

C.1 Pure Diffusion

For the simulation of this models, following conditions were applied.

Hydrodynamic Dispersion Coefficient = 10^{-6} cm^2/sec

Partition coefficient = 0 (tracer)

Upper Boundary Concentration = 10 mg/L (Constant)

Length of Column = 60.96 cm (2 ft)

Hydraulic Conductivity = 1×10^{-8} cm/sec

Hydraulic Gradient = 0 (no advective mass transport)

Total Porosity = 0.40

Effective Porosity = 0.36

Dry Density of Soil = 2.70 g/cm^3

Diameter of Column = 20 cm (2 ft)

For the numerical solution, the following four conditions were included:

Height of Upper reservoir = 10.0 cm

Height of Lower Boundary = 1.0 cm

Space Interval = 1/100 of column length

Time Interval = 0.1 day

Figure C.1 shows the concentration-depth profiles after several different elapsed times. Before the breakthrough of solute occurs, approximately one year, the numerical solutions agree with the analytical solutions. After breakthrough occurs, the concentration-depth profile is affected significantly by the concentration in the lower reservoir. Figure C.2 shows the concentration versus time in the upper reservoir estimated by the analytical and numerical solutions. The numerical solution has slightly higher values than the analytical solution.

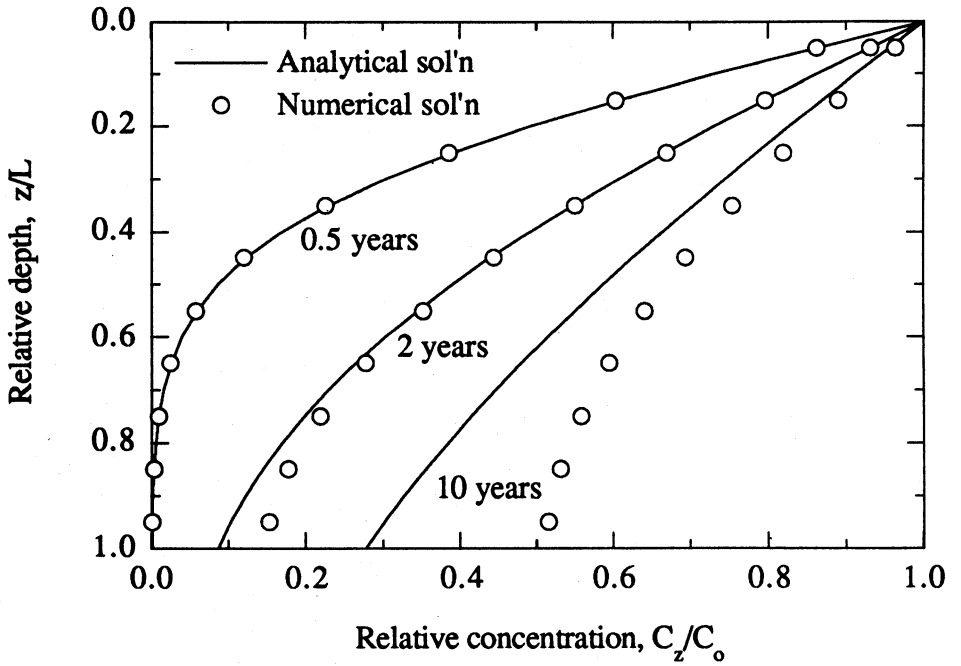

Figure C.1 Comparison between the analytical and numerical solutions of the concentration-depth profiles for the pure diffusion case.

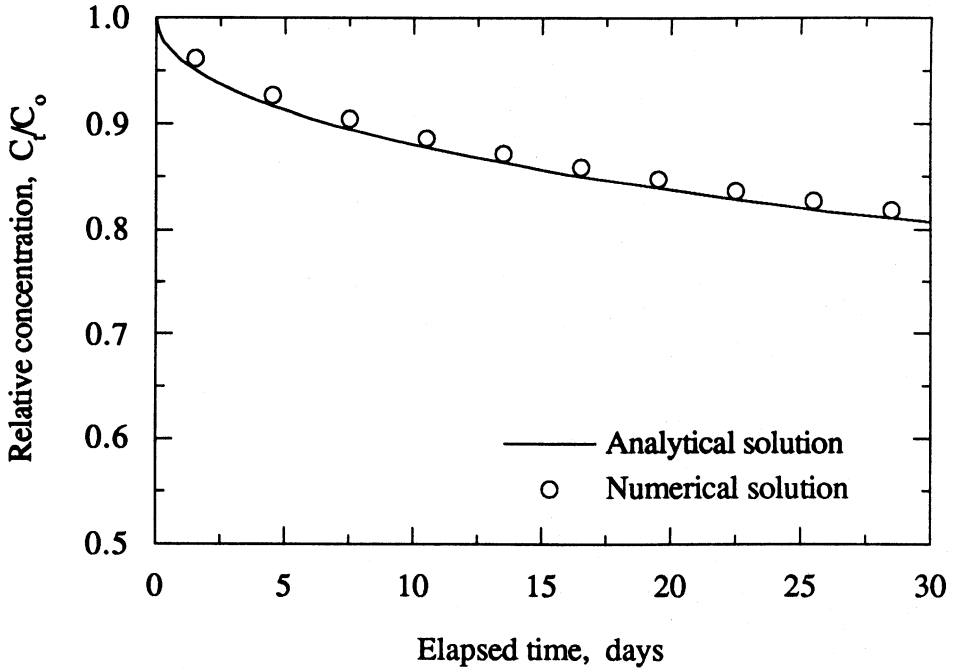

Figure C.2 Comparison of analytical and numerical solutions of the concentration in the upper reservoir for the pure diffusion case.

C.2 Advection and Dispersion

For this problem, the same conditions with the pure diffusion case were used. The applied hydraulic gradient was 1.5. Figure C.3 shows the concentration-depth profile after several different time passed. Before the breakthrough of solute occurs, approximately one year, the numerical solutions agreed with the analytical solutions. After breakthrough occurs, the concentration-depth profile is affected significantly as mentioned in the previous section.

Figure C.4 shows the concentration versus time in the upper reservoir estimated by the analytical and numerical solutions for the advection-diffusion case. The numerical solution has slightly higher values than the analytical solution as for the pure diffusion case.

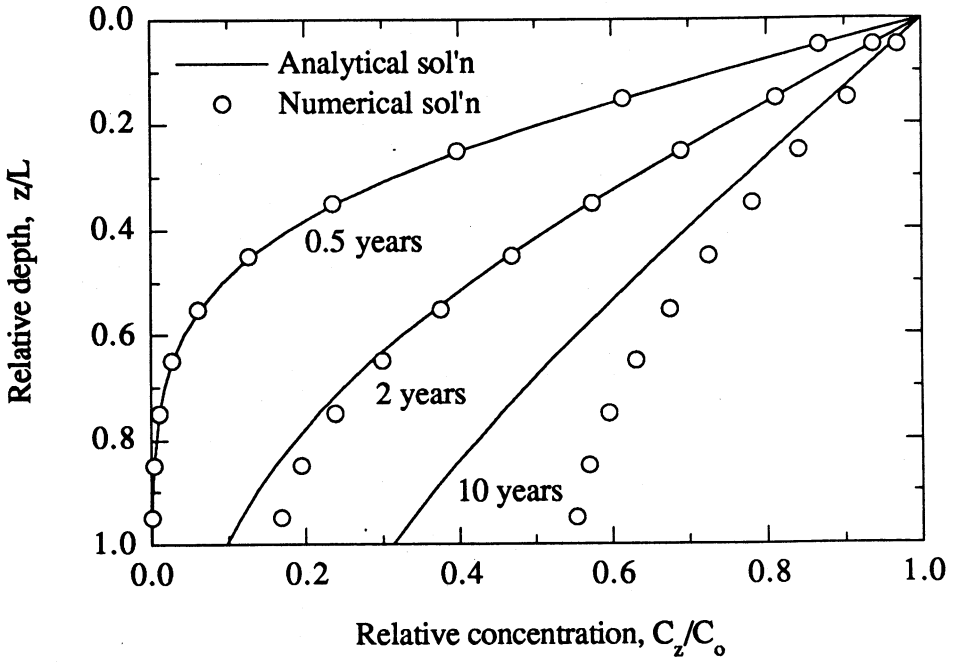

Figure C.3 Comparison between the analytical and numerical solutions of the concentration-depth profiles for the advection-diffusion case.

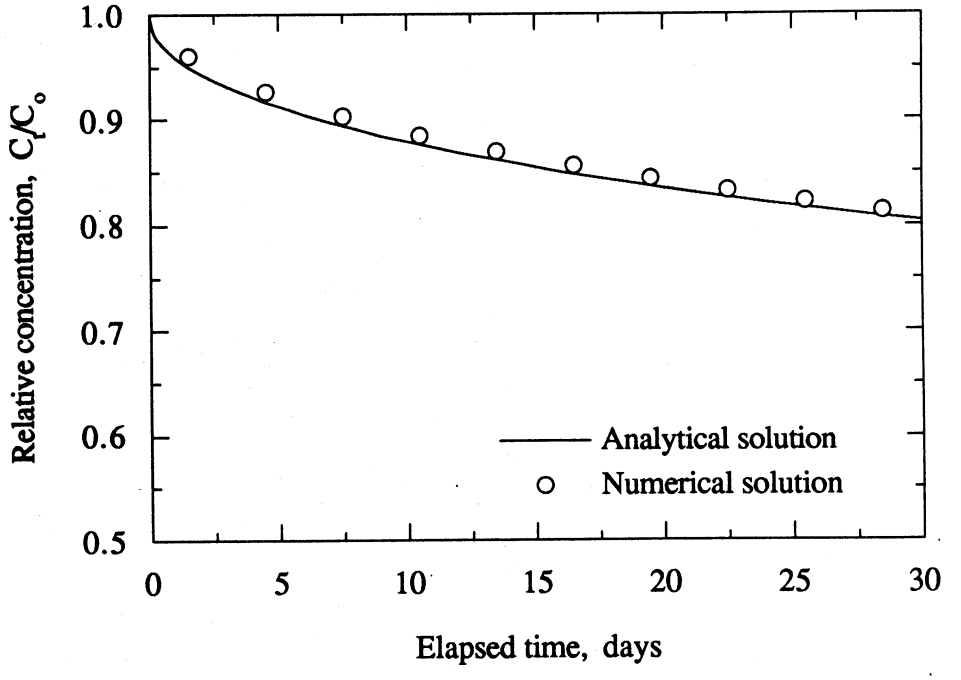

Figure C.4 Comparison between the analytical and numerical solutions of the concentration in the upper reservoir for the advection-diffusion case.

C.3 Effect of Lower Reservoir Volume on the Tank Model

As expected, the volume of the lower reservoir affects significantly the numerical solution. Figure C.5 is the results of the simulations based on different sizes of lower reservoirs. The volume of the lower reservoir was increased 10 times and 100 times greater than the previously used. The conditions were the same with those of the simulations previously conducted. As the volume of lower boundary increases, the breakthrough curve was expanded because of the lower concentration in the lower reservoir.

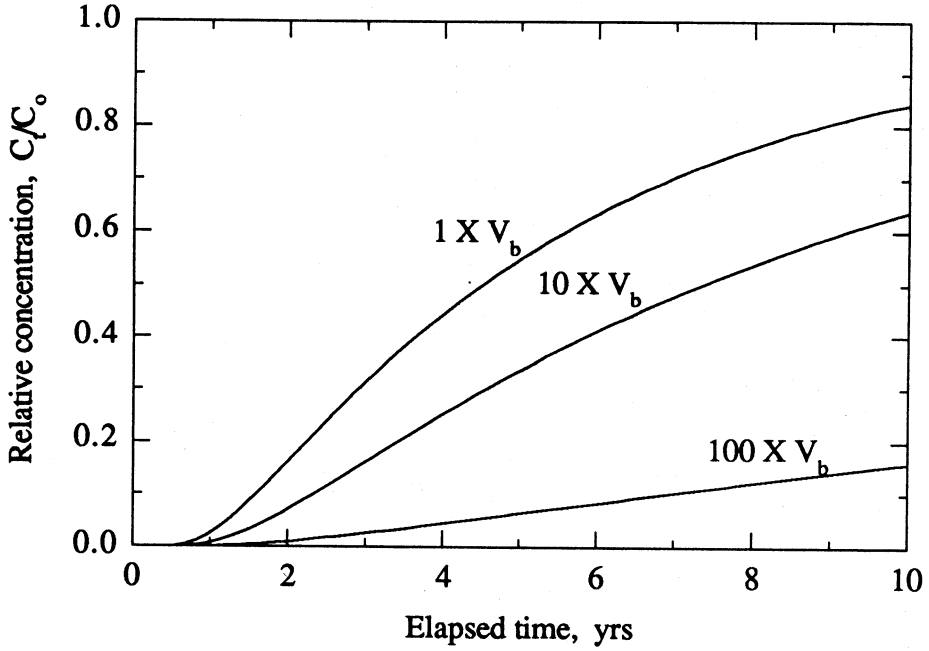

Figure C.5 Effect of the volume of the lower reservoir on the breakthrough curve for the advection-diffusion case.

C.4 Effect of Hydraulic Conductivity on the Concentration in the Upper Reservoir

According to Figures C.2 and C.4, the concentrations in the upper reservoir under pure diffusion and the advection and diffusion cases have no significant difference. It was

caused by the low hydraulic conductivity. If the hydraulic conductivity is increased, the advective mass transport will be increased and the difference will be greater. Figure C.6 shows the simulation results conducted under 10 times and 100 times increased hydraulic conductivity. The other conditions were the same with those of the previous simulations.

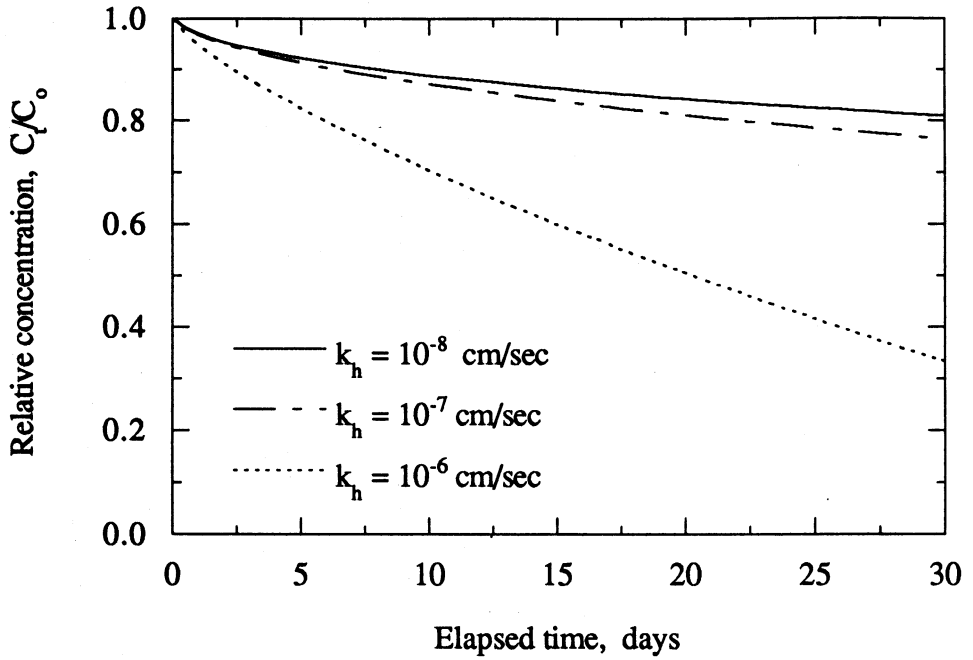

Figure C.6 Effect of hydraulic conductivity on the concentration in the upper reservoir for the advection-diffusion case.

APPENDIX D

PREPARATION OF STOCK SOLUTION

When the solution, which contains several organic compounds at the same concentration, is required for the experiment, the solution can be made by diluting a stock solution. The stock solution is prepared by mixing the same weight of each target organic compound. However, it is more convenient to measure the volume of organic compounds than to measure the weight of the compounds. If the stock solution which contains n different kinds of organic compounds, the volume of each organic compound for mixture can be calculated as follows:

$$V_1 + V_2 + \cdots + V_{n-1} + V_n = V_{total} \quad \text{(D.1)}$$

where V_1 = volume of 1st organic compound, mL;

V_2 = volume of 2nd organic compound, mL;

...

V_{n-1} = volume of n-1th organic compound, mL;

V_n = volume of nth organic compound, mL; and

V_{total} = volume of stock solution, mL.

Since the stock solution contains the same amount of each organic compound,

$$V_1 \cdot \rho_1 = V_2 \cdot \rho_2 = \cdots = V_{n-1} \cdot \rho_{n-1} = V_n \cdot \rho_n \quad \text{(D.2)}$$

where ρ_1 = density of 1st organic compound, g/cm^3;

ρ_2 = density of 2nd organic compound, g/cm^3;

...

ρ_{n-1} = density of n-1th organic compound, g/cm^3; and

ρ_n = density of nth organic compound, g/cm^3.

Now, the volume of each compound can be expressed in term of the first compound.

$$V_2 = \frac{\rho_1}{\rho_2} V_1$$

$$V_3 = \frac{\rho_1}{\rho_3} V_1$$

$$\cdots \qquad (D.3)$$

$$V_{n-1} = \frac{\rho_1}{\rho_{n-1}} V_1$$

$$V_n = \frac{\rho_1}{\rho_n} V_1$$

Then, Eq. D.1 can be rearranged as follows:

$$(1 + \frac{\rho_1}{\rho_2} + \frac{\rho_1}{\rho_3} \cdots \frac{\rho_1}{\rho_{n-1}} + \frac{\rho_1}{\rho_n}) \cdot V_1 = V_{total} \qquad (D.4)$$

and

$$V_1 = \frac{V_{total}}{(1 + \frac{\rho_1}{\rho_2} + \frac{\rho_1}{\rho_3} \cdots \frac{\rho_1}{\rho_{n-1}} + \frac{\rho_1}{\rho_n})} \qquad (D.5)$$

If the volume of stock solution is decided, the volume of one organic compound can be obtained by solving Eq. D.5 and the volumes of the other compounds also can be obtained using Eq. D.3.

When the target concentration and the volume of the diluted solution are decided, the volume of the stock solution to be diluted with water to meet the target concentration can be calculated.

$$C_{1,target} = \frac{(V_{stock} \cdot \frac{V_1}{V_{total}} \rho_1)}{V_{sol}}$$

$$C_{2,target} = \frac{(V_{stock} \cdot \frac{V_2}{V_{total}} \rho_2)}{V_{sol}}$$

$$\cdots \qquad (D.6)$$

$$C_{n-1,target} = \frac{(V_{stock} \cdot \frac{V_{n-1}}{V_{total}} \rho_{n-1})}{V_{sol}}$$

$$C_{n,target} = \frac{\left(V_{stock} \cdot \frac{V_n}{V_{total}} \rho_n \right)}{V_{sol}}$$

where $C_{1,target}$ = target concentration of 1st organic compound, mg/L;

$C_{2,target}$ = target concentration of 2nd organic compound, mg/L;

...

$C_{n-1,target}$ = target concentration of n-1th organic compound, mg/L;

$C_{n,target}$ = target concentration of nth organic compound, mg/L;

V_{stock} = volume of stock solution diluted, μL; and

C_{sol} = volume of diluted solution which will be made, L.

The volume of stock solution diluted, V_{stock}, can be calculated using one of Eq. D.6 as follows because all target concentrations of n compounds are the same.

$$V_{stock} = \frac{C_{i,target} \cdot V_{sol}}{(V_i/V_{total}) \cdot \rho_i} \qquad (D.7)$$

APPENDIX E

BATCH ISOTHERM TESTS

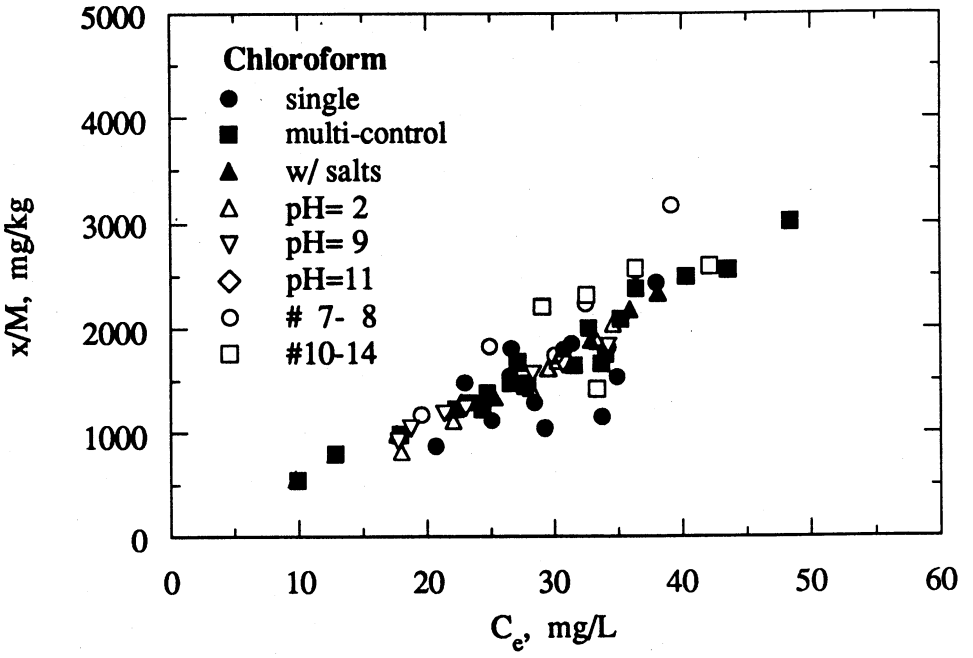

Figure E.1 Chloroform batch isotherm tests.
(# 7- 8 = 2.38 < d < 2.83 mm, and #10-14 = 1.41 < d < 2.00)

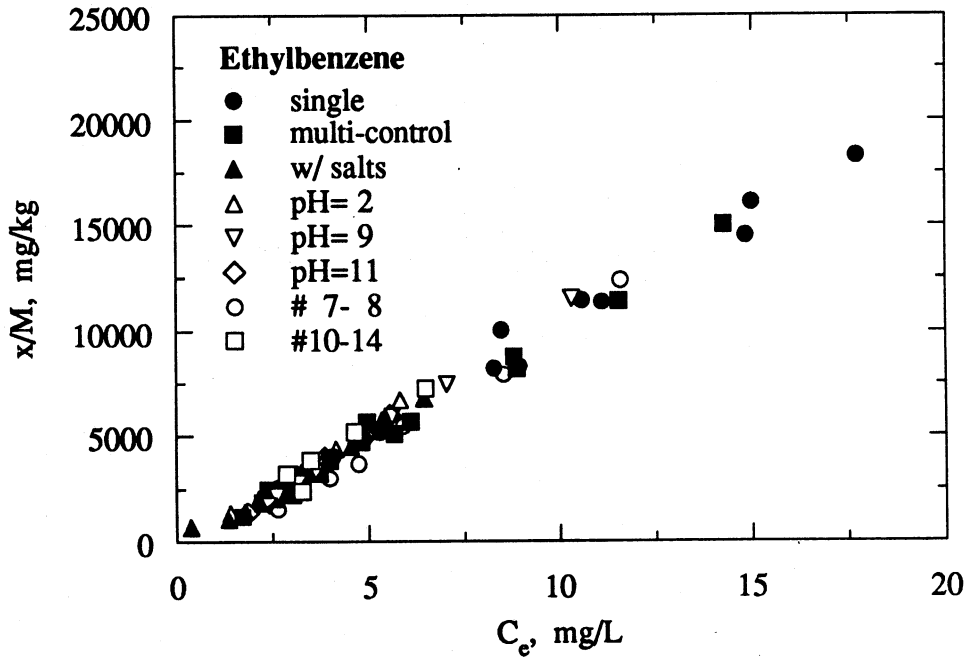

Figure E.2 Ethylbenzene batch isotherm tests.
(# 7- 8 = 2.38 < d < 2.83 mm, and #10-14 = 1.41 < d < 2.00)

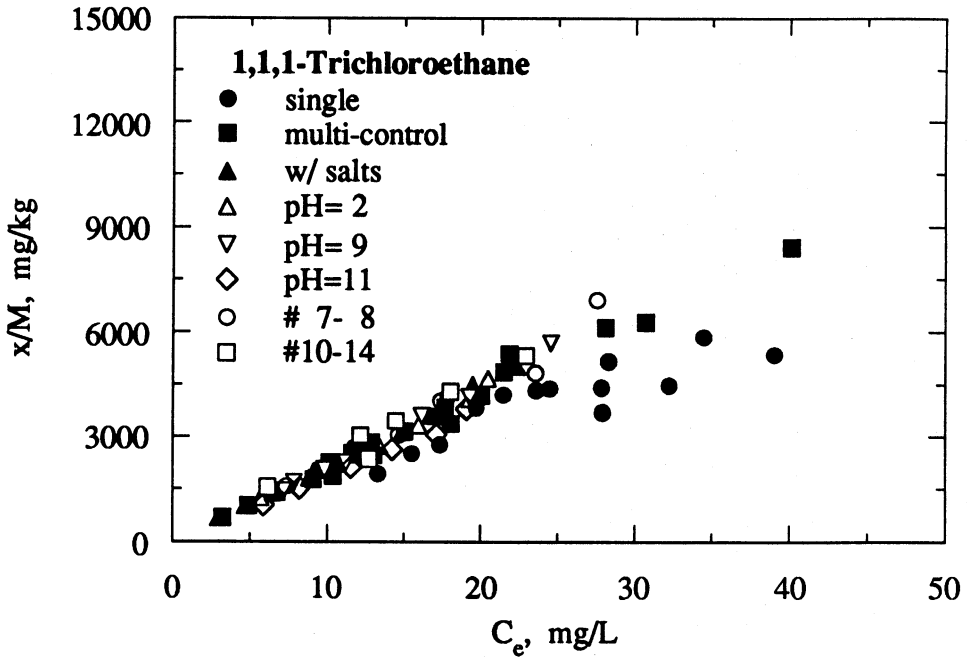

Figure E.3 1,1,1-Trichloroethane batch isotherm tests.
(# 7- 8 = 2.38 < d < 2.83 mm, and #10-14 = 1.41 < d < 2.00)

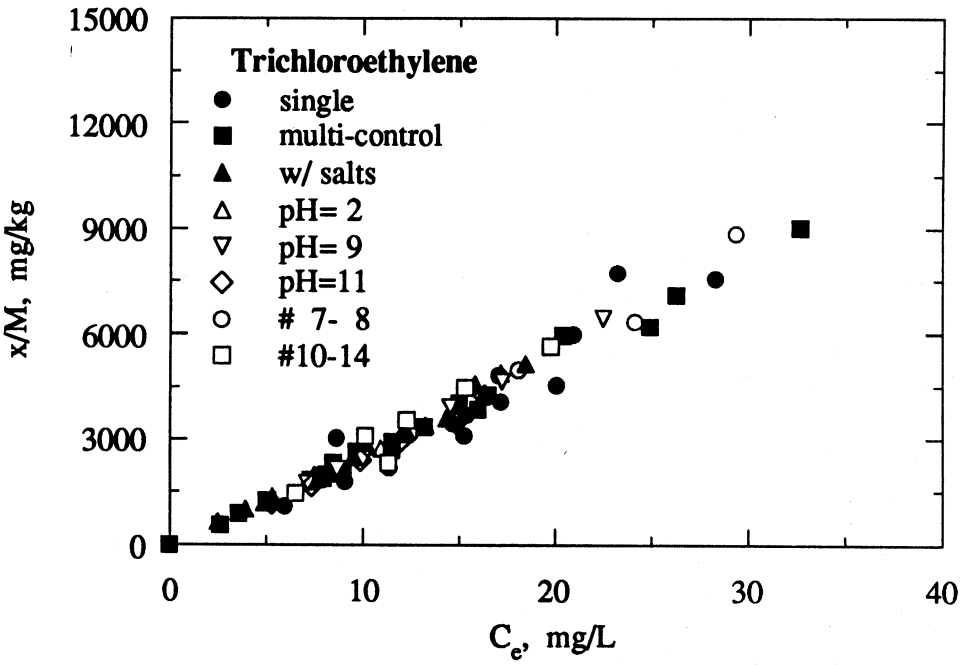

Figure E.4 Trichloroethylene batch isotherm tests.
(# 7- 8 = 2.38 < d < 2.83 mm, and #10-14 = 1.41 < d < 2.00)

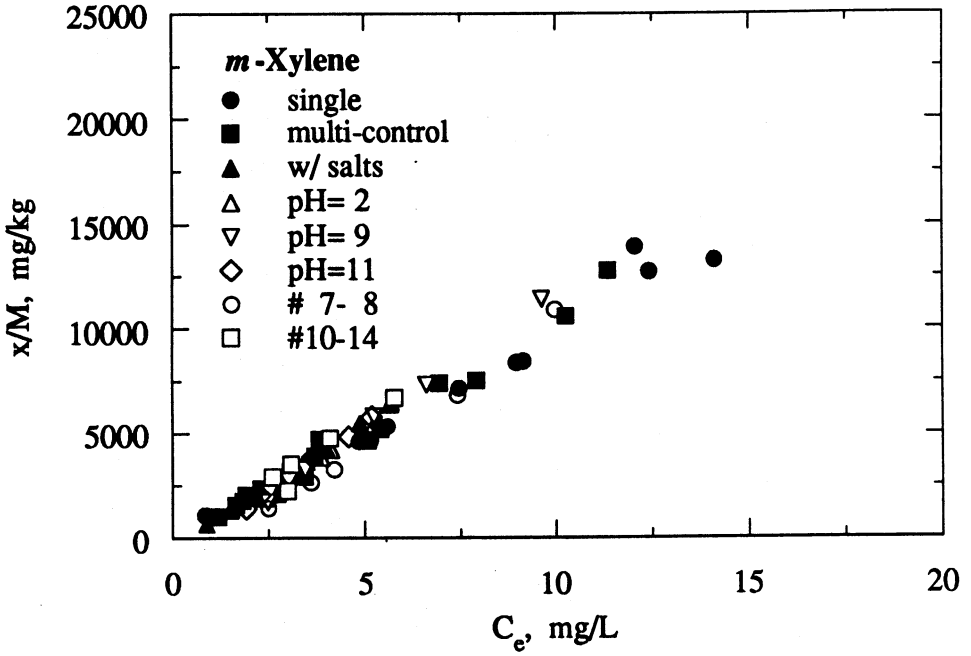

Figure E.5 *m*-Xylene batch isotherm tests.
(# 7- 8 = 2.38 < d < 2.83 mm, and #10-14 = 1.41 < d < 2.00)

APPENDIX F

HYDARULIC CONDUCTIVITIES IN TANK TESTS

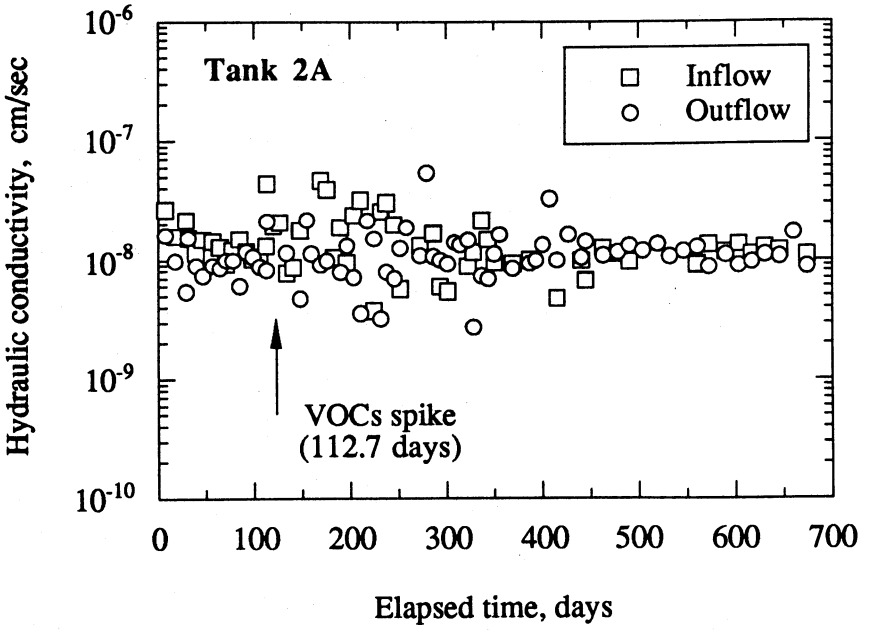

Figure F.1 Hydraulic conductivity in tank 2A.

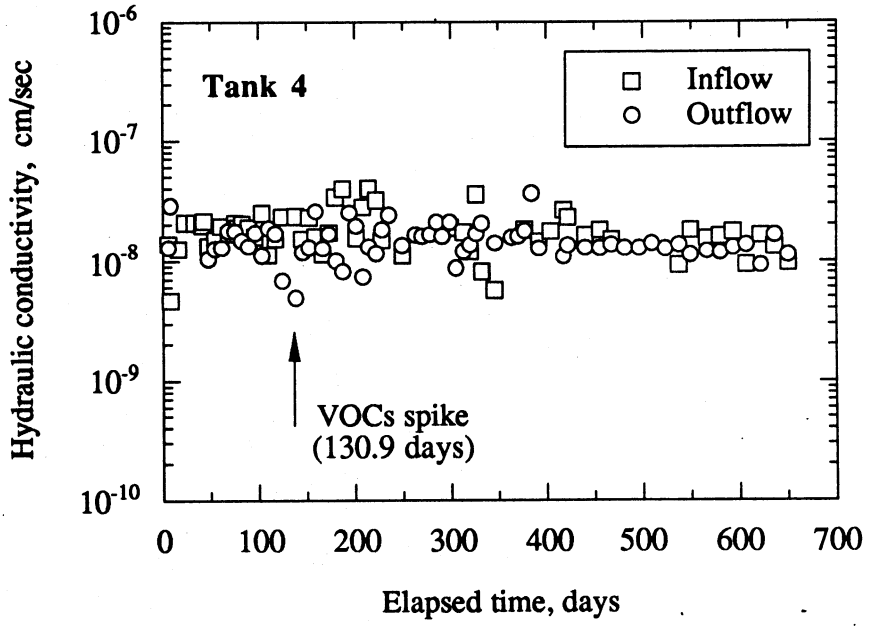

Figure F.2 Hydraulic conductivity in tank 4.

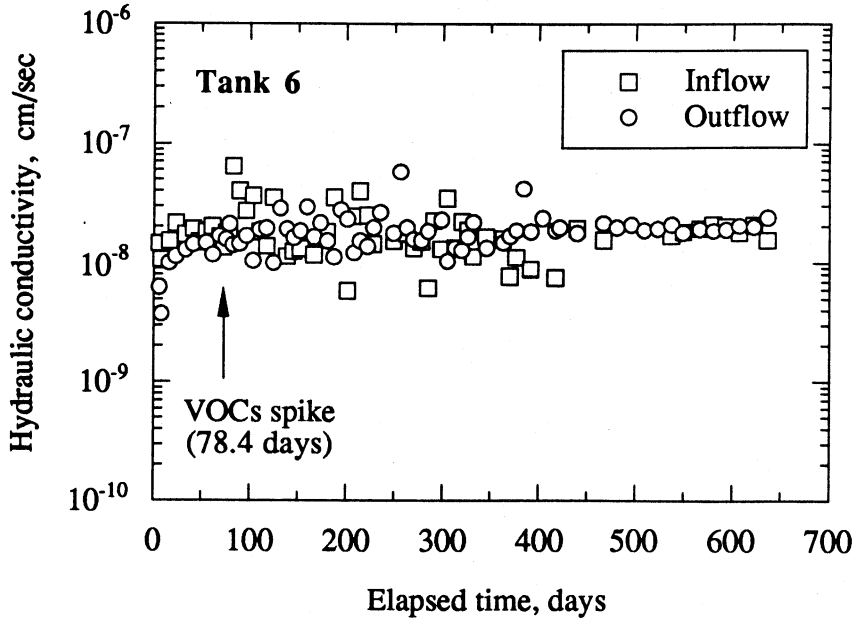

Figure F.3 Hydraulic conductivity in tank 6.

APPENDIX G

BROMIDE BREAKTHROUGH CURVES IN TANK TESTS

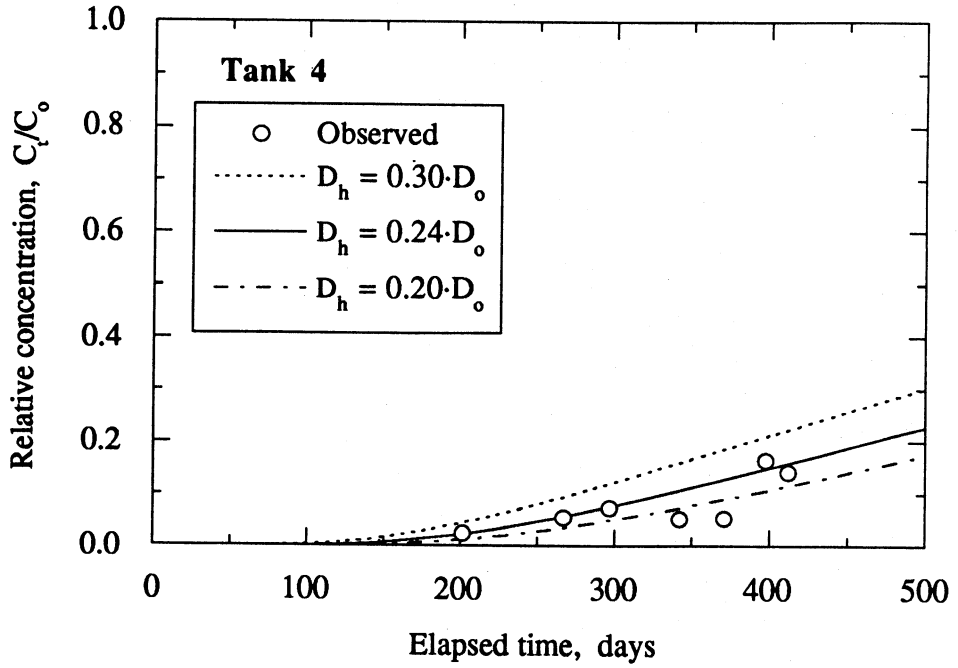

Figure F.1 Bromide breakthrough curves in Tank 4.

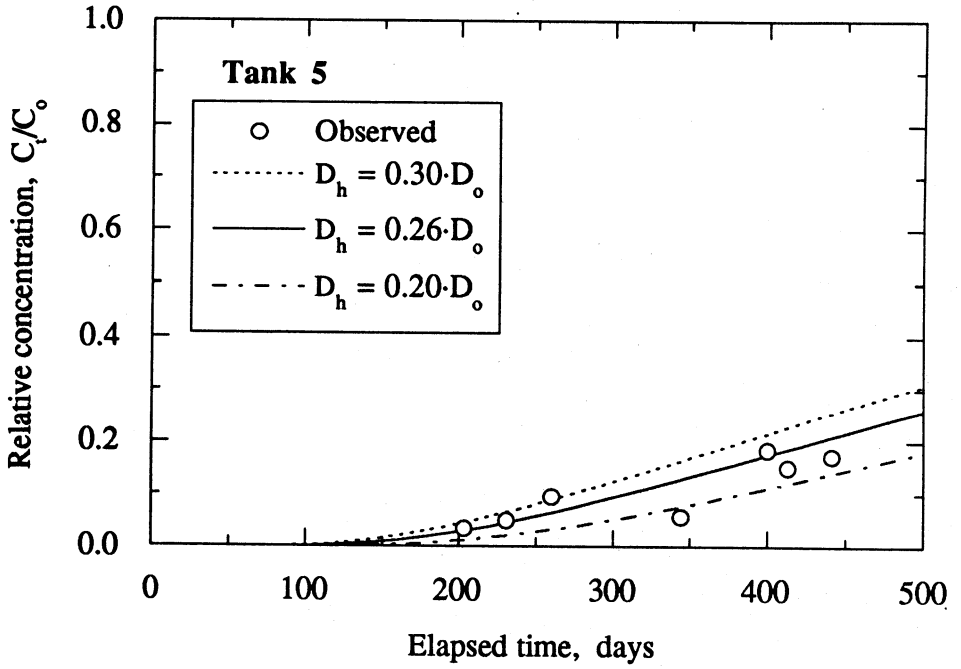

Figure F.2 Bromide breakthrough curves in Tank 5.

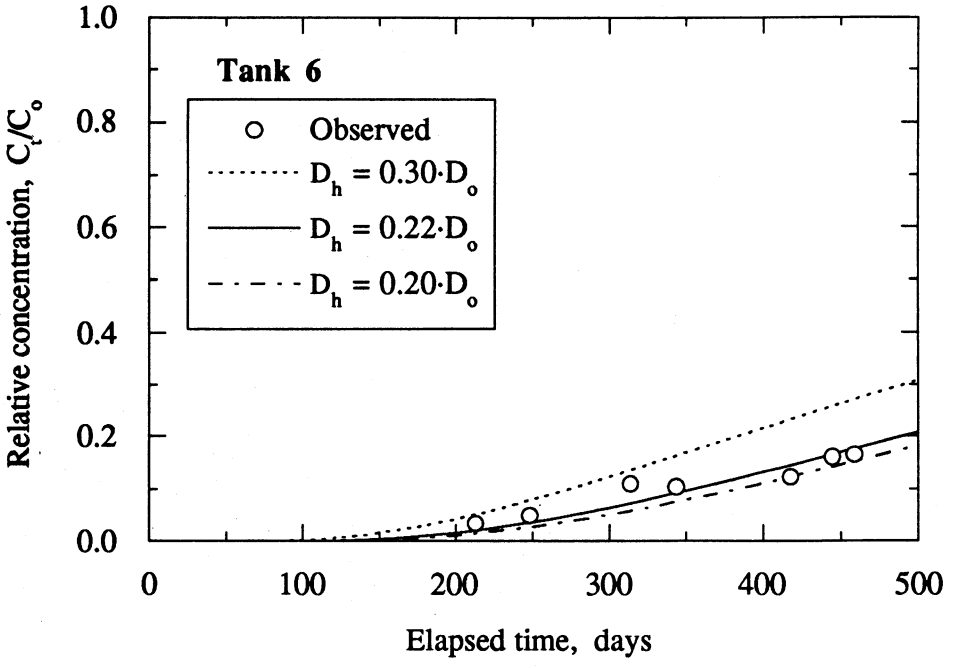

Figure F.3 Bromide breakthrough curves in Tank 6.